Highly Selective Attentional Modulation of Task-Appropriate Neural Populations in Primary Visual Cortex

A DISSERTATION
SUBMITTED TO THE FACULTY OF THE GRADUATE SCHOOL
OF THE UNIVERSITY OF MINNESOTA
BY

Scott Gerald Warren

IN PARTIAL FULFILLMENT OF THE REQUIREMENTS
FOR THE DEGREE OF
Doctor of Philosophy

Geoffrey Ghose

June, 2017

Acknowledgements

I have enormous gratitude toward the many who supported me along this journey.

The support staff of both the Graduate Program in Neuroscience and the Medical Scientist Training Program, most notably Ms. Susan Shurson, Mr. Nicholas Berg, and Mr. John Paton, provided a crucial foundation upon which my studies could be assembled.

Leaders of these same training programs, including Dr. Tucker LeBein, Dr. Yoji Shimizu, Dr. Timothy Ebner, Dr. James Ashe, and Dr. David Redish, each provided unique and valuable insights and advice during my personal and professional growth in these formative years. Dr. Stephen Engel provided valuable insights at every stage of my research, and for both his advice and his continual challenges to improve the rigor of my work I am grateful.

However, of greatest academic importance is my adviser and friend, Dr. Geoffrey Ghose, who is a daily exemplar of the scientist and scholar. His insight, dedication, and perseverance provided life to all of my research endeavors.

I thank my parents, Grant and Claudia Warren, for fostering a love of knowledge from the youngest ages. My trajectory was determined long before I left their home. My brother, David, and sister, Laura, were among my first and favorite teachers as we explored this world together.

None of this would be possible without the continual love and support of my wife, Teresa, and my new son Cameron. I thank her for all that she has endured in these years, and I treasure both Teresa and Cameron for their continuous inspiration.

Abstract

A wide variety of different forms of attention have been described in the human and non-human literature, however the recently developed Input Gain Model of visual attention proposes that a simple neural mechanism, multiplicative gain, may be employed to explain much of the available data on visual attentional modulations. On this basis, we hypothesized that a better explanation for distinct forms of attention may be that this simple attentional mechanism is in fact highly specific: attentional modulations are only present within task-appropriate neurons or neuron groups, and it is the location (and not nature) of these modulations which defines the observer's current attentive state. We present the results of two orthogonal attention tasks, both targeting distinct but specific and well defined sub-populations of primary visual cortical (V1) neurons. In both experiments we observe that attentional modulations are grossly targeted to neural populations that are selectively tuned for the cue. When humans attend to one orientation, voxels reflecting orientation selective neurons tuned toward that orientation are selectively enhanced. When monkeys were trained to attend to a very small region of space, attention modulated the V1 representation of stimulus elements near that location in space. In both studies, these modulations are predictive of observer behavior, providing evidence that attentional modulation of V1 meaningfully impacts the perceptibility of the attended stimuli. Systematic imprecision in these modulations suggest that attentional modulations of V1 are mediated through corticocortical feedback, hypothetically from secondary visual cortex. This provides a strong constraint for further refinement of general models of attention.

Contents

List of Tables

List of Figures

Chapter 1

Introduction

Human sensory attention is enormously flexible, but decades of evidence support the view that similar cellular mechanisms underlie the most well-studied attentional states.

Herein I present a series of arguments and experiments in support of my thesis that visual attention is best described as a selection process that matches simple neuromodulations with the most task-appropriate cells in the brain. This matching operation is non-trivial: I show that attention acts with millimeter precision in cortical space, and is capable of selectively enhancing even the most primitive stages of visual processing. I will present biologically plausible implementations of this process, and argue that this level of neuromodulatory specificity is sufficient to explain much of the published literature.

- Chapter 2 summarizes the state-of-the-art in the scientific study of sensory attention. Starting with a definition of attention, I present psychophysical studies that establish the effects of attention on sensory processing and conclude with a brief discussion of how attention may be implemented at a neuronal level.

- Chapter 3 acknowledges the central knowledge gap that this thesis aims to address. Humans can selectively attend to an enormous variety of stimuli across sensory modalities and time, yet it is not clear from single-neuronal experiments how such a wide variety of attentional states maybe invoked. I propose a simple extension of the current attention models to address this. I close with a discussion of attentional selectivity and targeting as used in this thesis and I describe the general experimental framework within which we will address this question.

- Chapter 4 briefly introduces ultra-high field functional magnetic resonance imaging as one tool to realize the experimental design goals discussed in Chapter 3. I will then present

the results of my first set of experiments, demonstrating that attentional modulations are indeed selectively targeted to the neural populations within primary visual cortex that are most well-suited to processing the attended stimulus. Moreover, we show that this modulation is temporally specific, implying that selective modulations can also explain temporal modulations of attention.

- Chapter 5 follows the logic of 4 to its extreme. Here I will ask how precise this process of selective targeting is by explicitly measuring the extent of attentional modulations in cortical space using an invasive form of optical imaging which affords a vastly improved resolution over the previous attempts to address this question. We show that attentional modulations differentially modulate closely packed stimuli, with precision on the order of the horizontal connections within neocortical layer 1 of V1.

- Chapter 6 considers the model of selective attentional targeting in the context of the known anatomy and histology of primary visual cortex. I will discuss how this model might be plausibly realized in the biological brain, then close with a brief acknowledgment of remaining knowledge gaps both within and outside of primary visual cortex.

Chapter 2

Sensory Attention: Psychophysical and electrophysiologic evidence

2.1 Introduction

Attention is a powerful modulator of our ongoing sensory experience. When we consciously select an object to be the focus of our attention, we are able to make more precise sensory judgments regarding finer details[14, 15] about the object under a shorter time frame[1, 16], and these attended stimuli are more likely to enter into our conscious thought[17] and to be preserved in our short- and long-term memories[18, 19, 20]. At the same time, the processing of non-attended stimuli is inversely suppressed- attention filters out distracting stimuli[21] and background noise[22], serving as a protection against sensory overload. This reshaping of our sensory world is ongoing, and is theorized to be an essential "bottleneck" in sensory processing[23, 24] as well as an important component of our greater conscious experience[25, 26].

Given its far-reaching effects on the human experience, the phrase "attention" has been ascribed to numerous effects and models throughout different fields of medical, biological, and social science. To facilitate rigor and to enable comparisons with previous work, in this dissertation I focus exclusively on attention defined as the differential processing of the same set of sensory stimuli as a function of the cognitive state of the observer. Classically, attention is manipulated by maintaining a constant stimulus and

- embedding a consistent long-term pattern into the stimulus sequence[27, 28],

- supplying or denying additional information about the stimulus[29],
- asking subjects to make simple or difficult judgments about the stimulus[30],
- and/or instructing subjects to make a response based upon one part of a composite stimulus[4, 3, 2].

By maintaining constant stimuli and controlling for variability due different sensory inputs, the remaining variability in task performance and in neurophysiologic measurements may be directly attributed to the manipulation of the observer's attentional state. Of these, the first type of manipulation deserves special mention. The great majority of attention studies utilize some form of *explicit cue* to instruct the subject as to the current state of the task[1, 2, 29, 3, 31, 32]. The use of explicit cues is scientifically powerful, because it ensures a rapid switch between distinct attention states that is driven solely by cue recognition and top-down modulation. While explicit cues do exist in both the natural world and in human society, a substantial amount of sensory learning and attentional orienting is done on the basis of learned patterns and regularities in the world which were *implicitly* trained by repeated presentation. Even in laboratory settings, such implicit cues result in the generation of unconscious attentional biases that improve task performance[27]. In the studies presented in this dissertation, we will utilize both explicit and implicit cues. While we do not make strong effort to distinguish between the modulations evoked by these cues, it will be important to consider these differences during our interpretation of the results.

To avoid confusion, there are several potentially confounding phenomena that are not considered within this dissertation. Here I focus on the *intrinsic, covert* attentional modulation of *sensory* cortex, namely attentional modulations that occur when attending to objects away from the current center of gaze due to an endogenously generated signal from within the brain of the observer. This is the form of attention that is associated with task history, learned patterns, symbolic cues, and the beliefs of the observer. Intrinsic attention is distinct from *extrinsic* attention, which is the subconscious orienting of ones attentional processing to a sudden cue of exogenous origin[33]. This alternative form of attention is associated with an unexpected sound or flash of light, or non-symbolic attention cues such as a blinking light in the same location as an upcoming stimulus. Intrinsic and extrinsic attentional signals originate in different regions of the brain[33] and it is not clear that they have the same effects on visual processing. To avoid confusion on this topic, all experiments herein will utilize attention paradigms in which subjects are instructed in advance of the task which stimuli are likely to contain a target event and which are unlikely. Subjects then generate their own intrinsic attention to the likely targets.

In studying spatial attention, both extrinsic and intrinsic attention are directed to a location away from the center of gaze. This is because foveate animals, including human and non-human

primates, resolve visual information non-uniformly across space. There exists a region, the fovea, of high resolution vision which is associated with a high density of retinal photoreceptors and ganglion cells[34]. The foveal visual field is also associated with a physically larger surface area within the primary visual cortex[35]. Due to these advantages afforded to the processing of foveal stimuli, subjects have sharper visual acuity when responding to objects nearer to fixation[36, 37]. During normal daily life, the most natural way for primates to orient their visual attention is to foveate on different objects, a process called overtly attending[38]. Overt and covert (peripheral) attention are thought to involve similar neural processes[38, 39]. In studying overt attentional processing, however, it is difficult to disambiguate between increased sensory processing prowess that are due to an intrinsically generated modulation of sensory cortex from those due to the anatomic advantages of the foveal visual representation. When we describe a process of attention, therefore, we are careful to either design a stimulus for which fixation in a certain location offers no benefit (Chapter 4) or to design a task in which fixation away from the attended stimuli is carefully controlled and the subjects must covertly attend to stimuli in their non-foveal visual field (Chapter 5).

Finally, there are numerous human diseases in which attention is impaired. While a number of these diseases do in fact exhibit a measurable deficit in intrinsically generated sensory attention (including the autism spectrum disorders[40, 41] and Alzheimer's dementia[42]), in many conditions the attentional impairment manifests as symptoms of poor sustained control over one's attention (e.g. difficulty focusing)[43]. In these diseases, it is not clear that there is any impairment in sensory processing or sensory attention, but rather the deficit may exist in the executive control of attention and it may reflect impairments in higher-order cognition outside of sensory cortex. Among other psychological diseases, this includes the attention deficit disorders, in which the sensory effects of attention are often reported as normal[44, 45]. In this dissertation, we focus on the sensory consequences of attention under the conditions of appropriate executive control, with direct relevance only to diseases in which sensory processing is diminished.

2.2 Psychophysical evidence for the existence of attention

Among the many internally generated cognitive processes that humans effortfully employ during the course of normal living, attention is notable in that the its effects upon sensory task performance can be explicitly measured with psychophysical techniques[46]. By carefully manipulating both the timing and physical features of stimuli as well as the cues given to the observer, it can readily be shown that appropriate deployments of attention result in improved task performance.

This is most simply exampled by the classic paradigm of Posner[1]. While fixating upon a center point, subjects were asked to press a button as quickly as possible when any of four light-emitting diodes illuminated. Compared to a baseline condition in which subjects had no expectation as to which diode would light, subjects instructed by numeric cue to anticipate the target event at a specific diode enjoyed a modest decrease in their time to respond to the event. The reduction in reaction time is attributed to an enhancement in the processing of light from that diode compared to from others. However, when the cue is invalid and the target event occurs at an different diode (such that the cue was invalid), subjects showed a penalty in their reaction time. This suggests that attention was in fact oriented toward one diode and away from the others, emphasizing the role of attention as a non-uniform selection process.

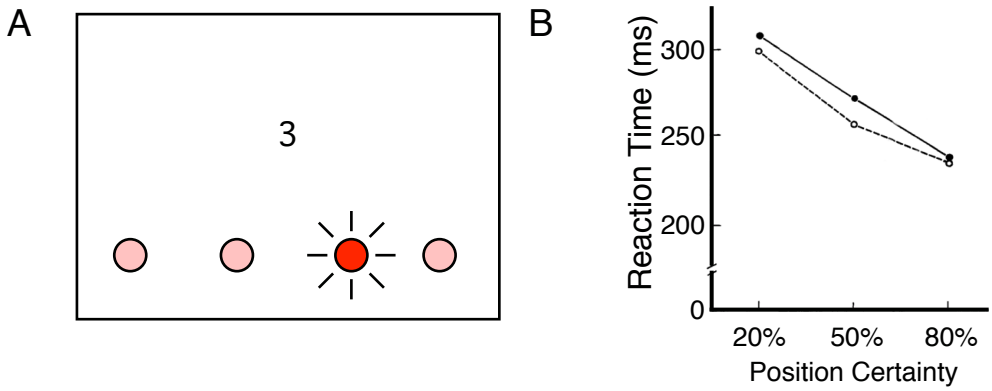

Figure 2.1: **The Posner Paradigm.** This experiment from Posner, Snyder, and Davidson was among the first to demonstrate a measurable effect of attention on task performance[1]. The data presented here are adapted from their report. (A) Subjects fixated at a central point and pressed a button as soon as any red light emitting diode below the screen illuminated. A cue in the middle of the screen either told the subjects which middle location would have an 80% chance of illuminating OR instructed the subjects that both middle positions were equally likely. (B) Subjects responded to light at the cued location more quickly than to light at the uncued location, even though both light sources were of equal character, intensity, and distance from fixation.

Changes in reaction time can be difficult to interpret- it is evidence that a change in processing occurred somewhere within the brain, but localizing those changes to a given stage of the sensorimotor response is challenging. Certainly, the effect of the cue may be due to attentive modulations of sensory processing. Drawing from the popular models of perceptual decision making[47], attention might speed responses because sensory information was integrated more quickly or with less noise, because this information was better retained over time, or because subjects lowered their decision making thresholds. However, the cue may also involve non-attentive changes to motor aspects of the task: *intentional* changes in the sensorimotor[48, 49],

premotor[48, 50, 51], or corticospinal[48, 52] stages of the motor response are also possible, because subjects anticipated the appropriate motor response. Indeed, the ambiguity between sensory and motor aspects of task performance may be inherent to attention, as models of attention often focus on its premotor effects[53, 54, 55]. Briefly, before a saccadic eye movement is made to a target location, it has been shown that the observer's attention is obligated to orient to the target location. Finer details of the relationship between saccadic planning and attention orienting remain controversial [55], but it is supposed that attention arose as a mechanism to plan upcoming eye and/or hand movements.

Further psychophysical studies have implicated alterations in early visual processing as an effector mechanism for visual attention. Modern reports investigate the threshold contrast of a cued target stimulus buried in external noise of variable contrast. Conceptually, by modeling the effects of signal and noise contrast on performance, one may distinguish between altered sensory processing that occurs before the neural representations of the signal and noise are mixed (presumably within the visual system) from processes that occur after these representations are fused into a single visual representation (presumably at the output of or external from the visual system). Attention to one location will decrease the signal-in-noise threshold contrast, implying attentive subjects may perceive fainter stimuli. Moreover, the effect of attention changes as a function of the intensity of background noise- the attention-noise function is very seldom found to be uniform, as may be expected from suggest a simple improvement in post-visual processing. Rather, modeling suggests that attention serves to both enhance the visual system's representation of the attended stimulus and to filter out the background noise *before* it interferes with target stimulus' neural representation[46]. Both of these effects have been observed within single neurons of the intermediate visual system, even on the same task[2].

The results from different attention studies/conditions often show differential effects of these modeled attentional mechanisms. These distinct task-related differences in attention emphasize an important trait- attention is incredibly flexible. Even in the context of simple visual tasks, attention demonstrates subtle differences in its effects on visual processing that may be optimized to meed the demands of the specific task. This flexibility is essential, as attention must adapt to a near infinite range of task conditions: attention may enhance specific targets or suppress noise. Attention may be directed to a location in space[1], to a single object[15], or even to statistical features of visual stimuli such as to all objects sharing a certain color or orientation[29]. Observers can also orient to temporal patterns[28, 29], attention is not exclusively visual. Attention may be directed to auditory[10], tactile[9], proprioceptive[56], olfactory[8], or gustatory[7] cues. Moreover, each of these states may be naturally assumed by the naive observer (although training certainly improves the potency of attentive states[57]). Any general model of attention must be able to account not only for the ability to attend across an enormous variety of physical

and temporal stimuli, but also for the ability of attention to flexibly adapt to the demands of specific tasks.

2.3 Attention changes sensory neuronal computation

In agreement with the psychophysical literature, neuroimaging studies have provided direct evidence that attention to a stimulus increases the blood-oxygen level dependent (BOLD) signal, an indirect hemodynamic response to neural activity, in the the regions of the cerebral cortex responsible for processing stimulus-relevant sensory information (reviewed in Chapter 3). Attentional modulations in BOLD (or EEG) signals are by definition non-specific in that they reflect a non-linear aggregation of neural activity of both visual and non-visual origin[58] from a large region of cortical space reflecting the net modulation of millions of neurons[59]. Greater insight into the cellular nature of the attentional modulations is made possible by the study of model animals. Attention is not a uniquely human phenomenon- with training, non-human primates exhibit the same reaction time advantages with attention to cued stimuli that were described with human subjects above[60]. Invasive recordings from the cerebral cortex of the attending animal has provided great insight into how attention fundamentally changes the processing of cortical sensory neurons.

Due to the incredible variety of possible attentional states and manipulations, it is useful to limit study to only attentional states that interact with stimuli whose cortical representations are well-understood. Historically, because vision is both the primary sensory modality of primates and is also the most well-studied sensory system in the macaque brain, the greatest efforts have been put toward understanding visual attentional modulations (and we follow in this tradition). The primate cortical visual system is hierarchically organized[61]. Visual information from the retina is relayed through the lateral geniculate nucleus of the thalamus to the primary visual cortex (V1), the earliest level of cortical visual processing. Within V1, the earliest visual features such as stimulus orientation[62, 63] are extracted from the retinal image. This featural representation is relayed through several cortical areas, including visual areas V2 and V4, where higher-order features and shape primitives are extracted from each processing stage. At the apex of the ventral visual stream, neurons in anterior temporal cortex fire selectively to the presence of specific objects or actors[64] and relay this information to perirhinal [65] and prefrontal[66] cortex to inform decisions and long-term symbolic memories[67, 68].

Because attention to objects is very common in daily life, and because of the close association between the object-encoding anterior temporal cortex and the more cognitive forebrain, it may seem appealing to study interactions between object attention and object perception in temporal cortex. Indeed, very large attentional modulations in inferior temporal (IT) cortex have been

reported[3, 6, 69]. However, the underlying tuning functions of IT neurons remains elusive. While their role in encoding objects is widely accepted, we lack a strong model for how individual neurons, local microcircuits, and the greater population of all IT neurons transform visual information into object representations. Without understanding these processes in their baseline condition, it is challenging to interpret the effects of attentional modulations within the circuit.

Because of this, most studies emphasize attention to low-level visual stimuli designed to activate neurons in early visual ares such as primary visual cortex (V1) and nearby low-intermediate visual areas (including visual areas V2 and V4)[3, 4, 2]. (The available exceptions do not provide strong counter-examples to the general findings summarized here[69, 3, 70].) The tuning functions of neurons within V1 are particularly well understood, and these have formed the basis set for stimuli in numerous visual experiments. Even at this early level, the receptive field of a given V1 neuron is a complex and multidimensional function: V1 units have a preference for stimulus retinotopic location[71], orientation[35, 71], contrast level[72], stimulus width and height[71], spatial and temporal frequencies[73], motion direction[73], eye-of-origin[71], and interocular disparity[74]. Of these, location and orientation tuning account for a large portion of the total receptive field structure, and manipulation of these variables (commonly in the form of either small bars, or localized sinusoidal gratings[75] called Gabor filters ("Gabors") after Hungarian-British scientist Dennis Gabor) has formed the basis for many visual attention experiments.

A new branch of neuroscience was initiated with the classical work of Moran and Desimone[3], in which rhesus macaques were trained to discriminate between two stimuli co-localized within the classical receptive field of a V4 neuron. One stimulus of the pair was aligned with the preferred orientation of the V4 neuron under investigation, while the other was anti-aligned. When the aligned stimulus is presented in isolation, the V4 neuron responds strongly, and conversely a weak response is seen to the anti-aligned stimulus in isolation. When the two stimuli are presented simultaneously, the V4 neuron has an intermediate-strength response, as though the strong and weak responses are in competition. When subjects attended to the aligned stimulus, the neuron responded more vigorously- conversely, attention to the anti-aligned stimulus produced V4 neuronal responses near baseline, again as though only the anti-aligned stimulus was presented. The conclusion was that attention biases a "competitive" process within the V4 neurons, allowing subjects to select one or the other stimulus for further sensory processing. This paradigm was repeated by multiple research groups (Figure 2.2) in several levels of the visual hierarchy, with verification of the same basic phenomenon in in V2[31, 76], V4[31, 2, 76, 77], and IT[3]. Biologically plausible models for this process were proposed, generally proposing that the synaptic input to the cell under investigation was re-weighted by an unexplained attentional modulation in order to drive the cell to respond to one or another stimulus.

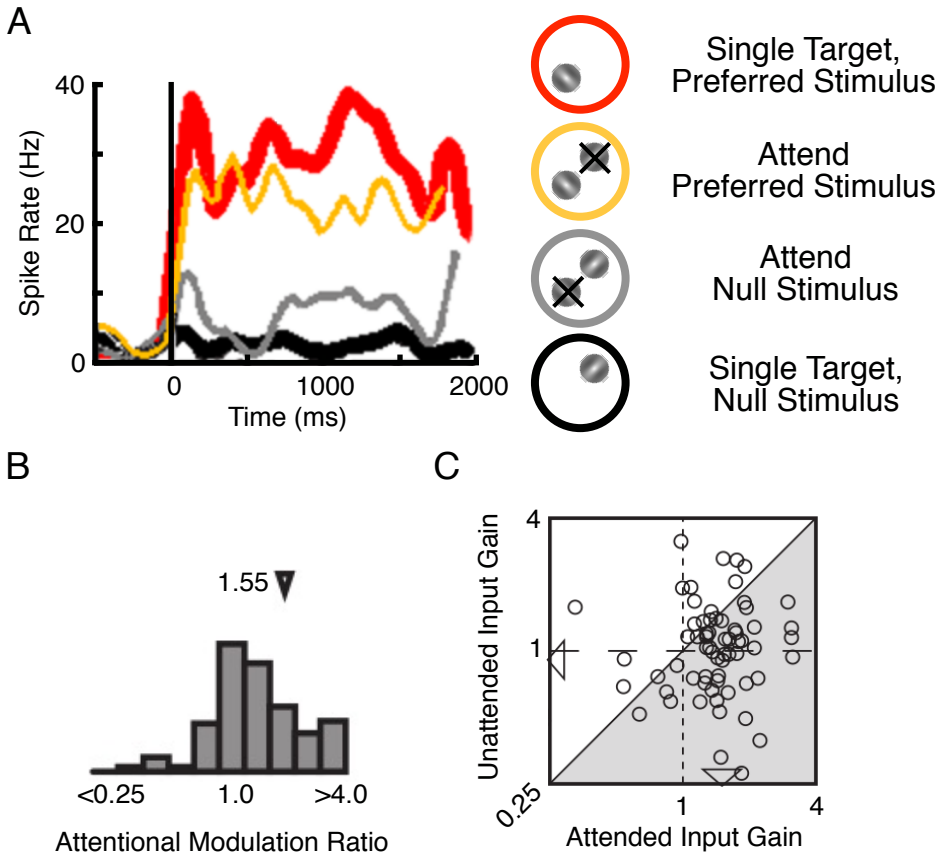

Figure 2.2: **Biased Competition during Visual Attention.** This experiment from Ghose and Maunsell[2] is representative of several studies of attention in the context of competing stimuli[3]. The data presented here are adapted from their report. (A) An example neuron from V4 exhibiting the biased competition phenomenon. When a stimulus aligned with the neurons preferred orientation is shown in isolation, the neuron fires robustly (red). When a non-preferred or null-oriented stimulus is shown, the neuron is unresponsive (black). When both stimuli are shown simultaneously, the neuron fires strongly when attending to the preferred stimulus (orange) and weakly otherwise (gray). (B) A histogram of ratio of V4 cell's firing rates to the preferred versus null stimulus is strongly positively skewed, suggesting that most recording V4 cells behave in the manner of (A). (C) The authors modeled each recorded neuron as a filter that combines independently modulated inputs from the two stimuli. The model suggests that, for most neurons, the input from the attended stimulus is amplified (gain > 1) while the non-attended input is suppressed. Even the non-linear phenomenon of biased competition may be explained by simple gain modulations that are targeted to elsewhere in the brain.

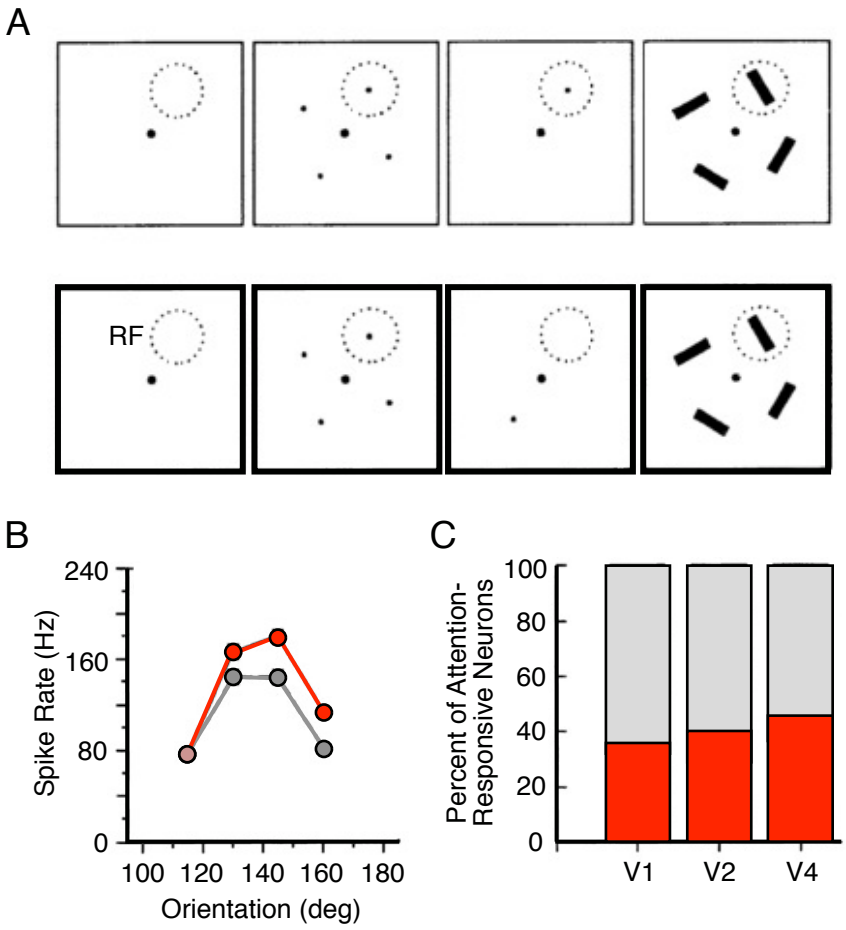

Figure 2.3: **Attentional Modulation to Single Objects.** This experiment from Motter provided direct evidence against the biased competition model[4]. The data presented here are adapted from his report. (A) Subjects fixate on a central point and are cued with dots where four different stimuli will appear on screen (second column) and then cued again as to which of the individual targets the subject should report on. After the cue, an array of bars are presented with only one bar located in the receptive field (RF) of the neuron under study (dashed circle). Subjects must report whether the cued stimulus is tilted left or right. On some trials the cued stimulus is the stimulus in the neuron's RF (top row, attend-in condition), and on other trials it is not (bottom row, attend-out condition). (B) A representative V1 neuron has the same relative orientation tuning curve profile when the animal is attending in (red) or out (gray) of the neuron's RF. However, attention amplifies the entire tuning curve in a multiplicative manner. (C) Not all neurons are modulated in this task- only $\approx 35\%$ of neurons in V1, 40% in V2, and 45% in V4 showed significant attentional modulation at their preferred orientation. Most V4 neurons required a dense stimulus with multiple distractors to show strong modulations, even though these multiple distractors were all outside of the neuron's RF.

If attention can alter the inputs to a cell at a synaptic level, then one would expect that attention might radically alter the receptive field properties of individual neurons. Further study would prove that this is not the case. A straightforward example is adapted in Figure 2.3[4]. In this experiment, bars are presented in four peripheral locations, and the animal is trained to make a judgment about the orientation (left- vs right-leaning) of only the bar in one cued location. Across multiple visual areas, attention to the single bar increased the responses of recorded neurons. Moreover, the observed response increases were of the most simple type: attention simply multiplied the output of the neuron by a constant amount. These gain-like modulations were observed in multiple other studies[78, 79], with the clear implication that attention did not fundamentally alter the receptive field structure of the neuron under study, but simply made the neuron globally more active. The receptive field location, preferred orientation, and other tuning curve features of the neuron to various visual stimuli remain constant with a linear response multiplication. Such simple response transformations could not easily account for the complex and non-linear changes observed in the biased competition studies.

A parsimonious solution to these seemingly distinct attentional effects has been proposed. Careful modeling of V4 neural responses under a biased-competition paradigm revealed that the best explanation for the nonlinear attentional responses is that a simple, gain-modulation is targeted not to the V4 neuron under investigation but rather to neural populations in earlier visual areas that individually encode the two stimuli and provide input to the downstream V4 neuron[2, 80]. Thus, a gain-model can explain both linear responses to single stimuli and non-linear responses to composite stimuli, *provided that the gain modulations are provided only to an appropriate sub-population of visual neurons.* Gain modulations are not applied uniformly throughout the visual cortex but rather appear to be targeted to the neurons that best discriminate between the attended and non-attended stimuli.

Non-linear attentional modulations of even greater complexity have been uncovered by the use of dense multi-electrode recording arrays that can obtain activity from many neurons simultaneously during an attention task. When measured in area V4, these multicellular recordings verify that gain modulations are appropriately targeted to neurons that respond to the attended stimulus, but it appears that these gain modulations are not fully sufficient to explain the behavioral benefits of attention[81]. The majority of the animal's task improvement instead appears to be due to the fact that attention causes activity across the population of neurons to be less correlated- this reduces the tendency of the neural population to transmit noise signals and improves the throughput of visual information. However, the reduction in noise correlation between two neurons is strongly correlated to the gain modulation experienced by the neural pair, suggesting that both gain modulations and reduced noise correlations reflect a common attentional modulation that is again targeted to the most task-appropriate neurons. Cohen et

al. argue that innate normalization circuitry[82, 83] within V4 may translate the common attentional gain modulation into a reduction in noise correlations. Therefore, it is not necessary to discard the targeted-gain model of attention in light of these observations, but rather one must remember that gain modulations are merely a simply-measured reflection of a more complicated attentional process that is none-the-less targeted to the neurons recorded in these tasks.

Superficially, these studies suggest that attentional signals and visual signals within a task are strongly correlated. This invites a simple but appealing model of attention wherein, during a given task, attentional modulations are directed to the neurons that are most optimal for detecting the attended stimulus. Here, "optimal" is defined as having a tuning preference toward the attended stimulus such that the neuron responds strongly to the stimulus even in a non-attentive baseline state. However, the nature of both electrophysiologic recordings and of the canonical gain-like modulation itself leave considerable room to doubt this conjecture.

Consider first the nature of electrophysiology experimentation. In both acute and chronic recordings, a small number of neurons is stochastically selected for analysis by inserting electrodes into the brain. One obtains data only from the neurons whose active processes happen by chance to be near the recording electrode surface. The experimenter then measures the neuron(s) tuning curve(s), and chooses a stimulus set that is optimally designed to stimulate the neuron under investigation for further study. It is inherently difficult to generalize from the activity of this single neuron under such optimal task conditions to explain the activity of the hundreds of millions of other neurons which must operate under non-optimal conditions during normal daily living. One might assume the unsampled neurons behave similarly for their own optimal stimuli, but their contributions to the current task are unknown. There is even greater challenge in observing population-level effects of attention, such as the reduced noise correlations described above[81], in the activity of small numbers of neurons.

Moreover, the gain modulation itself, exemplified in the simple equation $A = kA_0$, where k is a gain constant, may arise through several neurobiologically distinct mechanisms. Grossly, one may separate these into two categories. The modulation may act as a relatively diffuse gain that is applied to wide swath of sensory cortex. Neurons that are well matched to the attended stimulus will naturally have a high baseline and thus enjoy a higher gain modulation than neighboring neurons that are less well-matched to the stimulus and thus have a smaller absolute change in firing rate, even though the gains are identical. In tandem with innate normalization processes, even a diffuse gain may give rise to complex emergent non-linear attentional phenomena[81, 83]. This form of attention is simple to implement in a biologic circuit- multiple mechanisms exist that may potentiate synaptic activity and allow the same visual inputs to evoke stronger synaptic outputs[84, 85, 86, 87, 88].

However, this implementation of gain modulations would also be quite easy to confound. The

precision of attention would be limited by the diffuse nature of the modulator. In the extreme, such a mechanism would predict that attention could not be used to distinguish between two stimuli that activate two adjacent neurons, as both neurons would be equally modulated. While such a concept may seem to directly contradict the studies of biased competition performed above, recall that these studies typically present only two stimuli presented on an otherwise blank screen. Even a massively diffuse modulation can still be oriented to exclude one or the other of two stimulus elements 2.4.

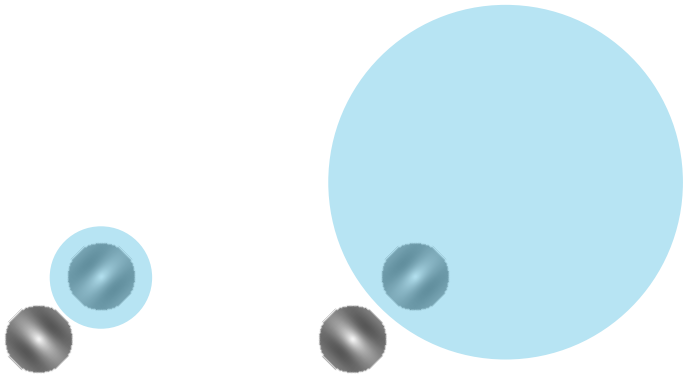

Figure 2.4: **Two-target competition is not evidence for a small spotlight.** The traditional biased-competition stimulus involves two stimuli presented adjacent to one another. An attentional modulation that selected one of the two stimuli (cyan) might be tightly restricted to only one stimulus, or might alternatively be quite diffuse and involve much of the blank background. Both distributions of attention are sufficient to selectively enhance one of the two stimuli and thus perform the task.

A more flexible alternative to this diffuse implementation of gain modulation exists. Instead of a constant modulation, attention may be graded such that the strength of the modulatory input to a neuron is a function of the baseline tuning of the neuron to the attended stimulus. The net effect is identical: stronger modulations are seen in neurons tuned toward the attended stimulus. However, this mechanism would allow for much greater flexibility across a number of different attentional states. For example, attention could be broadcast to neurons diffusely located across a visual area, or attention could be localized very precisely to a small subset of neurons and exclude confounding neighbors. While theoretically appealing, a biologic implementations of this specific targeting model of attention is much more complicated. Some template for the attended stimulus must be generated and propagated to sensory cortex, wherein a comparison operation between the template and the local neural population's tuning preferences occurs. Indeed, a very high burden of proof should be placed upon such a complex alternative.

A crucial difference between diffuse and targeted attentional modulations is the prediction for

what attentional inputs are received by neurons uninvolved in the task. Do attentional modulations spill over into neighboring cells, or are modulations targeted to individual task-appropriate cell groups? Modulatory inputs are difficult to directly measure- it is not sufficient to measure extracellular action potentials as such measurements would not sample a subthreshold modulation that did not reach the axon hillock but would have none-the-less influenced visual activity. Intracellular recordings and local field potentials are thought to sample synaptic membrane potentials and so may be more sensitive to subthreshold modulations, but one is still limited by sampling bias. We propose that functional neuroimaging methods offer a potential solution. Imaging methods sample space without bias, allowing equal sensitivity to task-involved and uninvolved regions of cortex. The signals recorded using imaging methods may also be sensitive to synaptic membrane depolarization (voltage-sensitive dyes)[89], or to activity-related metabolic (flavoprotein)[90] or hemodynamic (intrinsic signal, blood-oxygen level dependent)[91, 92] disturbances in neurons- both sub- and super-threshold modulations are resolvable.

Chapter 3

Selective Targeting: How precise are attentional modulations?

Chapter 2 demonstrated that one may attend to a wide variety of stimuli, but also that steps toward unifying these distinct forms of attention under a common neurological mechanism have been made: simple gain modulations may explain a wide variety of both linear and non-linear effects of attention across variety of visual tasks. It remains unclear, then, what actually distinguishes the current attentional state of the subject. What in the brain changes when attention is shifted between stimuli?

In my thesis, I propose that it is better not to ask, "what changes," but rather, "where do changes occur?" I hypothesize that the selection of an attentional state is synonymous with the selection of a population of sensory neurons to be modulated. In support of this, I will provide evidence that attention supports two very distinct perceptual tasks in a fundamentally similar way: targeting simple gain-like modulations to the most appropriate population of V1 neurons.

3.1 The localization of attentional modulations

The advent of positron emission tomography (PET) and functional magnetic resonance imaging (fMRI) provided direct neuroanatomic methods to address the question of where attention acts within the brain. From the earliest efforts, it became clear that attentional modulations consistently occur within the sensory cortical region associated with the task (Figure 3.1). On a fundamental level, the relationship between PET/BOLD signal modulations and changes in the underlying neural computations is not clear. Differences in the nature and magnitude of attentional modulations observed between human neuroimaging and non-human single-unit

electrophysiology have elicited controversy[93]. Briefly, in simple attention tasks, individual V1 neurons typically show small ($< 10\%$) multiplicative (gain) modulations[4], whereas BOLD modulations in V1 tend to be additive (the same for all stimuli) and large (20-100%)[94]. It is not the case that one or the other of these measurements is fallacious, but rather these two measures are sensitive to distinct components of the attentional modulation. BOLD measurements naturally sample the combined hemodynamic response to activity from millions of neurons per voxel[93]. While it is not clear whether the physiologic processes that couple neural activity to the changes in blood flow are more directly correlated with dendritic membrane potential changes[95] or with synaptic spiking activity[96], it should be expected the combined activity of so many neurons should be sensitive to even small attentional modulations[93][1] . Similarly, one should not be concerned that the signal is additive at the BOLD level, as it is possible that the sustained attentional modulation has an additive metabolic cost even if its downstream effect on unit spiking is multiplicative.

Given this understanding that the BOLD signal may not directly mirror but may be none-the-less reflective of single-unit physiology, there is reason to suspect that imaging techniques may be the better tool to determine where attention acts within the brain. BOLD imaging will have greater sensitivity to subthreshold modulations which may not affect spike rates but none-the-less have a real metabolic cost. Indeed, a local field potential study in V1 found that attention effected changes in the current source density of V1 intracolumnar signaling even in the absence of spike-rate changes[70], demonstrating that subthreshold attentional modulations are not simply a metabolic artifact but rather a real electrophysiologic phenomenon. Moreover, when one studies attention with invasive recordings, one's measurement is inherently biased to a small region of cortical space near the electrode contact(s). It is not guaranteed that even a series of recordings will sufficiently sample all possible tuning functions, and so it is difficult to demonstrate a specificity of modulations as a function of the identify of the neurons under investigation. In contrast, neuroimaging techniques may sample an entire region of visual cortex in an unbiased manner. Because imaging is sensitive to subthreshold modulations and because all available population tuning functions are simultaneously sampled in each trial, neuroimaging provides an optimal method to localize attentional modulations across the cortical surface.

3.2 Mapping attention at a mesoscopic scale

A major disadvantage of metabolic or hemodynamic neuroimaging techniques is that spatial resolution is sacrificed in exchange for the ability to image a greater spatial extent of cerebral

[1] This discussion does not include the concern that attention may interact with the BOLD signal without changing neural activity at all, by altering the relationship between neural activity and blood flow[97].

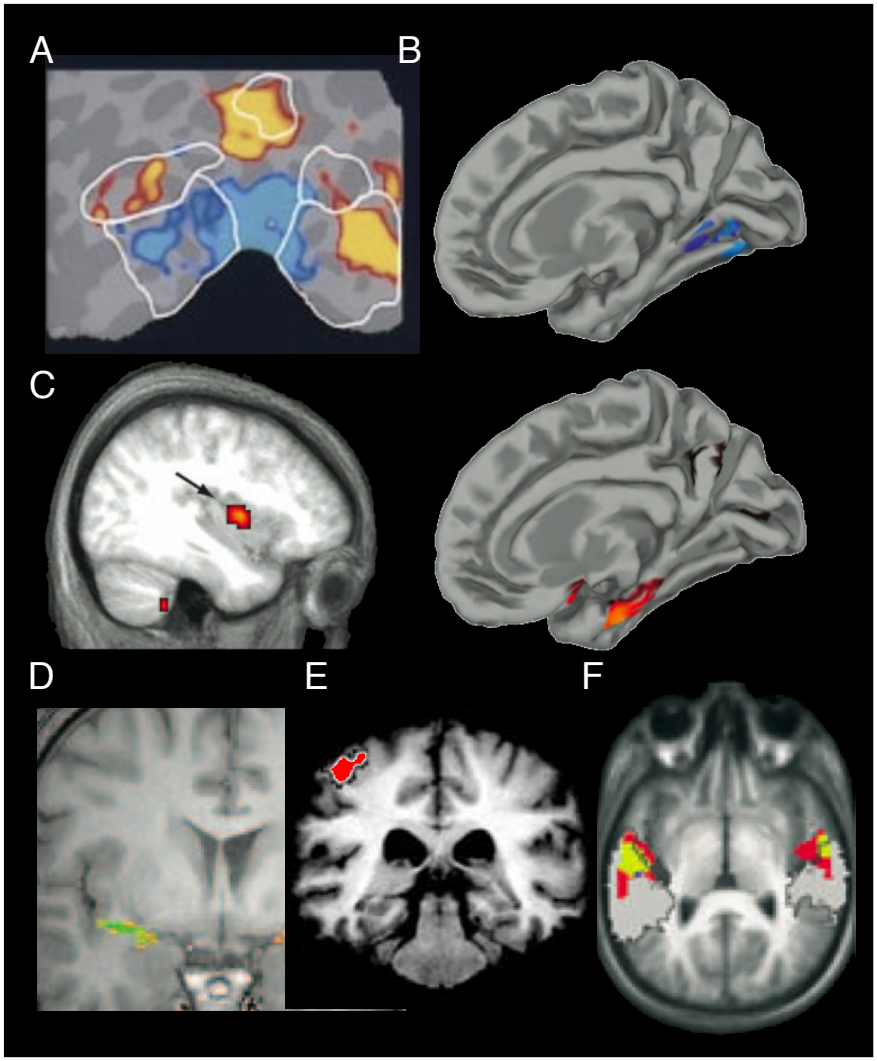

Figure 3.1: **Attentional Modulation of Sensory Cortex** (A) Spatial attention to a visual quadrant activates quadrant-specific representations in early visual cortex[5]. (B) Attention to faces modulates magnetoencephalographic activity from the fusiform face area (blue), while attention to houses modulates the parahippocampal place area (red)[6]. (C) Subjects performing a taste discrimination task (versus passive tasting) show increased BOLD activity in the insular gustatory cortex[7]. (D) Discriminative (versus passive) olfaction similarly modulates primary olfactory cortex[8]. (E) Attention to mechanical stimulation modulates primary somatosensory cortex[9]. (F) Primary auditory cortical voxels shown in red are recruited only when actively attending to sounds [10].

cortex. Single-unit recordings provide enormous insight into the functional properties of individual neurons, commonly considered the smallest computational units in the brain. While under certain circumstances the modulation of individual neurons may be perceptually important[98], it is more common to think of visual processing as occurring within computational units of interconnected neurons with similar functional tuning properties. Because these units span all six layers of neocortex, they are referred to as cortical columns and have been found throughout the cortex[99, 71, 100, 101]. The column is not defined anatomically but rather functionally, and the size of these columns varies by their functional definition. Because of this functional grouping, our efforts to measure where attentional modulations occur within the visual system (as always, on a given task) may not require the resolution of single neurons or even local multiunits. Provided that our imaging studies resolve or infer activity at or beyond the resolution of the cortical columns employed in solving our task, we assume that to a first approximation our studies will have an appropriately mesoscopic resolution to ascertain which functional units are modulated by attention.

A major limitation is that we must choose a stimulus set for which the underlying brain response patterns are relatively well-understood and verifiable. The most likely candidates are stimuli that either follow a known mapping within the brain (e.g. tonotopy, somatotopy, or retinotopy), or that exhibit a known or suspected columnar organization (e.g. direction tuning in 7a[102], object tuning in IT[100], or orientation tuning in V1[99]). Stimuli with more sparse cortical representations are not exempt from this model of attention, but rather are less likely to provide a robust and repeatable measurement of the cortex's response to the attended stimuli and are not suitable for our studies.

For many visual tasks, particularly those involving higher-level visual features, the underlying columnar scale (if any exists) is not known and therefore it is unclear how spatially precise imaging needs to be. While one may infer population-level tuning properties to individual high-level stimuli such as faces[15], the failure to observe such tuning and/or a corresponding attentional modulation can not be interpreted as an absence of attentional modulations. This is because a negative result could simply be due to the poor resolving power of the technique being used. For this reason, we limit our localization attempts to attentional tasks involving stimuli for which the functional distribution of relevant neural signals is well-understood and for which an appropriate mesoscopic resolution can be obtained or inferred with established neuroimaging techniques.

Here we focus on two orthogonal attention tasks both targeting V1 neural populations: attention to one orientation (over all spatial locations), and attention to restricted spatial locations (including stimuli of all orientations). Orientation columns in human V1 have been very precisely measured using in-plane ultra-high resolution fMRI, and are known to have a width of

$\approx$ 0.80 mm with a spatial periodicity of $\approx$1.6 mm[103]. While 0.8 mm resolution BOLD fMRI at ultra high field strength (7 Tesla) is rapidly developing, the signal-to-noise ratio of these images is typically poor [personal communication]. Rather, most studies image V1 at lower field (3 T) and lower resolution (2-3 mm)[15, 104, 105], where it is well established that neural activity from orientation columns is not resolvable within individual voxels. The point spread function of conventional 3 Tesla fMRI is approximately 3.5 mm[59]. A simple ratio of the column area to the voxel's 2D area along the cortical surface suggests that 20 or more orientation columns may influence a single voxel. Averaging the tuning of so many columns is expected to yield a population with minimal overall orientation tuning.

In spite of the poor column-to-voxel ratio, it is possible at low resolution to resolve whole-region differences in activity when viewing e.g. two different orientations[104], and these whole-region patterns are modulated by attention[106], the visual system does not utilize such patterns. Quite the opposite, it appears that information is encoded sparsely even at the level of V4. For example, a during a shape-in-noise detection task V4 neurons were found to encode information independently[107], and neurons that better represented the shape contributed disproportionately to the observer's behavior[108]. Rather than utilizing coarse, areal activity patterns, it rather appears that the brain utilizes the highest possible resolution for information processing-that of the single neuron. Single-cell imaging may in fact be necessary for areas such as IT, which have demonstrated little columnar structure for some stimulus sets[109], and heroic efforts toward two-photon calcium imaging of single cells in the awake monkey have been made[110]. By targeting our studies toward V1, we may utilize its known columnar and topological structure to establish a floor to the necessary imaging resolution, permitting us to utilize well-established techniques.

Advances in high-resolution imaging have delivered sufficient resolution in both the human and non-human systems. Ultra-high field fMRI (at 7 Tesla) provides an order of magnitude greater spatial resolution. For example, the same ratios within a 1.5 mm ultra-high field voxel suggest that as few as five orientation columns may be within each voxel. As this voxel averages tuning from fewer distinct orientations, we would expect the overall population within each voxel to have a measurable orientation preference. While this level of precision may be superficially unimpressive, it is sufficient in both theory[59] and practice[29] to observe neural tuning functions within individual voxels.

While the gross retinotopic map across the entirety of V1 is easily resolved with even conventional techniques[111], our second experiment will explore whether attentional modulations may be targeted to very small regions of V1, where "small" refers to the spatial extend of individual V1 neuronal receptive fields. On the basis of known electrophysiology, we expect this small range of the visual field to correspond to a $\approx$ 1 mm diameter extents of macaque V1[35]. As this

corresponds to only 1 or 2 voxels within even a high resolution fMRI data set, studying modulations at this scale is beyond the reach of current human neuroimaging techniques. However, we may in this case exploit the convenient anatomy of primary visual cortex in the macaque. V1 is a surface structure, and it may be readily observed using optical imaging techniques after the brain is exposed with only a simple craniotomy and durotomy[112, 58]. Were we limited only by optics, a resolution of ≈ 20 μm/pixel is readily attained with conventional lenses.

The optical signal we will explore derives from the autofluorescence of mitochondrial flavoproteins. The origin and response function of this proxy signal for neural activity have been extensively reported[90, 113]. Briefly, synaptic activity is metabolically demanding[114], and as neural activity increases the mitochondria correspondingly increase ATP production via the electron transport chain (ETC). Increased ETC throughput increases the proportion of oxidized flavoproteins, which naturally fluoresce (excitation: 420-490 nm, emission: ¿500 nm[90]). Thus the relative amplitude of fluorescence within this spectrum serves as a direct marker of local metabolic output, which itself tracks neural activity. However, with regard to localizing activity in the brain, it is unlikely that this metabolic signal will retain cellular precision. Mitochondria are located within synapses[115], providing a source of metabolic signal throughout a single neuron's axonal arbor. Activity at even a single synapse will also, for example, recruit nearby astrocytes participating in neurotransmitter reuptake[116]. Multiplied over all synapses, with even the activation of one cell a diffuse metabolic signal is to be expected.

AF images have provided clear maps of retinotopic, ocular dominance, and orientation tuning in V1[113], and so it is clear that the resolution is available, at worse, on the order of the size of a V1 orientation column. However, such images typically are acquired from anesthetized animals; images from the awake monkey performing a simple fixation task suggest that the point spread function may be large- up to 2mm in diameter[112]. To our knowledge, this is the first effort to image attentional modulations of flavoprotein activity in the awake monkey. It was unclear what even the basic features of these attention modulations might be, but none-the-less we determined that this non-hemodynamic, high-resolution technique provided the best possible option to measure attentional modulations within V1 of the awake animal with unprecedented resolution.

3.3 A general paradigm for attentional selectivity studies

Having established that both tuning to both orientation and to fine-scale retinotopy may be resolved with our available neuroimaging techniques, our experiments follow a similar framework to ask whether attention to an orientation (Chapter 4) or to a restricted region of space (Chapter 5) generates attentional modulations that are (A) specifically observed within the known

subpopulation of V1 that is tuned toward the attended stimulus, or (B) non-specifically to a larger extent of V1.

We have developed a general framework to measure the specificity of attentional modulations. Briefly, we select a set of stimuli that evoke differential neural responses patterns within V1, and we measure these patterns utilizing high resolution imaging methods. These will be stimuli of different orientations, activating distinct sets of orientation columns (Chapter 4), or stimuli at different monitor locations, activating distinct regions of the V1 retinotopic map (Chapter 5). We then, under the same task context and measurement conditions, cue subjects to attend to one or another of the mapped stimuli. We recover a pattern of attentional modulations evoked by this cue, and we test for a relationship between the activity patterns of the attentional modulation and of the underlying neural tuning functions. The strength of this relationship provides a measurement, to the precision of our imaging techniques, as to how precisely these attentional modulations are targeted to the most well-tuned neural populations within the brain for a given task.

Chapter 4

Functional Magnetic Resonance Imaging of Attentional Modulations at the Near-Columnar Scale

At higher magnetic fields, the hemodynamic signals recovered by BOLD fMRI are increasingly sensitive to signals from smaller venules which drain blood from more localized regions of cortex[117]. Leveraging this basic phenomenon, MRI physicists have developed the capability to recover, at ultra-high magnetic field, functional activity from visual cortex with 0.9-1.5 orders of magnitude greater precision than may be derived from conventional fMRI (0.8-1.5 mm isometric voxels versus conventional 3 mm isometric voxels)[118, 119]. While this increase in spatial precision does not yet deliver true resolution of the activity from individual cortical columns, it is close enough to permit the extrapolation of columnar circuitry from individual voxels.

Using this technology, we measured orientation tuning curves from V1 of human volunteers while simultaneously cuing the subjects to attend to one orientation. We found that this attentional cue resulted in the direct facilitation of orientation-tuned responses from individual V1 voxels that had an orientation preference aligned toward the cue independent of the location of these voxels within the V1 retinotopic map. This result suggests that attention is in fact selectively targeted to individual neural subpopulations as a function of their ability to encode the attended stimulus.

4.1 Introduction

A defining feature of visual attention is its flexibility. Subjects may selectively attend to locations, objects, periods of time and visual features to enhance their perceptual capabilities[120, 121, 122, 46]. Of these, the selection according to location (spatial attention) is the most studied. Numerous studies have demonstrated that when subjects covertly attend to a location, the sensory responses of neurons representing this location are enhanced throughout the visual hierarchy[123, 78].

Studies of single neurons in monkey visual cortex suggest that non-spatial attention is similarly targeted, such that attention preferentially enhances neurons selective for an attended feature[124] and attentional modulations are strongest during times that the animal is maximally focused[28]. These attentional modulations may be divided into two broad categories: linear, gain-like increases in a neural firing[125]; and more complex non-linear modulations. While a variety of non-linear effects have been reported[126, 81, 83], similar gain modulations have been observed in spatial[78, 2] and featural[127] attention studies. Moreover, computational modeling suggests that some non-linear effects may actually arise from simple gain processes[80].

These findings lead us to hypothesize the existence of a single common mechanism for visual attention: while attending to a stimulus, simple but computationally powerful[85] gain modulations are targeted to the neurons and times most appropriate for the task at hand. Testing this theory requires the ability to systematically map the representation of a visual feature representation across an entire visual area to first identify the neural subpopulation best matched to the task and then measure how responses within that subpopulation change with attention and over time. To this end, the encoding of stimulus orientation within primary visual cortex (V1) is ideal. Within V1, a single cortical column contains neurons tuned towards a common orientation[63], and recently developed functional magnetic resonance imaging (fMRI) techniques are capable of measuring orientation tuning at columnar resolutions[103]. Moreover, orientation tuning can be observed even in voxels, which are larger than a cortical column[128]. Such tuning offers an opportunity, for the first time, to map a non-spatial visual representation within a single cortical area and to study how that map is dynamically changed with attention.

To address how representations of visual information are altered by non-spatial attention, we therefore imaged V1 using ultra-high field fMRI (7 T) while subjects performed a periodic non-spatial attention task[128, 101]. We discovered that both orientation tuning and attentional modulations of that tuning, are present within individual voxels. Both the orientation preferences and the response timing of voxels systematically shift towards the featural and temporal foci of attention. These shifts can be explained by a model in which featural and temporal attention cause linear changes in activity preferentially directed during behaviorally appropriate times to neurons with appropriate feature selectively. Our results suggest that representations

at the earliest stages of visual processing can be profoundly altered by cognitive influences and that all forms of attention may act by common mechanisms to selectively enhance behaviorally relevant sensory representations throughout cerebral cortex.

4.2 Results

4.2.1 Attention biases single-voxel orientation tuning

Human subjects (n = 9, 7 male) participated in a visual change-detection task. Over a 5 min trial, subjects viewed a continuously rotating (20 s period, 15 rotations per trial), full field, counter-phasing Gabor grating and quickly responded by button press when the spatial frequency (SF) of the stimulus briefly (50-83ms) doubled (Figure 4.1A) This task was demanding (60% hit/17% false alarm rate), and required the subjects' continuous vigilance. To manipulate attention, there was a non-uniform probability of SF changes occurring; subjects were cued prior to each trial to the range of orientations at which changes were most likely. Two types of attention trials were presented: one in which changes were more likely around 45° (Attend 45° (A45)) and the other at 135° (Attend 135° (A135)). Subjects responded quickly to expected SF changes and suffered a small but significant penalty in reaction time to unexpected SF changes (Figure 4.1C, 15-22 ms, Rayleigh test, $P<0.01$). The range of orientations associated with quick reaction times (95°, Figure 4.1C) was nearly identical to the range of orientations at which changes were most likely (87°). However, during a control condition in which change probability was constant over all orientations (No-Cue), subjects were uniformly quick to identify the changes with no behavioral bias in favor of one orientation. The uniformly fast No-Cue reaction times suggest that our attentional manipulation behaviorally encouraged subjects to ignore the stimulus during periods when the SF change was unlikely. During an alternative control in which the stimulus was fixed to vertical and did not rotate but change probabilities still varied (No-Rotate), subjects still showed the penalty towards unexpected changes (21 ms). We concluded that subjects selectively attended to the stimulus when changes were likely, although with an anticipatory advance between peak attentional effect and peak stimulus probability.

To study how such selective attention altered representations in early visual cortex, we obtained ultra-high field, high resolution blood-oxygen level dependent (BOLD) functional images from a large volume of occipital cortex (7 T, GE sequence, 690-1,050 cm^3 image volume, $1.5 \times 1.5 \times 1.5$ mm voxel size and TE/TR 20/1,500 ms), while subjects performed the task. We discarded data from one subject due to substantial motion artifacts. For the remaining eight subjects, we explored response tuning for individual voxels within a V1 region-of-interest (ROI) that was defined on the basis of anatomy and retinotopy. During all trials, the stimulus rotated at the same constant rate (Fig. 4.1A). Thus, for orientation-selective voxels, we would expect

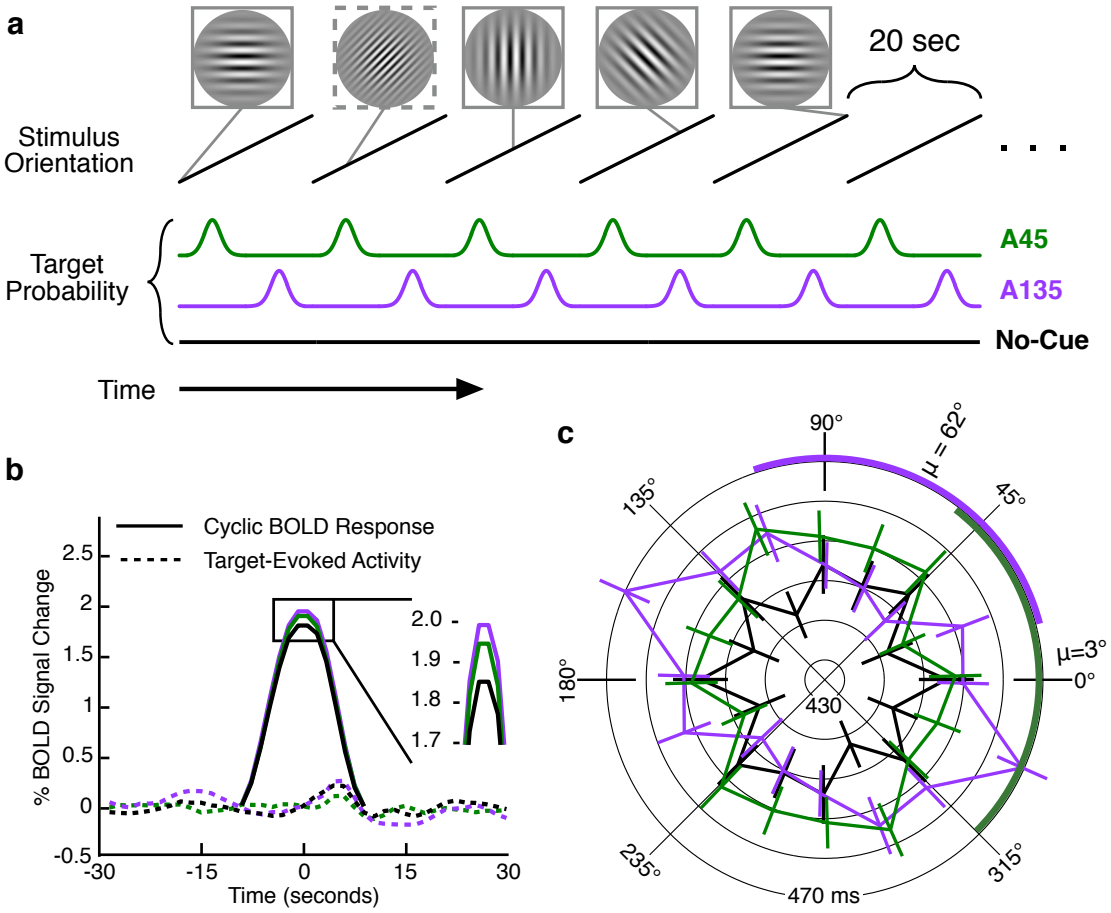

Figure 4.1: **Selective attention in a change-detection task.** (a) Human subjects viewed a full-field, continuously rotating Gabor and responded by button press when the spatial frequency of the stimulus briefly changed (dashed outline). During attention conditions, these target events were more likely to occur at a single orientation (green, A45; violet, A135). Prior to each trial, a static grating indicated to the subject the orientation about which targets are likely to occur. In one control condition, the target probability is static over time (No-Cue, black). (b) Mean event related response to stimulus rotation (aligned to preferred phase, solid) and to target events (dashed, aligned to individual target events per condition) averaged across all voxels with significant orientation selectivity. The response to individual target events was negligible, but removed via linear regression in all future analyses. The mean global response increased with attention. (c) Reaction time, indicated by radius, is fastest prior to the cued orientation when subjects anticipate target events. μ, orientation with the fastest mean response during each Attend condition; colored arc, full-width at half-maximum (FWHM) range of fastest reaction times (A45 FWHM 98° and A135 FWHM 92°).

that the BOLD response would show modulations over time at this frequency[103]. The phase of such modulation could reflect the preferred orientation of the voxel, while the amplitude would reflect its orientation selectivity. Alternatively, a voxel with a 20 s periodic response could also be temporally selective and show activity during a specific time point in the stimulus cycle without any orientation-specific visual processing. Thus the peak of a voxel's cyclic response could correspond to a preferred orientation or to a preferred time; we will use the term 'preferred phase' to avoid the assumption that all cyclic activity is necessarily orientation selective. A major goal of our analysis will be to determine the relative contributions of orientation and temporal attention within V1 (see below), but to study such contributions we must first establish that voxels are all modulated according to the orientation/temporal rhythm.

In all runs from all subjects, we observed single voxels with significant tuning to our stimulus as evidenced by BOLD modulation at the orientation frequency. An example voxel is shown in Figure 4.2A. To quantify this selectivity, we computed the likelihood that each voxel's maximum and minimum BOLD activity could be used to distinguish between the voxel's preferred and anti-preferred stimulus phase. This is analogous to a classical decoding framework, only adapted for our continuous paradigm (see Methods). We found that a substantial proportion of individual voxels could distinguish between orthogonal orientations with >95% accuracy (Figure 4.2B). This is in sharp contrast to most fMRI studies of human V1[104, 106], which have been unable to find individual voxels with significant decoding performance. Moreover, the performance of many individual voxels in our sample exceeds the overall performance reported in previous studies ($\approx 70\%$) when thousands of V1 voxels were analyzed together.

A notable exception exists for studies utilizing ultra-high resolution over a restricted volume of V1 (less than and equal to four slices)[103, 128], which have demonstrated orientation-selective responses from single V1 voxels. To enable comparison to these reports, we also computed a coherence coefficient (CC) to estimate the degree to which each voxel is entrained to the stimulus frequency. While Sun et al.[128] reported 35.3% of voxels were significantly coherent with the stimulus, we only found such coherence in 15.6% of voxels at baseline (Figure 4.2C). Thus, while our imaging parameters allowed for the greatest sensitivity to orientation tuning that has yet been reported for high-volume imaging using isometric voxels, these parameters did not afford a functional resolution equal to that of dedicated ultra-high resolution/low-volume methodologies.

To restrict the remainder of our analyses to voxels that exhibited a significant degree of tuning, we utilized regression analysis to make a binary decision, for each voxel, as to whether its response was significantly entrained by the stimulus. In comparison to the coherence analysis above, this regression analysis was performed without detrending or other manipulation of the frequency content within each voxel. Across all subjects, we found that 14.3% of voxels exhibited such significant tuning (regression F-test, restricted to 5% false positives) during No-Cue

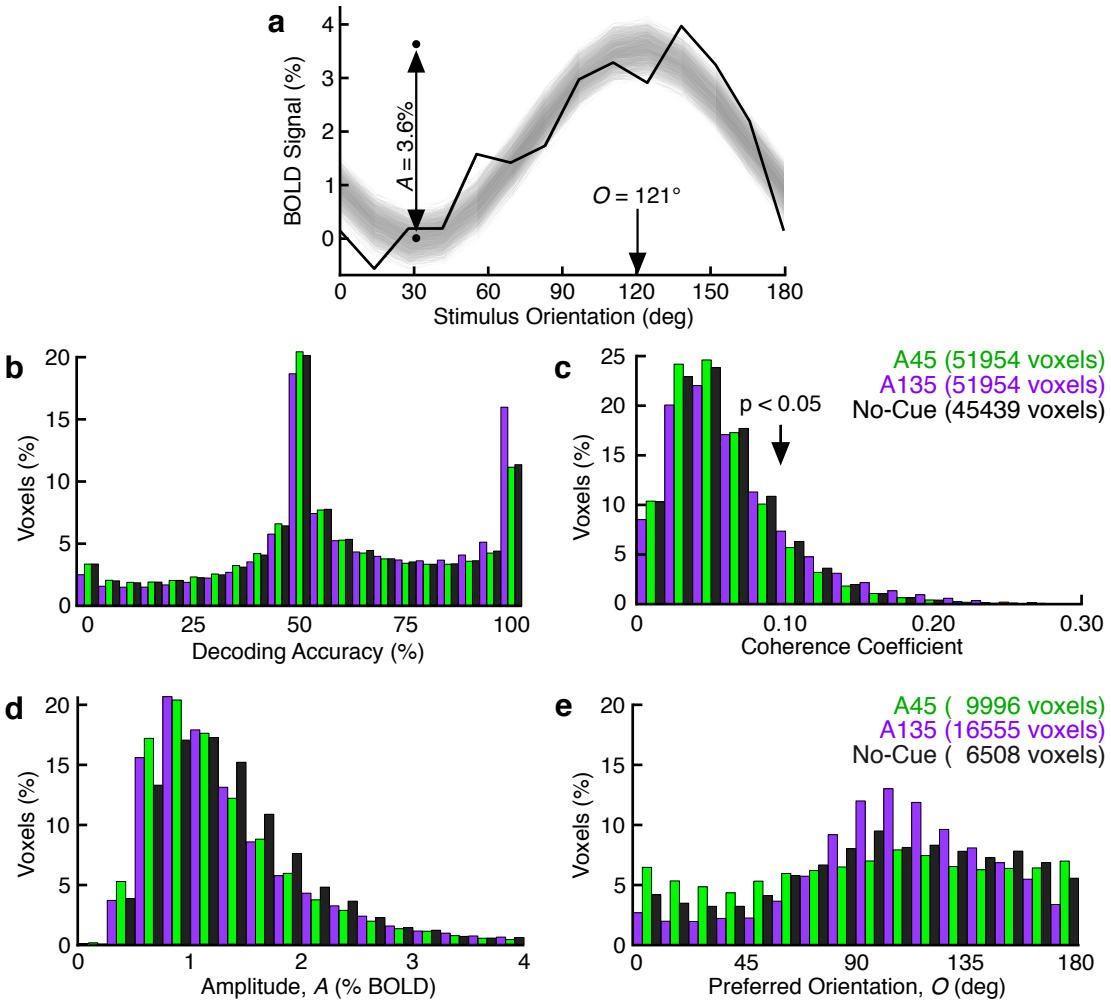

Figure 4.2: **Orientation-selectivity in single V1 voxels.** (a) Fourier and regression analysis (see Methods) provides the amplitude (A) and peak (O) of each voxel's orientation tuning curve. Peaks are offset to account for the hemodynamic lag between stimulus presentation and BOLD response. Shaded region shows a confidence interval of the fitted sine wave for this example voxel. Orientation-selectivity metrics for this voxel: coherence coefficient=0.2131 (P=1.7×10^{-5}), decoding accuracy ≈100%. (b) Many individual voxels accurately discriminate between their preferred and anti-preferred orientations (mode at 50% represents chance performance). (c) Many voxels have significant coherence at the signal frequency. Coherence coefficient of 0.0984 (arrow) is the threshold for statistical significance. (b,c) include all V1 voxels. (d) Among orientation-selective voxels, attention recruited weakly orientation-selective voxels. (e) Among orientation-selective voxels, the distribution of preferred orientations is biased towards the attended orientation.

conditions (Figure 4.3A).

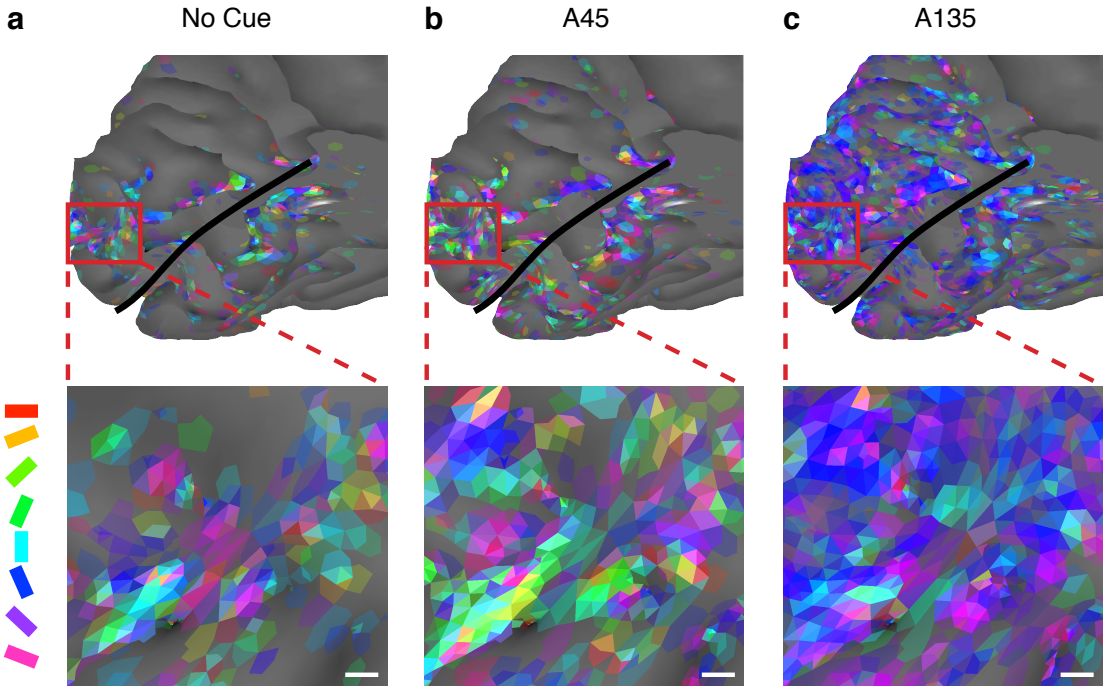

Figure 4.3: **Attention biases the orientation preference map.** (a) Preferred orientation from one subject, coded by color and measured during No-Cue task, plotted on a medial view of occipital cortex. Inset is a flattened representation of the occipital pole. Greater color saturation indicates a higher certainty in preference estimate. Orientation selectivity was greatest along gyri, likely due to the use of a surface coil. (white scale bar, 2 mm; black line, calcarine sulcus). (b,c) As a, with orientation preference measured during the attention conditions. Attention increased the extent of orientation-selective activity across the occipital cortex (top) and biased population orientation preferences at the hyper-columnar scale (bottom).

We then repeated these analyses for our Attend trials. We found that attention to a cued orientation increased the median decoding accuracy and CC among all V1 voxels, as well as the prevalence of selective voxels in all subjects: 19.2% (A45, Figure 4.3B) to 31.9% (A135, Figure 4.3C) of voxels collected during attend conditions were significantly correlated to the stimulus. This recruitment is consistent with known neurophysiology: attention to one orientation causes orientation tuning to emerge in otherwise non-orientation-selective neurons in V4[78], and an attention-mediated increase in activity should cause weakly selective voxels to show a more robust and detectable modulation. The stronger attentional effects of the A135 condition, as compared with the A45 condition, likely reflect the predominance of vertically tuned voxels in our sample (Figure 4.2C) and the behavioral (Figure 4.1C) evidence, suggesting that subjects

anticipated likely changes and accordingly increased their attention prematurely (that is, during the presentation of vertical lines during the A135 condition).

Attention increased the mean amplitude of cyclic activity across V1/V2 (Figure 4.1B), though increases in the number of both low- and high-amplitude voxels are observed (tails of the distribution in Figure 4.2D). In addition to increasing stimulus selectivity, attention powerfully biased voxels' baseline (No-Cue) phase preferences. The distribution of phase preferences spanned the entire range of orientations, but was non-uniform in all conditions. During the No-Cue condition we saw an innate bias towards post-vertical phases (90°-135°), whereas preferred phases were biased from the No-Cue distribution towards the cue during the Attend conditions (Figures 4.2E and 4.3). Thus attention both increased phase selectivity and shifted phase preferences towards the cued orientation. If these were the only task-related changes occurring within the brain, we would expect that such changes would decrease subjects' reaction times, as information about the stimulus is accumulated faster. We, however, observed the opposite: the cue instead increased average reaction times across all stimuli (Figure 4.1C). This suggests that task-related nonspecific changes, such as motor preparation or vigilance, which are likely to present in numerous areas other than V1, significantly contributed to the overall behavior.

Such non-specific behavior effects open up the possibility that V1 changes might simply reflect overall task parameters, rather than task-related changes in stimulus representation associated with attention. To examine whether such changes in BOLD response phase may occur irrespective of the actual stimulus presented, we applied identical analysis techniques for data from No-Rotate trials. During this condition, only 0.5% of voxels were cyclically active and no single voxel cycled during two different scans. Thus the temporal pattern of SF changes was not sufficient to evoke V1 activity; the cyclic activity we observed is a result of cyclic visual stimulation. Moreover, cyclic changes in BOLD response cannot be explained by the biased distribution of SF changes, because such changes failed to evoke a measurable BOLD response (Figure 4.1B) and would therefore be unable to skew the BOLD signal at the paradigm's fundamental frequency. Thus the observed changes in orientation tuning were due to a top-down modulation of innate orientation-selective responses in V1 and do not reflect differences in stimulation between the attention runs.

Because we observed voxels with tuning preferences across the entire 180° range for all three conditions, we could examine whether attention modulations were selectively directed to neural populations appropriate to the particular attention condition. We first identified those voxels which had significant phase selectivity during both the No-Cue and attention conditions (voxels that 'Stay-On' with attention, $n = 7,969$). During attention trials, Stay-On voxels on average reached peak activity earlier, such that they either had a more clock-wise preferred orientation (5.40°) or had a more rapid hemodynamic response (0.60 s, Upton's angular mean test, n =

7,969, P$< 10^{-10}$). However, this tuning advance was a function of voxel phase preference: when a single orientation was cued, the response of voxels with a preference at or after the cue was shifted towards the cue (Figure 4.4A,B). As expected, the cue-selectivity of attention effects was largely orthogonal between the A45 and A135 conditions (as was observed with subject reaction times). By directly comparing voxels that were selective during both attention conditions (Figure 4.4C), we found that 36.3% of voxels had a significant difference in orientation preference (likelihood estimation, 356-716 Degree of Freedom (DOF), $q_{FDR} < 0.01$).

We also explored the effect of attention on the amplitude of single-voxel tuning curves. Across all voxels, the cue increased tuning amplitude by 0.0340.015% BOLD (95% confidence interval, t-test, 7,968 DOF, P=0.041). This increase was less robust and only reached significance in 14.7% (likelihood estimation, 356-716 DOF, $q_{FDR} < 0.01$) of Stay-On voxels (Figure 4.4D) But, as with phase preference, these effects were selective and depended on preferred phase: attention to a cue increased the response amplitude of voxels whose preference aligned with the period of maximal behavior effect (before the cue).

Because our task utilized a full-field stimulus, subjects should gain no benefit from applying spatial attentional strategies. However, because spatial attention was not explicitly controlled, it is possible that subjects focused their attention spatially and that focus differed between our A45 and A135 conditions. If this were true, one would expect attentional modulations would vary significantly across the visual field and differentially between the two attention conditions. We therefore examined whether phase preferences of individual voxels, and attentional modulation of those preferences, varied according to retinotopic position. Consistent with previous reports[105], we found a significant correlation between preferred phase and retinotopic polar angle (angle-angle correlation, r^2: 0.07-0.13) at parafoveal eccentricities. However, our attentional effects were uniform across the visual field: retinotopy was uncorrelated with the changes in preference or amplitude seen in our attention trials (regression analysis). This confirmed that the modulations we report were targeted to individual V1 voxels solely as a function of their featural tuning.

4.2.2 Attention linearly increases BOLD activity over all of V1

While these results establish that appropriate neuronal populations in human V1 are preferentially modulated by attention, they do not speak about the nature of this modulation. Numerous imaging and electrophysiological studies suggest that spatial attention has a simple linear effect on responses[125]. In these studies, attention either multiplies ('gain' effect) or increases ('additive' effect) responses across a range of stimulus conditions. In the context of neurons tuned to a particular parameter, such as orientation in early visual areas, the model predicts

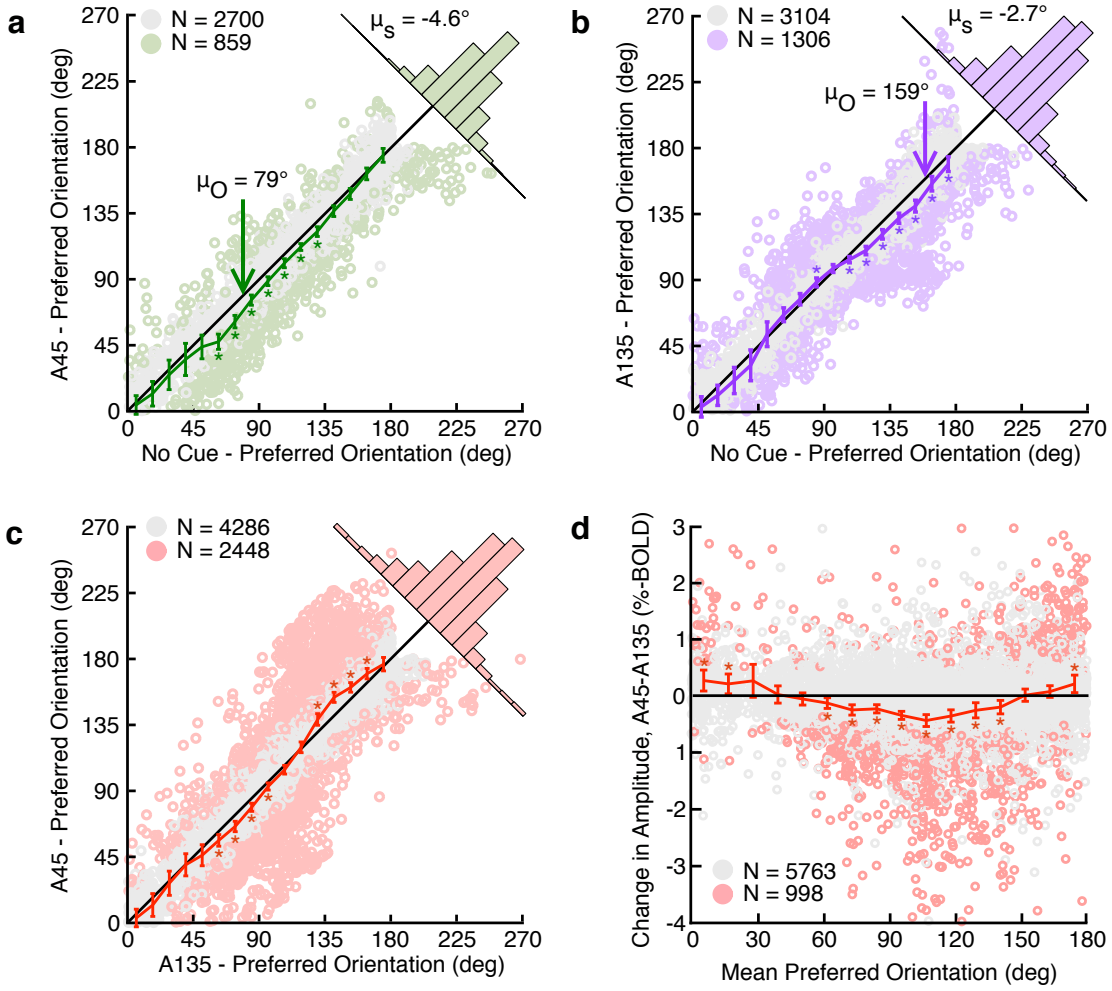

Figure 4.4: **Attention selectively advances and amplifies orientation tuning curves.** (a) Voxels with an orientation preference near 79° respond sooner (have a less positive orientation preference) during A45 condition. Error bars show 99.9% confidence intervals of the mean. Note that 270° is equivalent to 90°. Inset histogram shows distribution of tuning preference shifts as distance from the identity line. (black line, identity line; μ_O, center of range with significant tuning advance; μ_S, mean tuning curve advance over all voxels). Color indicates individual voxels that are at a significant ($q_{FDR} < 0.01$, likelihood estimation) distance from the identity line. (b) As a, showing an orthogonally distributed tuning curve advance during A135. (c) Direct comparison between A45 and A135 conditions reveals a strong and orthogonal relationship between preferred orientation and changes in tuning preference. (d) As c, comparing tuning amplitude between A45 and A135. Amplitude increases for voxels with preference prior to the attended orientation ('*' indicates significant change, von Mises (a-c) or t-test (d), variable DOF, P< 0.001).

that attention will increase orientation tuning curve amplitudes without any changes in preference. When a neuronal population with a variety of preferred orientations is sampled, such as individual voxels in our study, this model permits that the overall orientation tuning of the sampled population may change in preference, in accordance with our observations. However, because previous studies have been unable to reveal and map functional preferences other than retinotopy in the human it has not been possible to examine linear non-spatial attention models in humans. By contrast, our ability to observe significant tuning in a large number of voxels within V1 enables us to systematically compare tuning curves across our attention conditions.

To do this, we first grouped Stay-On voxels according to their preferred orientation relative to the attended orientation, combining A45 and A135 into a single normalized Attend data set. We tested whether a linear model could explain how the mean orientation tuning curves (computed over all voxels, grouped by orientation preference into 13 bins and over all 13 sampled time points) changed with attention (Figure 4.5). Across all orientation preferences and all points of time, a simple linear regression provided a good explanation of the effects of attention on V1 activity. Having demonstrated that orientation tuning curves between two conditions were linearly related, we wanted to further determine whether the effects of attention might also be well-described as linear modulations within the voxels that gained or lost tuning with attention. Thus we repeated this analysis using voxels that only showed significant phase selectivity during the Attend conditions (voxels that 'Turn-On' with attention, n=13,876 across both attention conditions) or only during the No-Cue condition (1Turn-Off', n=5,047). Even in the absence of well-defined single-voxel tuning curves, we found that the average BOLD signals between the Attend and No-Cue conditions were also well-described by a simple linear model (Figure 4.5). Across all voxel groups, we also observed positive linear correlation coefficients between the *single-voxel* tuning curves estimated from No-Cue and Attend data, even when these tuning curves were not significantly tuned (median correlation coefficient: Stay-On 0.72, Turn-On 0.36 and Turn-Off 0.31).

Although our ultimate goal is to determine whether attentional modulations act with specificity over features and time, we used these linear fits both within single voxels and over the entire data set to justify the assumption that any featurally or temporally specific effects should be linear as well. This simplifying assumption enabled us to utilize a two-dimensional model to disambiguate between temporal and featural attentional mechanisms.

4.2.3 Dissociation of featural and temporal attention mechanisms

The possibility that attention is modulated both over time and feature preference presents a potential challenge, because both featural and temporal modulations may enhance neural activity in a subset of voxels. Moreover, our periodic stimulus naturally confounds orientation

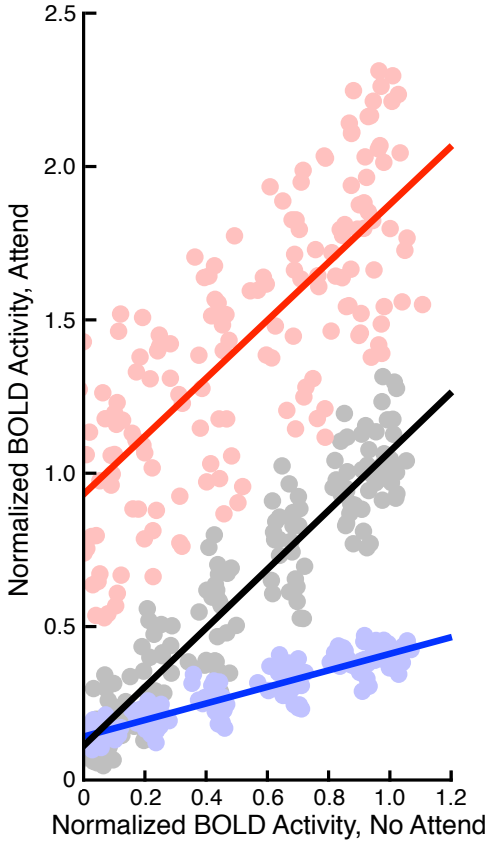

Figure 4.5: **Attentional modulations are linear over V1.** Normalized activity (see Methods) during No-Cue and Attend conditions is highly similar in Stay-On voxels (gray). Each point represents the mean normalized activity of all voxels with a set range of phase preferences over a single sample interval; preference and time are sampled to 13 points each, providing 169 data points. The effect of attention over all points is well-described by a linear fit ($R^2 = 0.92$, slope 0.96, y-intercept 0.11). Changes in tuning curves observed in Turn-On (red) and Turn-Off (blue) voxels are also relatively well-described by linear functions (Turn-On: $R^2 = 0.61$, slope 0.95, y-intercept 0.93; Turn-Off: $R^2 = 0.86$, slope 0.27, y-intercept 0.14).

and time at the level of single voxels. However, we can use the fact that the full range of orientation preferences exist among sample voxels to distinguish the two types of attention. This is because feature-specific modulations should cause modulation among voxels of an appropriate orientation selectivity but irrespective of time. Similarly, time-specific modulation should cause modulations in all sampled voxels irrespective of their feature preference. Thus, a model that simultaneously incorporates both types of modulations can be used to quantify the effect that can be attributed to each type of attention.

To evaluate such a model, we computed a population activity surface in which normalized BOLD responses from Stay-On voxels in the No-Cue condition are binned according to stimulus time relative to the attended time and by the preferred orientation of the voxel relative to the attended orientation (Figure 4.6A). We then constructed a similar response surface for the same voxels in the Attend conditions (Figure 4.6C), using the same grouping as used for the No-Cue surface. Examination of this response surface reveals that maximal responses in the Attend case are not present at the cued orientation/time, but rather slightly precede the cue both in time and in preferred orientation. The anticipation is consistent with our behavioral (Figure 4.6C) and amplitude (Figure 4.4D) data, in which maximal effects precede the cued orientation.

Having constructed these two response surfaces, we then tested whether global, temporally specific and featurally specific modulations could explain the effects of attention. Consistent with the global effect of attention seen across all voxels (Figure 4.5), we first modeled our attention data by invoking a non-specific modulation (Figure 4.6E) that has uniform effects across all neurons and time. In this model, we found a systematic pattern of error along the diagonal of the surface. To account for these errors, we introduced a global response advance to the Attend responses of our model. Such a term may represent a systematic decrease in the hemodynamic response latency of V1/V2 during Attend conditions or a selective increase of the leading tail of all orientation tuning curves. This is consistent with our previous observation of a change in orientation preference across all voxels (Figure 4.4). Once this global phase shift was introduced, along with global attentional effects, we found a pattern of errors consistent with specific and directed allocations of spatial and featural attention. Accordingly, we then found the specific featural, and temporal attention functions, that when applied over the rows (featural dimension) and columns (temporal dimension) of the No-Cue activity surface best explains the Attend surface.

Our full model contains four attentional mechanisms: a global modulation; additive featural and temporal modulations; and the feature-time interaction. Notably, these mechanisms are consistent with previous reports: attention is typically observed to be an additive/constant modulation in BOLD studies[93] and human visually evoked potentials suggest that featural and temporal attention may act synergistically[129].

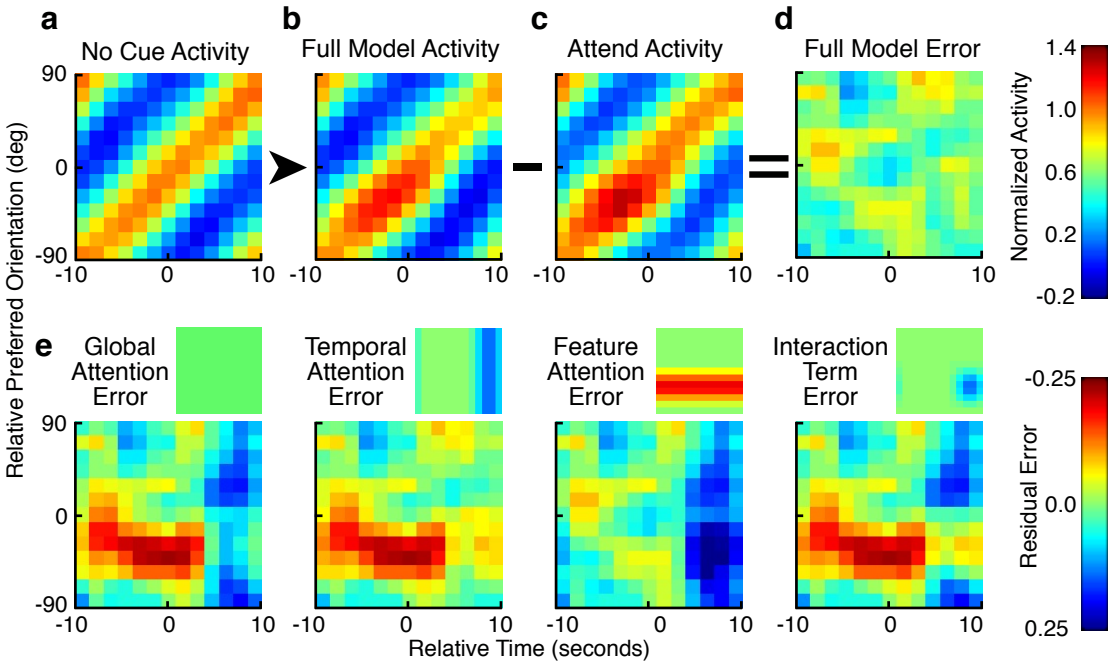

Figure 4.6: **A combination of featural and temporal mechanisms is required to explain attentional changes in orientation tuning.** (a) Normalized BOLD activity during No-Cue condition, averaged across all subjects and retinotopic locations, for the Stay-on voxel group. Each row represents the mean tuning curve (response over the stimulus cycle) for voxels that share a common orientation preference relative to the cue. Orientation and time are given relative to the cue, which occurs at 0/0 s. (b) The No-Cue activity surface is enhanced by a linear transformation and phase advance (0.6 s) to most closely approximate the corresponding Attend activity surface (c) defined from the same voxels with the same scaling. (d) The residual difference between the observed (c) and predicted (b) Attend activity is small ($R^2 = 0.99$, $R^2_{ajd} = 0.82$ after removing variance due to global effects (see Methods)). The Bayesian information criterion is used to compare this full model with simpler submodels to determine which mechanisms of attention are most consistent with these data. (e) The model in b is generated from the sum of four different attentional mechanisms (small images): a global term which modulates all data points equally, featural and temporal terms which act purely as a function of either the feature (row) or time (column) dimension, and an interaction term which acts with both featural and temporal specificity. All terms may incorporate both a multiplicative and additive component (that is, are linear functions of the form $y = mx + b$, see Methods); however only additive effects are shown in this and in Figure 4.7 as multiplicative modulations were not statistically justified. Each attentional mechanism alone is insufficient to explain the effects of attention, as shown by the patterned error surfaces produced when only one mechanism is modeled.

The parameters of this model are shown in Figure 4.7, and were 90/10 cross-validated. While the mode of the feature attention facilitation anticipates the cue by 32°, its width averaged across all voxels (80°) is comparable to the width of orientations over which behavioral events were most likely to occur (87°) and over which behavioral responses were most altered (95°, Figure 4.1D). Conversely, we found a temporal suppression across all voxels after the cued time. Thus our feature and temporal attention functions are well-matched to the behavioral manipulation. The interaction term is negative and compensatory to the feature attention term, acting to limit the feature-based modulation to only the most relevant points of time (Figure 4.7D).

To further test the model, we examined whether attentional changes in a tuning parameter that was not explicitly fit, namely the selectivity of individual voxels, were also accurately predicted. Although there was considerable variance in this tuning width data, on average, a clear bimodal pattern of width changes as a function of phase preference was present in both the A45 and A135 data (Figure 4.8). Moreover, both the shape and amplitude of this bi-modal pattern of tuning width changes was largely replicated in our attentional model.

To further validate these findings, we independently repeated the modeling analysis on the Turn-On and Turn-Off voxel subgroups. As a group, these attentional surfaces had greater noise and greater model errors. However, the featural, temporal and feature-time interaction parameter estimates derived from both Turn-On and Turn-Off voxels (Figure 4.7E,F) are well-correlated with those estimates obtained from Stay-On voxels. In all voxel subgroups, featural attention was characterized by a facilitation, which was maximally directed to voxels whose preference preceded the cued orientation but restricted in time by a negative interaction term, and temporal attention was characterized by a suppression that was maximal after the cued orientation was presented. We concluded that across all subjects and all voxels, the major mechanisms of attention were an increase in activity that is targeted to voxels with an appropriate feature preference and a suppressive effect gated as a function of the temporal rhythm of the task.

4.3 Discussion

We have shown that population activity in V1 is selectively enhanced during non-spatial forms of visual attention. While V1 cortical columns are tuned across several dimensions, the most prominent are tuning to retinotopic location and to stimulus orientation (spatial and featural tuning). Just as spatial attention enhances activity in populations that are tuned towards the attended region of space regardless of their feature tuning, we found that attention to a visual feature selectively enhances neural populations tuned towards that feature irrespective of spatial tuning. Considering the findings that modality-specific attention enhances stimulus selectivity in primary auditory[130] and somatosensory cortices[131], we interpret our data as consistent

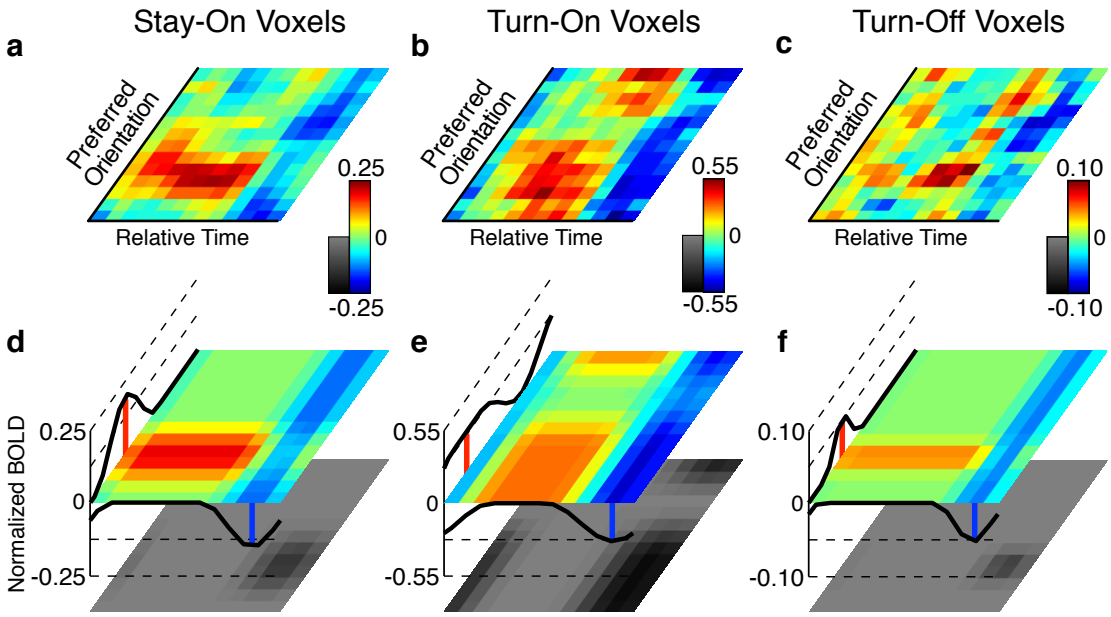

Figure 4.7: **Attention model parameters from three separate groups of voxels are nearly identical.** The optimal model (lowest BIC) is comprised of three attentional mechanisms: a feature-specific additive enhancement, a time-specific subtractive inhibition and an inhibitory interaction term, which gates the feature-attention to the relevant period of time. (a) The empirical attention surface generated from Stay-On (SO) voxels, computed as the difference between the Attend and No-Cue activity surfaces. Variance that is explained by global changes in activity over all voxels (the trend line in Figure 4.5) has been removed. The middle of this surface represents the cued orientation/time. (b,c) As a, showing the attention surfaces generated from Turn-On (ON) and Turn-Off (OFF) voxels. All surfaces show an increase in activity within voxels that prefer an orientation just prior to the cue, and all surfaces show a global suppression after the stimulus passes the cued orientation. (d) The best-fitting model surface for the SO voxel attention surface. Curves along the left and bottom sides show the modeled featurally and temporally specific modulations, while the black-and-white surface shows the feature-time interaction term (always suppressive). The sum of all three attentional mechanisms provides the colored model surface. (e,f) As d, showing models derived for the ON and OFF voxels. All three models approximate their respective attention surfaces well ($R^2_{adj,SO} = 0.82$, $R^2_{adj,ON} = 0.80$, $R^2_{adj,OFF} = 0.44$), and all three models agree as to when and where V1 attentional modulations are found (featural attention peaks: SO -32°, ON -52° and OFF -34°; featural attention widths: SO 51°, ON 115° and OFF 30°; temporal attention peaks: SO 63°, ON 71° and OFF 66°; temporal attention widths: SO 47°, ON 64° and OFF 36°).

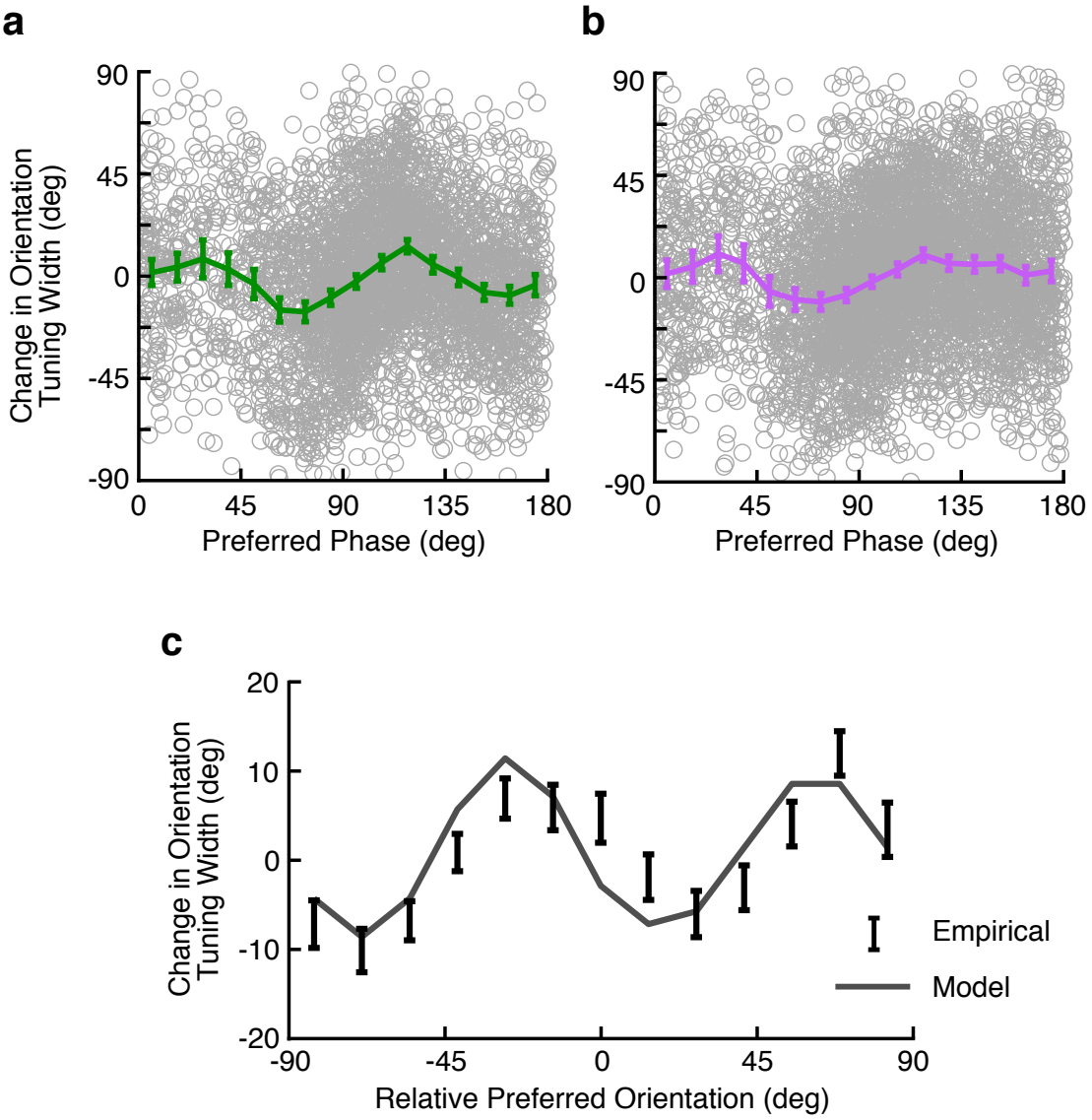

Figure 4.8: **Attention changes the width of orientation tuning curves.** Tuning width was estimated by fitting a circular Gaussian function that was modified to fit widths wider than 90° (see Methods). A. Compared to width measured in the No-Cue condition, widths during A45 follow a complex bimodal distribution. line, mean change in width versus preferred phase, error bars 95% confidence interval for the mean. B. During A135, a similar distribution of tuning width changes is observed. Note that, although there is substantial noise in the width changes, the bimodal curves are similar in shape with respect to the focus of attention (A: A45 and B: A135). C. Mean changes from A and B are aligned (error bars), and compared to predicted changes in tuning width derived from the attention model for Stay-On voxels (solid line, model shown in Figure 4.1). The model recovers the overall bimodal distribution of width changes.

with the overarching hypothesis that attention selectively targets the neural sub-populations within the earliest levels of sensory processing that are best suited for a task irrespective of modality.

We were able to simultaneously measure featural tuning and attentional modulations across large portions of V1. The sensitivity of the BOLD signal to attentional modulations is well-known[132, 94] even within V1, where the effect of spatial attention on single-unit activity is very weak[78, 4, 133]. This is likely due to the BOLD mechanism's sensitivity to sub-threshold synaptic activity[93]. However, our data suggest that even presumably weak single-unit modulations can profoundly alter the distribution of population activity over a cortical region[134], biasing neural representations in favor of the attended focus be it a location or a visual feature.

In stark contrast to resolving attentional modulations, the ability to resolve V1 voxel-level orientation tuning has been largely limited to ultra-high resolution studies that only image a small volume of V1[103, 128]. We found that imaging with 7T fMRI afforded a superior spatial selectivity and signal sensitivity[135], permitting orientation tuning to be measured over a large enough volume of V1 to exclude the possibility of spatial confounds[105]. This difference in signal quality is highlighted by our finding that, in our data set the decoding accuracy of many single voxels for orthogonal orientations rivals or exceeds the accuracy of the entire V1 volume obtained at lower resolutions.

Single unit studies in non-human primates have suggested that attention modulates responses according to a gain-like mechanism where all responses are multiplicatively increased. Such gain modulations, when combined with non-linearities such as response normalization, can explain many physiological observations[83, 80]. Our finding that feature attention caused a simple additive increase in V1 population activity is seemingly at odds with gain-like mechanisms. However, this finding likely reflects a known discrepancy between the electrophysiology and fMRI literatures: processes which are known to evoke gain-like modulations in single units are typically associated with additive increases in the BOLD signal[93, 136]. In our data, although additive attentional models were superior to gain-based models, the basic features of the multiplicative model's gain terms (early facilitation in the feature domain and late suppression in the temporal domain) were completely consistent with our additive model (data not shown). Thus our observations, while not able to provide direct support for gain modulations at the neuronal level, are certainly consistent with such modulations underlying a broad spectrum of attentional phenomena.

Consistent with the independence of spatial and featural attention[136, 137], we also find that independent featural and temporal attention is necessary to explain our observations. However, an interaction term is additionally required to explain the absence of net response modulation among appropriately tuned voxels after the times of likely change. This is consistent with

both human event related potential[129] and monkey single unit data[28], in which temporal expectations restrict spatial attentional modulations to behaviorally relevant periods of time. We suggest that the cumulative effect of these attentional modulations is to provide targeted feedback to neuronal populations specific for the focus of one's attention (be it an object[15, 138], a location in space, or a distributed visual feature) during periods of time that are most behaviorally relevant.

The sensitivity of BOLD measurements to attentional modulation highlights the need for extreme caution when using imaging to study the functional architecture of cerebral cortex. Columnarly organized orientation tuning within V1 is among the most consistent phenomena in the neurophysiological literature. Its underlying basis is well-understood[63, 139, 140], and efforts to resolve orientation selectivity in V1 have served as a litmus test for the resolution of columnar activity with fMRI throughout the past decade[103, 104]. However, our results demonstrate that measurements of orientation tuning based on population activity, such as fMRI, may be heavily influenced by the observer's mental state. In our present study, we control a subject's attentional state and can therefore distinguish between intrinsic orientation tuning and attentional tuning changes. However, this control depended on our prior knowledge of feature selectivity in V1: namely, that neurons within V1 are strongly tuned for orientation. For areas or regions in which the underlying functional properties are less well-understood, the potential of uncontrolled behavioral factors to alter responses is a great concern. Many imaging experiments do not control for attention or attentional fluctuations, and if they do so, concentrate on spatial, but not temporal or featural, controls (for example, tasks at fixation). Even a mild, idiosyncratic preference for one of two stimuli (for example, for a face instead of an inanimate object) may cause a profound attentional modulation throughout the cortex[134]. This is particularly true for regions that are known to be modulated by subjects' cognitive state, including association cortex and limbic structures, but as shown in our data can be a factor even at the earliest, presumably most 'sensory', levels of processing.

Attentional modulations at such early stages can significantly bias downstream processing and allow for complex attentional changes to emerge at higher stages of processing in the visual system[80]. For example, in the case of orientation and form processing, a weighting of particular orientations could bias the sensory preferences of higher order object representations, which include that orientation, and thus be responsible for observations of 'biased competition' reported in single neuron studies of higher areas such as V4[2]. However, such a reweighting of early features would also have consequences for all the higher order visual areas receiving input from V1, including parietal areas associated with spatial and motion processing. Therefore, for tasks in which specific higher order features, such as faces or objects, are particularly behaviorally

relevant it may be advantageous to directly modulate the populations that encode those higher-order features without changing all visual representations. If such higher order feature selectivity is spatially localized within a particular visual area[109, 141], high field imaging may be able to reveal single-voxel tuning, and attentional modulation of that tuning. Such studies could be used to directly test the hypothesis suggested by our data that all forms of attention may rely on simple linear modulations of activity that are selectively directed to task-appropriate neurons.

4.4 Methodology

4.4.1 Subjects

Nine human volunteers (including the author, two female volunteers, ages 20-48) participated in this study: nine performed the two Attend experiments, eight performed the No-Cue experiment and six performed the No-Rotate experiment. Data collected from one male subject were discarded due to motion artifacts. All subjects gave informed consent and the human subjects protocol was approved by the institutional review board at the University of Minnesota.

4.4.2 Stimulus and Behavioral Analysis

The stimulus consisted of a large continuously rotating, counter-phasing, achromatic Gabor ($\approx 30^\circ$ field of view, counter-phase frequency 2-4 Hz and rotational frequency 0.05 Hz) with a central fixation point. Use of a periodic stimulus provided enhanced statistical power to detect stimulus-evoked BOLD activity[128, 101]. At random times, the SF of the Gabor would briefly double (from 0.5 to 1.0 cycles per degree). Subjects were required to quickly respond by button press when these SF changes occurred. To manipulate attention, subjects were notified prior to each trial (by the presentation of a 20 s static cue) whether the probability of SF changes would be uniformly distributed around all orientations (No-Cue test condition) or whether there would be a bias in the probability of SF shifts such that approximately twice as many shifts (20-fold increase in hazard function) would occur in a 45° range (full-width at half maximum (FWHM) $= 87.15^\circ$) centered on either 45° or 135° orientation (A45 and A135, respectively). Two subjects performed an alternative No-Cue task in which they identified a change in the color of the center fixation point. No difference in results was noted between subjects performing the SF-change detection and the color-change No-Cue task, and these data are presented as one condition in this report. In a final control condition, the stimulus did not rotate but SF shifts still occurred with a predictable and sinusoidal timing (No-Rotate).

Subjects received performance feedback (brief color change) at fixation, but eye movements were not monitored and fixation was not overtly instructed. A button press within 250-750 ms

of a SF shift was counted as a correctly identified target. These reaction times were averaged and used as weights in a statistical test of the second-order angular mean[142] to determine whether reaction times were uniform across all orientations.

4.4.3 MRI Acquisition

Subjects viewed this stimulus via projection onto a mirror while supine in the 90 cm bore of a 7 T MR scanner, controlled by a Siemens (Erlangen, Germany) console equipped with a head gradient insert operating at up to 80 mTm^{-1} with a slew rate of 333 $\mathrm{Tm}^{-1}\mathrm{s}^{-1}$. A half volume four-channel radio-frequency coil was used for transmission, and a nine-channel surface receive array was used for reception. We took gradient-echo (GE) echo-planar BOLD contrast functional images from a volume perpendicular to the occipital pole with a variable field of view (96×192 mm or 144×144 mm) and number of slices (25-34) but with a constant temporal and spatial resolution across subjects (repetition time (TR) = 1,500 ms, echo time (TE) = 20 ms, flip angle 65°, 1.5 mm isometric voxels). Retinotopic maps, when obtained, were measured using the same functional sequence over the same volume in the same session. Also in the same session and with the same hardware, high-resolution T1-weighted and proton-density anatomic images of the occipital cortex were obtained. All anatomic analyses, including volume registration, white/gray matter segmentation, and surface modeling, inflation and flattening, were performed on proton-density-normalized T1-weighted partial-volume anatomic images[143].

In MATLAB, utilizing the third-party NIFTI Toolbox (**http://www.mathworks.com /matlabcentral /fileexchange /8797-tools-for-nifti-and-analyze-image**), raw BOLD images were visually inspected for aliasing artifacts, which were present in six subjects and manually masked. The 21st volume (the first volume after 30 s of data was discarded) of the first set of functional images collected for each subject was designated as the reference volume. All functional images from all experiments for that subject (including retinotopic mapping) were aligned via rigid-body transformation (fMRI of the Brain Software Library[144], mcflirt function) to this reference volume, such that a given row-column-slice index referred to the same volume of cortex for all test conditions.

4.4.4 V1/V2 ROI selection

In eight subjects, standard phase-encoded retinotopic maps[111] were either collected (one 5-min scan each for polar angle and eccentricity maps, six subjects) or acquired from past experiments (two subjects). Retinotopic maps were visualized on a flattened representation of occipital cortex using FreeSurfer[145], a V1 ROI was selected on the basis of reversals in polar angle, and this ROI was transformed into the functional image space to determine which voxels would be

included for further analysis. Because the retinotopic maps were not of optimal quality (derived from a single 5-min scan instead of a typical 1 h session), we consider it likely that the V1 border was not precisely defined and that our ROI likely contains a small portion of V2 voxels. For one subject, no retinotopic data were available and anatomic volumes were manually registered to the anatomic volume of subjects with known retinotopy. This manual registration focused exclusively on aligning the calcarine sulcus, an anatomic landmark for V1. After alignment, these two subjects used the same functionally defined ROI. No difference in major results was observed between subjects with functionally and anatomically defined ROIs.

All analysis of correlation between retinotopy and orientation tuning were performed exclusively on the subjects for whom retinotopic and orientation images were acquired in the same session with the same resolution over the same volume[105].

4.4.5 Single-voxel statistical analysis

All single-voxel analysis was performed using custom software written in MATLAB, except where noted. Following motion correction, the time-series of each voxel was analyzed independently with no spatial smoothing. Not all subjects performed each control experiment; in total 51,954 voxels from V1/V2 were studied during A45/A135 (eight subjects), 45,349 voxels during No-Cue (seven subjects) and 32,226 voxels during No-Rotate (five subjects). Except when repetitions are explicitly compared, analysis was performed on concatenated data in which the time series of all repetitions of a given task were analyzed at once. Any time data from two or more conditions are compared, the comparison is made on the same voxels from the same subjects.

The first 30 s of data from each scan were discarded to eliminate start-up artifacts. We removed signal means and applied a Hamming taper to limit the effect of edge discontinuities, and a 1-dimensional, discrete Fourier transformation provided the spectral content of each voxel. From this, we estimated the phase of each voxel's 0.05 Hz component (the frequency of stimulus rotation). This phase was adjusted by 5 s (45°) to account for the hemodynamic response latency, which was assumed to be constant in all subjects. This sinusoid plus a constant term was regressed against the raw voxel time series, where the ratio of the mean square model to the mean square model error provides an F-statistic of the goodness-of-fit of the sinusoid model. This is similar to a standard general linear model approach, except only one regressor was used. No detrending, artifact removal or other temporal filtering was performed prior to identifying modulated voxels.

To limit false positives without compromising statistical power, we used the method of False Discovery Rate (FDR) to choose a critical value for our data such that only 5% of selected voxels would be false-positives[146]. A voxel with an F-statistic beyond this critical value was defined as orientation-selective, where the peak of its tuning curve, that is, orientation preference, was

given via Fourier analysis and its tuning amplitude is twice the regression coefficient for the sinusoidal component. FDR-controlled data are denoted by use of a q_{FDR} value instead of a P value in this text.

Once a voxel was defined as significantly modulated, its time series was detrended by regressing out a second-order polynomial. In addition, to account for the possibility of a BOLD response to individual target events, we regressed from each voxel a predictor consisting of a target-event impulse function convolved with a canonical hemodynamic response function with a latency of 5 s. Tuning parameters of amplitude and orientation preference were then determined by finding the best-fitting sinusoid. To define a confidence interval on these tuning parameters, we computed by numerical approximation the second derivative of each voxel's likelihood function with respect to each parameter. This derivative may be converted to a confidence interval for each tuning parameter[147]. We confirmed that our data generally met the assumptions for this form of confidence interval estimation, namely that the likelihood surface is bivariate normal at its maximum.

To derive a non-parametric tuning curve for each voxel, we averaged its response to all cycles of the stimulus. These tuning curves were used to derive an estimate of the decoding accuracy (DA) for each voxel by computing the likelihood that each voxel could be explained by a sine-wave modulation at each voxel's preferred versus anti-preferred phase. The log-likelihood ratio between preferred and anti-preferred phases ($LLR_{pref/anti}$) provides the probability that a maximal voxel response was due to a stimulus at the preferred versus null orientation:

$$DA = LLR_{pref/anti}/(1 + LLR_{pref/anti}). \tag{4.1}$$

The DA values reported in Figure 4.2 were obtained by using 75% of cycles as training data to estimate the voxel's orientation preference and the remaining 25% of cycles as validation data to obtain likelihoods relative to this orientation. For all other analyses, a single tuning curve (the mean of all cycles) is used.

To compare our orientation tuning results to previous reports, we also computed a correlation coefficient (CC) at the stimulus frequency for each voxel:

$$CC = \frac{|F(f_{stim})|}{\sqrt{\sum_f |F(f)|^2}} \tag{4.2}$$

where F refers to the Fourier coefficient at a given frequency f. The CC is also computed after detrending and is F-distributed under the assumption of white noise[128, 111].

To estimate the tuning width of each voxel, we required an angular distribution that might accommodate widths larger than a sine-wave to describe voxels with very poor tuning specificity. This required us to modify the standard circular Gaussian function, as the FWHM of a circular

Gaussian may not be wider than a sine-wave ($\lim_{\sigma \to \inf} FWHM = \pi radians, Amplitude = 0$). Our modified circular distribution consists of a square-wave with sinusoidal on- and off-ramps. It is identical to a circular Gaussian function for FWHM $< 90°$, but becomes artificially wider with a flat peak for larger widths. This permitted us to estimate tuning widths from the entire range of [0°,180°).

For all analyzed data, we performed a minimum of two scans (5 min each) of each condition with at least 30 min between repeats. Voxels which were significantly active during both scans had highly similar orientation preferences (A45 3.9% of voxels, A135 7.4%, No-Cue 2.8%; mode difference 0°; 95^{th} percentile 33.6°). We concluded that our estimates of orientation tuning were reliable enough to justify concatenating all data from each condition into a single data set for all future analysis. These concatenated data gave substantially more power to detect cyclic activity. Notably, no voxel was active during two repetitions from the No-Rotate data set, leading us to conclude that these data did not contain orientation-selective information.

4.4.6 Attentional modeling

As the attentional changes observed during A45 and A135 are orthogonal (Figure 4.4) and independent of visual field location, we combined data from the A45 and A135 to create a single Attend data set by aligning both data sets to their attended orientation. After alignment, preferred orientation and time are reported as relative to the cued orientation/time, which occurs at 0°/0 s. We then normalized the Attend and No-Cue data sets such that each voxel's No-Cue tuning curve is defined as oscillating between 0-1. Values <0 and >1 are permitted, as these values represent real peaks above/valleys below the estimated sinusoid component. The same scaling factors were then applied to the Attend data. Thus if tuning in the Attend condition is of a larger amplitude than in the No-Cue condition, then Attend tuning curves will vary between 0 and a number >1 (Figure 4.6). Voxels were binned by preferred orientation and tuning curves are averaged to generate each row of the activity surfaces shown in Figure 4.6.

We grouped voxels into three groups: those which exhibited orientation selectivity in all conditions (Stay-On, 7,696 voxels), those which were only selective with attention (Turn-On, $n = 13,876$) and finally those which were only selective in the absence of attention (Turn-Off, $n = 5,047$). Compared to the other groups, Turn-Off voxels had lower tuning amplitudes (0.24% BOLD or 14% lower, t-test, 6,506 DOF, P$< 10^{-10}$) during the No-Cue condition, and we concluded that Turn-Off voxels were predominately associated with regions whose noise precluded our ability to observe attentional effects. For all three groups of voxels, we performed a regression analysis of attended versus unattended responses to determine the potential for simple linear models to explain our data and to quantify global effects of attention.

Our objective was to find the model of attention, as a function of relative preferred (Θ)

and stimulus (Φ) orientations that best predicts the attended responses (A45 and A135) from unattended (No-Cue) responses. First, we applied a constant phase shift to all standardized tuning curves

$$S'_{no-cue}(\Theta, \Phi) = S_{no-cue}(\Theta, \Phi - \omega) \tag{4.3}$$

as we found that during the Attend condition all voxels reached a peak activity ≈ 0.5 s ($\omega_{StayOn} = 0.60$ s, $\omega_{TurnOn} = 0.65$ s, $\omega_{TurnOff} = 0.36$ s) earlier than during No-Cue conditions. Then a complete attention model, including both additive (a) and multiplicative (m) featural and temporal attention effects can be described by:

$$S_{attend} = (a_G + a_F A_F + a_T A_T + a_I A_T A_F) + (m_G + m_F A_F + m_T A_T + m_I A_T A_F) \cdot S'_{no-cue} \tag{4.4}$$

$$A_F(\Theta, \Phi) = N_{circ}(\Theta, \mu_F, \sigma_F) \tag{4.5}$$

$$A_T(\Theta, \Phi) = N_{circ}(\Theta, \mu_T, \sigma_T) \tag{4.6}$$

where N_{circ} is a circular Gaussian function over preferred orientation (feature) or over stimulus orientation (time) with a peak at μ and with a s.d. of σ. A_F and A_T are functions describing the specificity of featural and temporal modulations, respectively. Again, to accommodate attentional modulations that might be wider than π rad (FWHM>90°), we used our modified circular Gaussian as described above.

Two of these parameters refer to a global non-selective attentional effect, whereby the entire surface is both multiplied (m_G) and incremented (a_G) by a constant. These parameters are derived by first regressing all observations across voxels and time from the Attend data set with all observations from the No-Cue data set (Figure 4.5), and are not allowed to covary with other model parameters. In addition, interaction parameters (a_I, m_I) test the hypothesis that these forms of attention may not be independent but rather may directly influence one another. This is an extension of an approach that has been used previously to determine the relationship between orientation preference and time during a V1 adaptation paradigm[148]: we have added the potential for additive parameters, the interaction parameters, and the potential for attention functions with a FWHM $> \pi$ rad.

As orientation is sampled to 13 bins, each activity surface consists of 169 points and a full model potentially consists of 13 parameters. In our data, the effects of featurally and temporally specific multiplicative gain (m parameters) were only marginally distinguishable from the effects of the corresponding additive parameters (a terms). Because exclusively additive models consistently performed better than exclusively gain models, we set the m parameters to zero to test

whether temporally and featurally specific modulations were present. Thus, because the global parameters were also set according to regression analysis on the entire data set, there were a total of three functions (featural, temporal, featural-temporal interaction) that could potentially contribute and seven parameters (a_F, a_T, a_I, μ_F, σ_F, μ_T, and σ_T) which needed to be evaluated and tested for significance. The maximum likelihood estimate of these parameters was found using global optimization methods (**http://www.mathworks.com/matlabcentral/fileexchange/24838-godlike-a-robust-single—multi-objective-optimizer**), and this likelihood estimate was used to compute the model's Bayesian Information Criterion (BIC). BIC is a tool to select the most parsimonious model by imposing a penalty upon models with greater complexity. The full model BIC was compared with the BIC of submodels, in which one of these functions were removed to determine whether any smaller subset of attentional mechanisms was sufficient to explain our observed data. Such analysis revealed that all three functions were justified and the full model's BIC was lower than that of any individual submodel. We performed a 90/10 split train/test cross-validation on this model; results from 10 repetitions gave almost identical model parameters and always provided a good explanation of the testing data. To test the generalizability of this model, we separately fit the three attention functions for voxel subsets with very different attentional modulation (Stay-On, Turn-On and Turn-Off; Figure 4.7).

Approximately 86% of the variance within our activity surfaces is due to the diagonal pattern of activity that is defined by the process of generating the surface and does not reflect an attentional effect. To account for this, when reporting variance we use a measurement of 'attentional variance', defined as the proportion of explained variance a given model accounts for, which was not accounted for by a model with only global attention terms:

$$Attentional variance \equiv R^2_{adj} = 100\% \times \frac{(R^2_{model} - R^2_{global})}{(1 - R^2_{global})} \tag{4.7}$$

where R^2 is the standard linear regression statistic commonly used to measure the amount of variance in a data set that is explained by a linear model. This adjusted attentional variance term is 0 for the global attention model, 100% for a model which perfectly recreates the observed effects of attention, and varies linearly between 0 and 100% for any model which improves upon the global attention model as measured by the R^2 metric.

Chapter 5

How Small is the Spotlight? Attention to Very Small Objects

5.1 Introduction

Attention is not only flexible across different sensory domains and stimulus features, but also may be deployed toward a given target in a graded fashion, much like a lens zooming in and out of an image[120, 149, 150, 151]. When attention is broadly distributed to a quadrant of visual space, matching attentional modulations occur within the retinotopically correspondent quadrant of early visual areas[149], but is it not known how well-matched are the most narrow, "zoomed in" attentive states. Given that humans may perform discrimination tasks with retinal spatial precision[152], it is plausible that attentional modulations within early visual areas might be similarly precise when attending to such small regions of space.

The more narrowly restricted attentional modulations are within the cortex, the greater the number of distinct arrangements of attentional modulation within cortex are ultimately possible. If attentional modulations may occur over a very restricted extent of sensory cortex, as we hypothesize, then this implies a large degree of flexibility in orienting attention toward distinct stimulus representations throughout the brain. Given the enormous flexibility of attention across different sensory modalities[10, 9, 56, 8, 7], different stages of sensory processing[1, 15, 29], and distinct cuing conditions[27, 28, 4, 3], measuring the limit to attentional precision may provide crucial bounds for developing a general model of attention.

While the precision of spatial attention have not been systematically probed, several studies point to early visual areas, specifically primary visual cortex (V1), as an area of interest.

Trained non-human primates are unable to base responses on one of two stimuli when the composite stimulus pair is small and located entirely within the receptive field of one V1 neuron[3], suggesting that a limit occurs near the scale of the V1 receptive field. The extent of attentional modulations within V1 scales appropriately with increasingly broad spatial attentional allocations[149], and robust, task-appropriate modulations have been observed in V1 populations and single-units during tasks that require the subject to process V1-relevant information such as small objects[153], oriented gratings[29], or curve-tracings[154]. Even complex, non-linear attentional interactions, such as those observed under paradigms of biased competition[3], in higher visual areas can be explained by theoretically simpler, linear modulation of early visual areas[2, 80].

However, efforts to demonstrate the modulation of V1 neurons in simple spatial attention tasks have historically failed, typically showing only weak modulation of V1 neural firing even when attending to single stimuli appropriately scaled for V1 neural receptive fields[31, 4, 3]. In this context it is not clear that attention to a small stimulus necessitates that attention be directed exclusively to a small region of space, as higher-level visual areas with larger receptive fields may still discriminate between small stimuli presented in isolation. Conversely, imaging studies show large modulations of V1[94, 155] but do not quantify the precision or behavioral relevance of such modulations. It is not known whether attentive modulations of the BOLD signal correspond to meaningful but sub-threshold modulations of V1 neurons or merely reflect non-specific feedback and behaviorally irrelevant task effects.

To explicitly measure the precision of V1 attentional modulations, we mapped the distribution of attentional modulations in primary visual cortex using invasive optical imaging[58] in two rhesus macaques trained in a task engineered to require the attentional recruitment of V1 neural populations. In this paradigm, we train the animals to develop a retinotopically small attentional template and then measure the spatial extent of attentional modulations across the cortical surface. In this chapter I show unpublished data demonstrating that even though the task was exceptionally challenging and that our animals performed this attention task imperfectly, attentional modulations were grossly appropriately targeted within V1 and that the distribution of modulations across V1 explained a large amount of the spatial variations in animal behavior. We argue that attention is in fact selectively targetable to very small regions of cortical space but only with a resolution on the order of the known feedback projections to V1.

5.2 Results

5.2.1 Attention to V1-scale Objects

We trained two rhesus macaques to detect the brief, perceptually faint contrast increment of the single Gabor elements positioned within a 3x3 array of stimuli (Figure 5.1). The size of the individual elements was 1-1.25 times the size of V1 receptive fields at the stimulated eccentricity (Monkey F: 0.15°; Monkey P: 0.2° radius), as estimated from known V1 electrophysiology[35], and the array was simple-cubic close-packed such that the individual elements lay in the surround fields of their neighbors. All other Gabor parameters were chosen to maximally activate local V1 neurons. Both animals maintained within ±0.5° fixation to a 0.125° target circle, with median single trial eye position variance less than the stimulus element size (50/95th percentile: Monkey F: 0.148°/0.222°, Monkey P: 0.106°/0.195° .

To manipulate attention, the probability that the contrast increment would occur within a given Gabor was non-uniform. The subjects were trained to utilize two pieces of information. First, in each trial block, subjects were instructed as to whether the left or the right stimulus array would host 96% of contrast increments. Both subjects readily followed this left/right cue between hemifields: sensitivity to detect increments in the cued hemifield was substantially greater than in the uncued hemifield (Monkey F: 64% versus 34%; Monkey P: 83% versus 38%; $p<0.05$ in both subjects, binomial distribution, variable DOF).

Attention between visual hemifields has been extensively studied, and historically the findings of attentional modulations within V1 are slight. It has been shown that attention over a smaller region of space modulates earlier stages of visual processing[156], and modeling predicts this trend will extend even to V1 with even smaller attentional foci[80]. To encourage our subjects to attend over the length scale that is relevant to local V1 computation, we also manipulated the probability that the increment would occur at a given stimulus position within the larger array. In both animals, one position close to the fovea and one position further in the periphery (separated by Monkey F: 0.85°; Monkey P: 1.13°) were each eight times more likely to host the contrast increment than were the other seven positions (Figure 5.1). The bias locations were fixed and never explicitly instructed to the subjects, but rather were trained over weeks of repetition. In behavioral training prior to physiologic measurements, both animals showed a relative increase in detection sensitivity toward one or both biased stimuli. However, this training occurred in the peripheral upper hemifield far from the expected representation of the imaged V1, and it was unknown whether and how this bias-benefit would persist when the chambers were implanted and the stimuli were appropriately scaled to the imaged region of V1.

After training with appropriately scaled stimuli, we found that both animals enjoyed a modest benefit to detecting increments at the two biased locations relative to the 7 more central

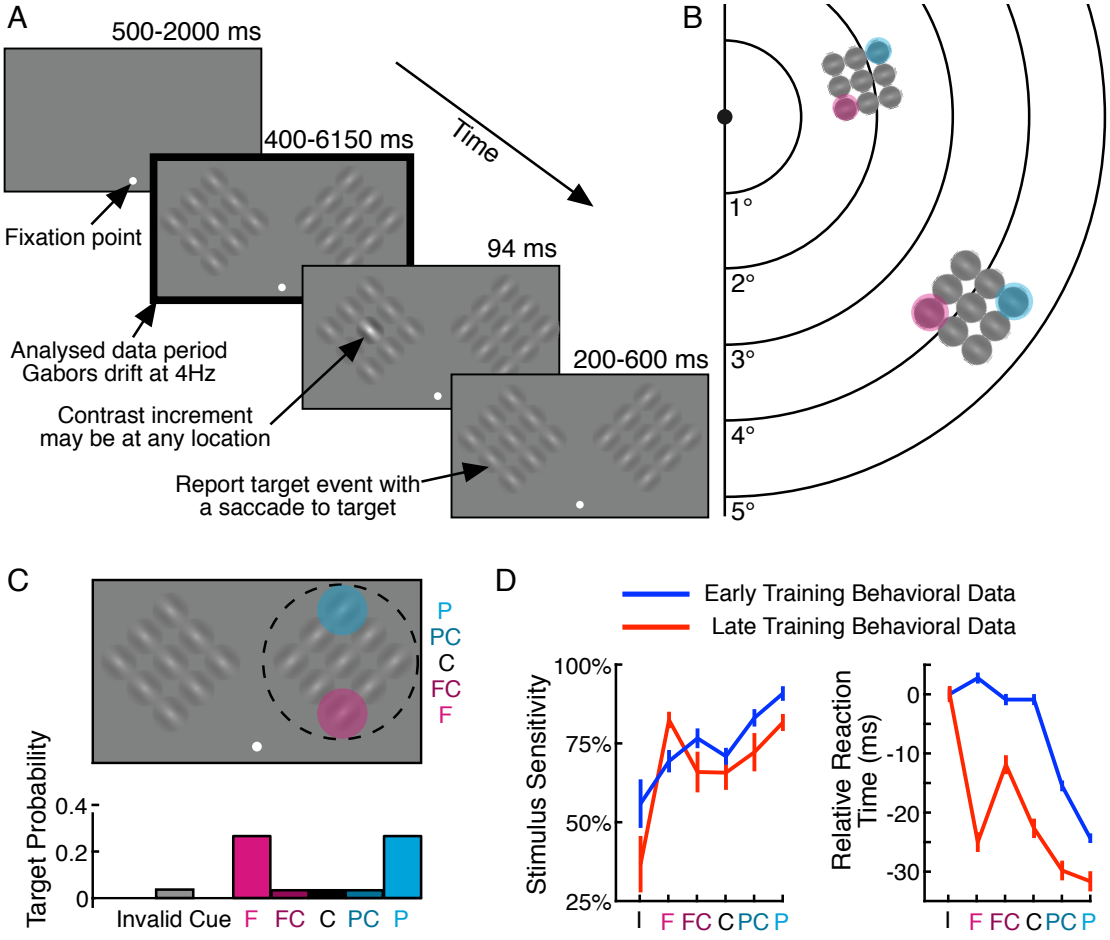

Figure 5.1: **Attention to Fine Objects.** (A) Outline of task. Animals fixate at a center point while a 3x3 array of drifting Gabors is presented in each hemifield. At a random time, one of the 18 Gabor targets will briefly increase in contrast. Subjects report detection of this increment by a saccade to the appropriate array. (B) The individual Gabors are approximately 50% larger than the expected receptive field size of V1 neurons at the stimulated location. When viewed at arms length (60 cm), this panel shows the location of the stimulus array to scale for each animal. Monkey F (P) refers to the subject with the more foveal (peripheral) stimulus array. (C) Each trial block (20-50 trials), subjects are cued (black circle) as to whether the increment is more likely (96%) to occur in or outside of the imaged region of V1. The cue is communicated via instruction trials (see text). Subjects were trained over several months that two locations (one foveal, pink, and one peripheral, cyan) are eight times as likely to increment. (D) Representative behavioral data from one animal. Peripheral increments were easier to detect, but with training performance increased at the foveal target.

locations (Figure 5.1). The overall sensitivity to bias-matched increments was higher (Monkey F: +17% Monkey P: +13%; $p<0.01$ at both bias locations in both subjects, binomial distribution confidence intervals, variable DOF) and the reaction time of saccades to biased-match increments was lower (Monkey F: -4.6 ms; Monkey P: -7.4 ms, $p<0.05$ at both bias locations in P and in peripheral bias location in F, *t*-test, variable DOF). The match between behavior and stimulus probability was however not perfect. The pattern of behavioral performance on the individual bias-mismatched elements (Figure 5.4) strongly suggests that both subjects struggled to attend focally on only the bias targets. Either some attentional resources spilled into neighboring elements, or read-out effects in later visual areas impaired V1 attentional targeting, in a subject-specific pattern. The individual behavioral patterns will be explored in combination with imaging data later in this report.

Because of the imprecision in behavioral performance and because these data are averages derived from hundreds of trials, we can not conclude that the subjects are simultaneously splitting attention to two distinct foci, a topic of controversy[46]. It is possible, for example, that the subjects rapidly alternated attention between the two biased locations. We more conservatively concluded that each subject's performance was influenced by the cue in a subject specific manner, and we then asked whether modulations reflecting this influence may be found in V1.

5.2.2 Physiologic Response to Individual Stimuli

Our primary objective was to explore the effect of attention on the V1 representation of each individual stimulus element. This required us to first carefully measure the V1 visually-evoked response to each single element of the stimulus array when presented in isolation. After mapping the retinal topography of the imaged region of V1 using standard methods, we determined that the chamber of one subject (Monkey P) was placed over the approximate region of V1 that was expected from known macaque V1 anatomy in the close peripheral lower hemifield (Figure 5.1). However, the other subject (Monkey F) showed strong visual responses only when the stimulus was placed near the fovea. In Monkey F, we therefore used smaller stimuli which were more closely packed. We also used a higher base contrast when mapping his chamber as these foveal signals were initially difficult to detect.

After the retinotopic location of the chamber was determined, subjects performed the same task as above except only one element was displayed on a given trial (this element was always the location of the contrast increment, so no selective attention was required). Notably, both subjects were unable to detect contrast increments at singly-presented locations with the same threshold for which they could be detected in the whole array- both subjects required stronger singleton contrast increments to perform the task (data not shown, this calibration was performed quickly online). This difference in contrast increment threshold can not be explained by integrating

signal over the entire array. Rather we concluded that both subjects solve the array task by comparing the relative contrast of neighboring stimuli, which requires spatial integration and comparison operations to be performed on the scale of the individual stimuli (on the scale of V1 neural receptive fields).

While both subjects' V1 showed a robust visually-evoked response to the array and to single elements, we found large differences in the spatial precision of single-target responses between animals. In Monkey P, consistent with past literature, we found that each stimulus element evoked a V1 response within a small locus (Figure 5.2A) The individual element evoked-responses were modest early in the trial, but were well-defined by a strongly negative hemodynamic signal late in each trial. This late, negative signal has been described previously[112], and we verified its hemodynamic nature with a separate series of red-illuminated images measuring the intrinsic hemodynamic signal[101]. The location of this well-defined response moved appropriately along the V1 cortical surface as the different singleton stimuli were presented. We also observed a strong and diffuse surround signal that typically to co-localize with nearby blood vessels. These regions of hypervascular response were masked out and not considered in future analysis. Thus we were able to unambiguously define a small region of V1, approximately 1mm in diameter, associated with each individual stimulus element.

In Monkey F, each singleton stimulus evoked a stronger but more diffuse response over the entire imaging window. This response matched the expected time course of AF activity (with onset <500ms after stimulus presentation) and did not demonstrate the negative response associated with broader hemodynamic signals. We interpreted this diffuse response as a real AF signal that may be due to the more foveal location of his chamber, the closer packed or higher contrast stimuli we used for this subject, or due to blurring of the V1 signal due to the need to image his V1 through an arachnoid neomembrane. None-the-less, while perfect retinotopy was not recovered from Monkey F's chamber, we still observed unique patterns of activity from the early period of each singleton's visually evoked response. In both animals, positional responses were distinguishable as quickly as 200 ms after stimulus onset (Figure 5.2).

The poor retinotopy of Monkey F's chamber prevented us from using a simple region-of-interest analysis for each position. However, as noted, single target response patterns across the chamber for each subject were distinguishable. Thus, as animals performed their full task with the composite stimulus array we were able to decompose V1 activity to the full array into a linear sum of the activity to each singleton using a multiple linear regression model where the regression β-statistics indicate the extent to which each singleton's V1 representation contributes to a composite-stimulus response. In these future analyses, we performed the regression only using pixels contained within a single manually defined region-of-interest (ROI) that included visually responsive center and surround pixels from all nine stimulus elements while discarding

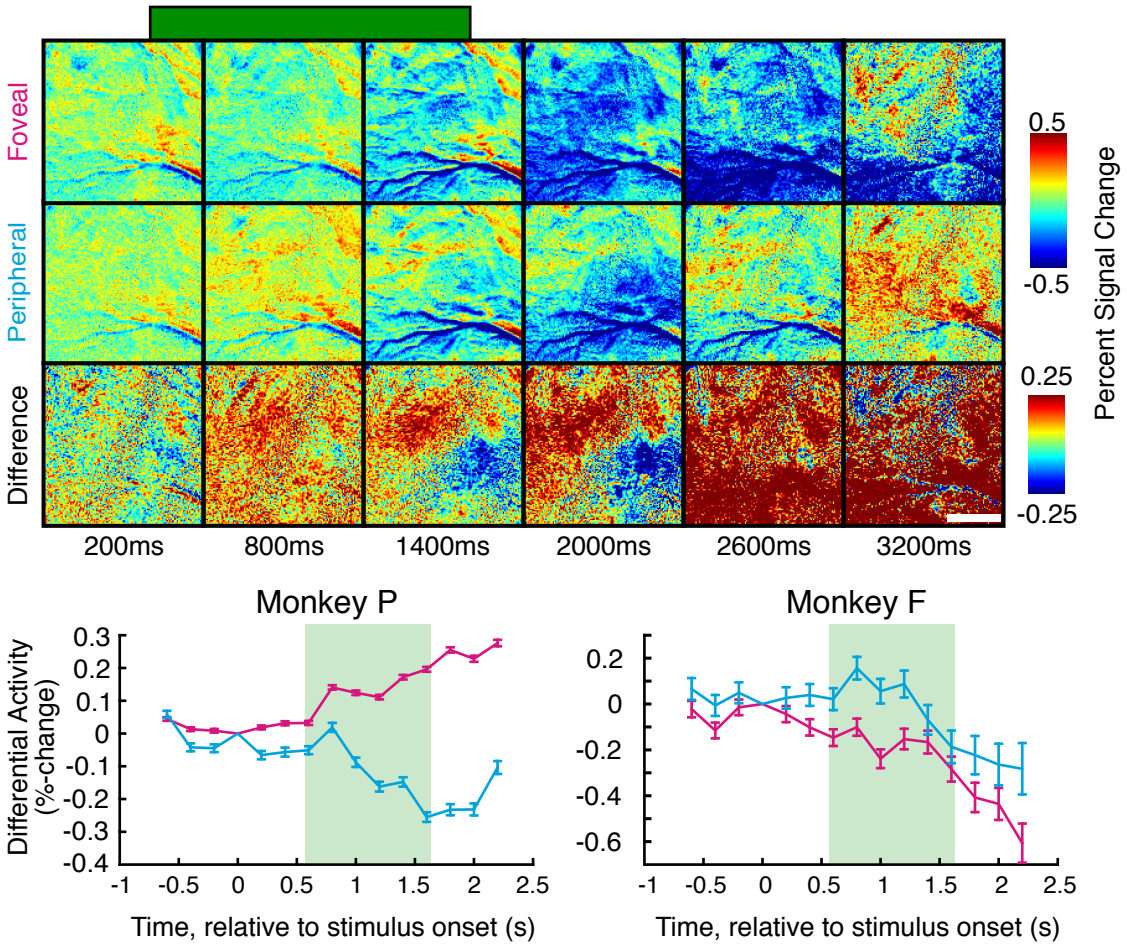

Figure 5.2: **Differential activity to individual Gabors.** In a separate task, each of the 9 Gabor targets was presented individually. The distribution of optical signal from V1 reliably changed as a function of Gabor location, consistent with the known retinotopy of V1. (A) Time series of averaged optical signal from Monkey P when only the foveal (top row) or peripheral (middle row) target is presented. Bottom show shows a a difference image between the top rows. Although the target centers are separated by only 1.13° in visual space, we may localize activity from one or the other target. The other 7 positions were also mapped with equal precision (not shown). (B) In both animals, differential activity as a function of stimulus location appears immediately after stimulus onset. Green highlight indicates the time frame from which the position-tuning of each pixel is estimated in future analysis. This time matches the time of observed attentional modulations (Figure 5.3).

regions of the chamber corrupted by blood vessels, image artifacts, or implant material.

5.2.3 Physiologic measurement of attentional modulations in V1

After singleton V1 responses were measured, subjects performed the contrast increment detection task on the full array of stimuli with left/right cues and the positional bias present. After discarding trials that ended earlier than 1 second, in which fixation was broken, in which large motion artifacts occurred, or in which uncorrectable software/hardware errors caused data loss, we were left with 2733 full attention task repetitions (F: 1005, P: 1728). The difference in trials is due to a greater tendency of Monkey F to make an early false positive report- in comparing the two subjects we always first compute and then compare inter-subject means, so P is not over-represented in our analyses. The behavioral data set presented in Figure 5.1 used the all available data from each animal, but the positional behavior described here uses only this restricted subset of trials. Because of the sparse sampling of unbiased targets, some noise in the estimation of behavior for each position was tolerated. Importantly, we only analyze trials collected before a saccade or a contrast increment occurs- the visually evoked signal from contrast increments (which we estimated to be real but minuscule, not shown) does not influence our measurement of preincrement attention activity.

In the early trial period (600-1600ms post-stimulus onset), both animals showed a net increase in the AF signal across the V1 ROI when attention was directed contralateral to the imaged V1 hemisphere (Figure 5.3, $p \approx 0$, t-test, DOF >3 million pixels $\times$ repetitions per animal at each time point). Later in the trial, the time course of chamber-wide activity remains distinct between the two attention conditions in both animals. However, in Monkey P the sign of this difference inverts as his stronger hemodynamic signal washed out the early AF signal. As it is known that the early stages of the combined AF/hemodynamic signal better reflect AF signal and are spatially more precise[112], we limit our analysis to the early attention period to avoid ambiguity in the sign of attentional modulations in the late in the trial (as both AF signal decrease and hemodynamic signal increase appear as a negative signal change).

On visual inspection, the mean two-dimensional pattern of early attentional enhancement over hundreds of trials has multiple clear peaks in each animal. We do not, however, claim that the animals are simultaneously attending to two locations- multifocal attention is controversial and we can not distinguish between a truly multifocal modulation versus other strategies such as attending to a continuous subset of the array or rapidly changing attentional allocations throughout the trial ("flipping" attention over multiple foci). Rather, we only interpret this non-uniform distribution as evidence that attention did not uniformly modulate the entire array's V1 representation but rather was targetable to only a subset of the V1 on the order of the size of the representation of individual stimuli. This implies that attentional modulations within V1

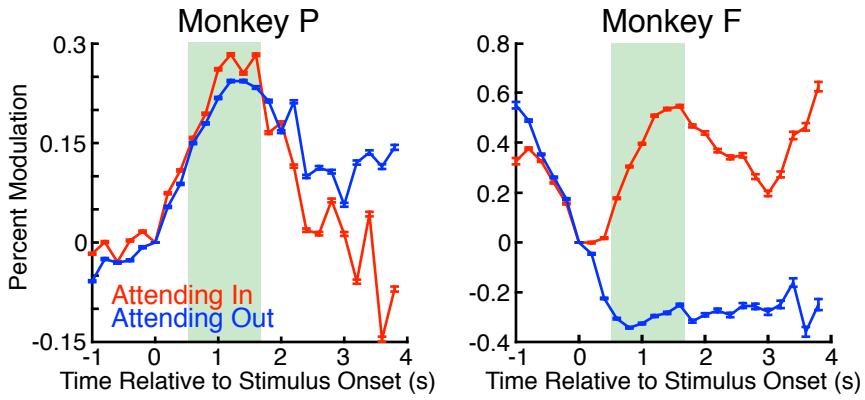

Figure 5.3: **Gross attentional dynamics.** Line traces show the average optical signal from a region of interest integrating activity from all 9 positions while subjects direct attention toward (red) or away from (blue) the imaged region of V1. In this and all figures demonstrating attentional differences, only images collected prior to a saccade or contrast increment are included. Early in the trial both attention increases activity across V1 of both animals. Late in the trial, the early mitochondrial signal from Monkey P is washed out by a negative signal of known hemodynamic origin. No such confounding signal was observed in Monkey F. To avoid ambiguity about the sign of the relevant signal, we analyze attentional activity only from the early trial period indicated in green.

may be targeted to as little as 0.5° of visual space.

Using the previously-measured singleton activity, we decomposed the map of attentional modulations for each animal into an attention vector of gain modulations for each individual element (Figure 5.4). We chose to model attention as a multiplicative gain because this type of modulation has been reported in several studies in V1 and other cortical areas. Moreover, gain modulations can explain numerous results of seemingly greater complexity by carefully modeling the effect of appropriate gains within non-linear neural networks.

Because our analysis regresses attention against the raw evoked activity from each singleton, it normalizes the magnitude of the attentional modulations by the magnitude of evoked visual responses. While Figure 5.3 suggests that the two subjects had vastly different attention modulation amplitudes, our regression analysis suggests that the amplitude of modulations attributable to individual positions is similar between subjects (±30%). This is because our decomposition regression includes a constant term so that non-specific attentional modulations are controlled in both subjects; this term is considerably larger in Monkey F than in Monkey P (Figure 5.4). While this may be due to individual differences in their stimulus configuration, overall task difficulty, or attention strategies, both subjects performed similarly and significantly worse on detecting cue-invalid targets in the non-attended hemifield (Monkey P: 38±13%, Monkey F: 32±20%, binomial distribution 95% confidence interval) than for cue-valid targets (P:

83±3%, F: 64±4%).

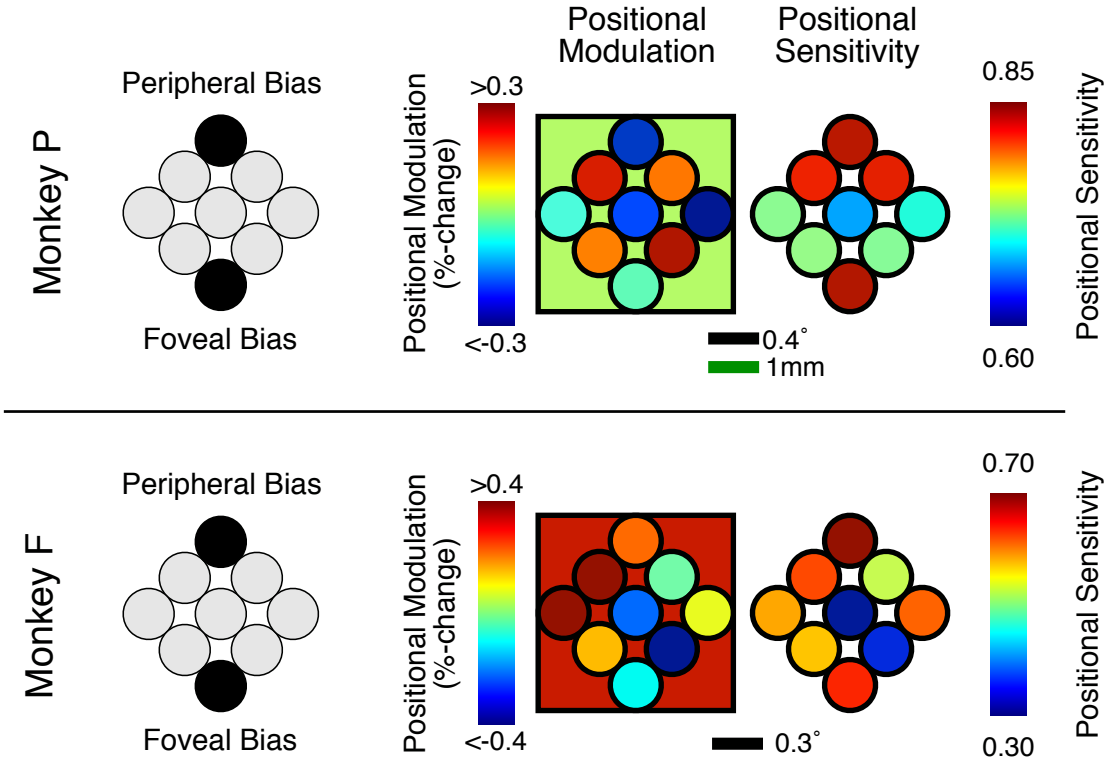

Figure 5.4: **Attentional modulation of individual targets.** We reconstructed the distribution of attentional modulations as a linear combination (see text) of the activity patterns observed when the individual stimuli were presented (Figure 5.2). Positive (negative) "positional modulations" imply enhancement (suppression) of the individual target's V1 representation. The colored background on the modulation distributions indicates the magnitude of a coincident global modulation that enhances or suppresses all stimulus representations. For both animals, neither the reconstructed attention distribution nor task performance perfectly match the probability schedule, however biases toward the cued sides of the array are evident. Scale bars show the extent of the stimulus array in retinotopic coordinates (black) as well as across real cortical space (green) where available.

In order to compare the positional distributions of both attentional modulations and detection performance, we first need to remove the effect of the probability distribution from each data set. This is because, plausibly, the biases could be implemented anywhere in the brain and have similar but independent effects on both distributions. By regressing the probability distribution out from both our behavioral and physiologic data, we better assess whether attentional modulations in V1 directly correlate with behavior. In Monkey F (but not P, who had larger

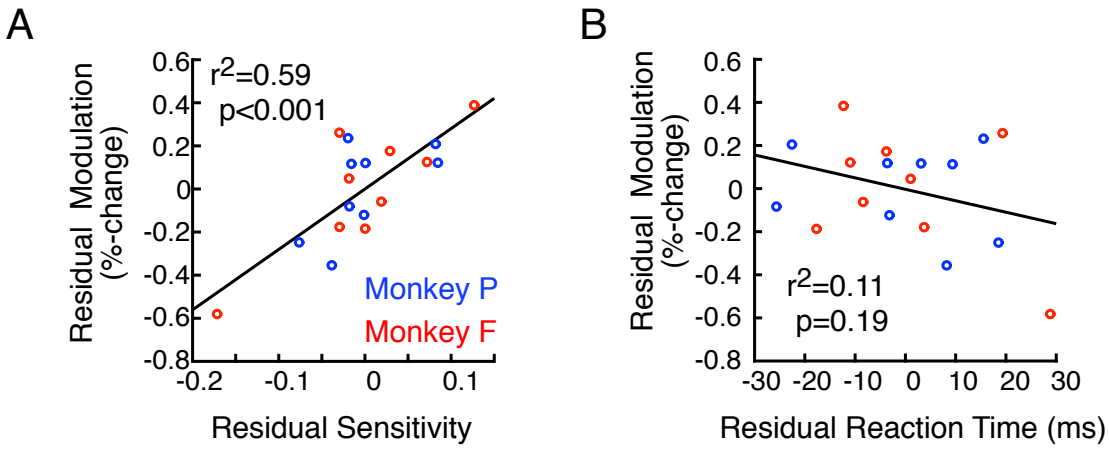

Figure 5.5: **Attention targeted to individual targets.** (A) The partial correlation between reconstructed positional attention modulations and stimulus sensitivity (controlling for each variables individual correlation with the probability bias) is high, strongly implying that attentional modulations at a given target's V1 representation enhances detection of changes at that target location. (B) A trend toward the same is seen in the correlation between attention and reaction time.

and more peripheral stimuli), we also found that a simple surround suppression model also significantly correlated with behavior (see Table 5.1). Thus we added to our partial correlations a surround suppression term, but the magnitude of this regressor was set to 0 for Monkey P.

Having regressed out the effects of the probability distribution, we found that attention toward a position strongly improves stimulus sensitivity (partial correlation, $r^2 = 0.51, p = 0.001$) after correcting for the influence of the probability distribution (and surround suppressive effects in Monkey F) on both distributions. We also observed a very weak trend toward attention reducing reaction time ($r^2 = 0.06, p = 0.34$). It is however evident that the match between attentional modulations and individual position behavior is imperfect- individual locations enjoy excellent behavior with minimal attentional modulations and vice versa. Moreover, in neither subject do the maps of behavior or attention perfectly reflect the trained probability bias toward two location. These differences are unsurprising, as the perceptual decision of whether an increment occurred relies on several further stages of cortical processing throughout the visual and oculomotor systems. It is plausible that attentional modulations, intraareal computations, and readout factors between other areas will non-uniformly effect processing of different stimulus elements. In the greater context of the entire visuomotor response, it is remarkable that as much as half of the positional differences in mean stimulus sensitivity may be explained by appropriately-matched V1 attentional modulation.

5.2.4 V1 modulations promote new behavior after task perturbation

Although we found a strong correlation between V1 modulation and stimulus sensitivity on a scale of less than 0.5 visual degrees, it remained unclear that this correlation represents the output of a flexible system that matches attention to task demands at this scale. First, the overall match between the cued pattern and the subjects' attention and performance is crude when viewed over all nine positions (see Table 5.1 in Methods). For example, Monkey F clearly misdirects his performance toward a bias-mismatched foveal location (Figure 5.4, far left stimulus position). It is not clear whether such mismatches reflect true attentional imprecision, poor task comprehension, or some fixed and non-attentive phenomenon such as the effects of normalization[157], surround suppression[158], or crowding[159] on V1 neuron responses. Second, recall that both subjects were exposed to the same positional bias for months of training. Although these data were collected from an untrained region of the visual field and thus we did not over-train the imaged region of V1, we may have yet trained higher-level, position-invariant attentional allocations to this bias pattern.

To test this, we abruptly changed the bias distribution for each subject. In Monkey P we rotated the probability distribution, while in Monkey F we removed the bias completely and presented a uniform distribution (Figure 5.6). Both animals behaviorally responded to the bias change- although performance remained superior at the obsolete bias locations (indicating preservation of the trained attentional strategies), performance also improved at or near newly biased locations (Figure 5.6, difference images).

Changes in the distribution of V1 attentional modulations, however, were more modest. Focal increases in the modulation of single positions may be seen, suggesting an increase in attentional resources being allocated to updated pattern, but modulation also remains undeniably strong at the formerly biased locations. Note, however, that the bias change did not impose an explicit penalty to detecting increments at the obsolete locations- subjects were given the same juice rewards for any successful increment detection, likely or unlikely. Thus, if the long-term training made attention to the obsolete locations more trivial, it might be advantageous for the animal to maintain old allocations while incorporating new information on the updated biases to increase overall task performance. Whether persistence of attention is beneficial in naturalistic stimuli remains uncertain, but in this task there was a real disadvantage from this mismatch in trained expectation versus current probabilities: Monkey F's sensitivity was significantly lower (-2%, $p<0.05$, binomial distribution), but a larger effect was seen in a significant reduction of the positive predictive value (PPV) of saccades in both animals (P: -4%, F: -6%, $p<0.05$ in each). Thus both subjects' overall task performance was impaired by the change in contrast increment bias distribution.

While attentional modulations were less adaptive to the new probability distribution, the

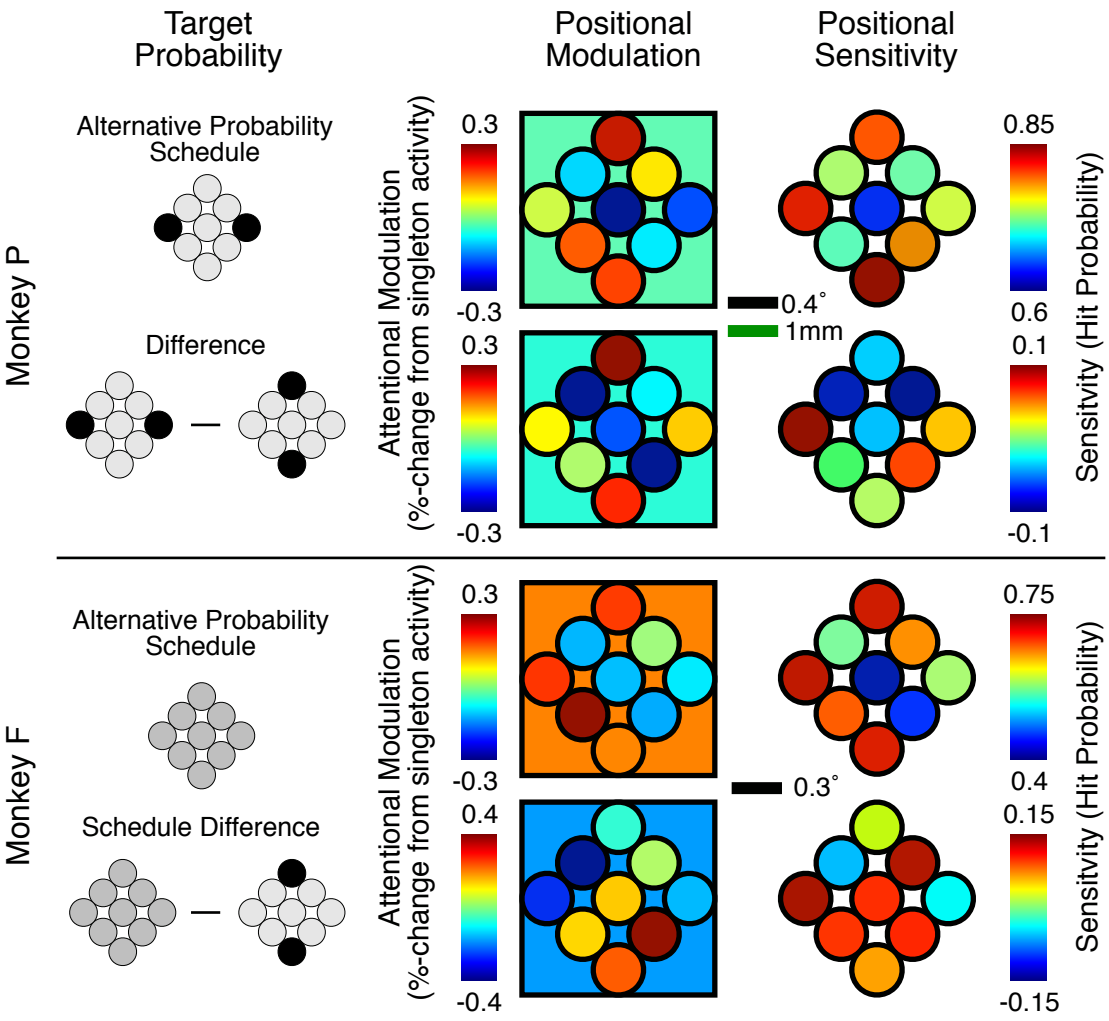

Figure 5.6: **Alternative Probability Schedules - Two-dimensional Distribution.** Abruptly, the long-term bias in target probability as a function of position was changed for each animal (left column). Monkey P was trained on a rotated probability distribution, where Monkey F was trained on a uniform distribution. Both animals changed their behavior (right) and attentional allocations (left) to accommodate the change, however performance remains imperfect. Top row for each animal shows the new distributions for the updated bias, and the bottom row shows a difference in performance between the two bias distributions. Format is otherwise the same as Figure 5.4. Both animals only partially adopted the new distribution and each had a tendency to maintain attention and improved performance at the obsolete bias locations.

correlation between positional modulations and positional sensitivity remained strong (Figure 5.7; sensitivity: r^2 =0.57, p<0.001), while reaction time now strongly correlated with the new modulation pattern (r^2 =0.56, p<0.001). Together with the increase in false positives, we interpret the reaction time data as a change in both subjects' strategies as they learn the new task. Correlating modulations with behavior across both probability distributions, we find that over half of the positional variation in increment sensitivity and one-fifth of the variation in reaction time may be accounted for by the appropriate allocation of attention to the V1 population representing each stimulus (sensitivity: r^2 =0.558, p<.001 reaction time: r^2 =0.219, p=0.004).

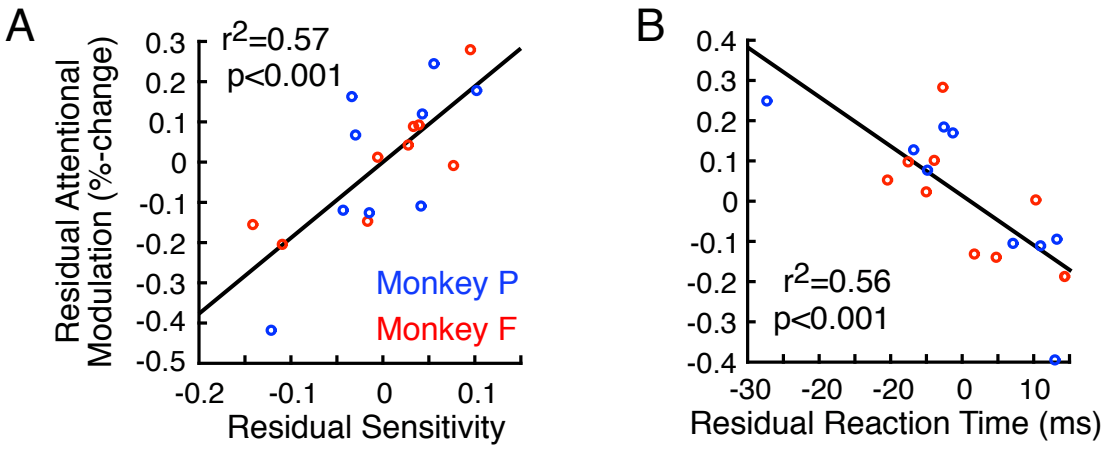

Figure 5.7: **Alternative Probability Schedules - Behavior Partial Correlation.** Under the new probability schedule (Figure 5.6), attentional allocations across V1 remain correlated with sensitivity (A) and with reaction time (B). The overall correlations between attention and sensitivity, including both the original and altered probability schedule across both animals (not shown), strongly suggest that these modulations are involved in stimulus perception (overall sensitivity: r^2 =0.558, p<.001; overall reaction time: r^2 =0.219, p=0.004).

It is still possible that the overall correlation across both task conditions hinges on a fixed, underlying mechanism as discussed above. This is particularly concerning given the suggestion that the subjects may not have fully abandoned their older strategies. To explore this, we performed a final correlation analysis between the differences in behavior and attentional modulation across the two probability biases (Figure 5.8). We found that increases in attentional modulation correlated with improvements in target sensitivity, with an additional trend toward correlation with decreasing reaction time (sensitivity: r^2 =0.26, p=.03; reaction time: r^2 =0.16, p=0.098). This suggests that, regardless of any common factors that influence our subjects across both task conditions, the distribution of V1 attentional allocations predicts the ability to detect changes in retinotopically matched objects.

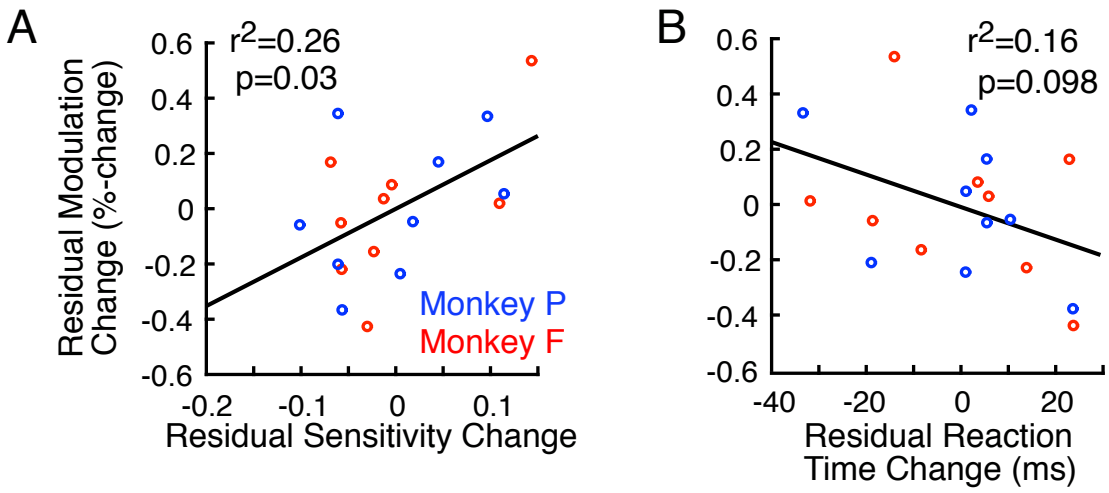

Figure 5.8: **Difference Between Probability Schedules - Behavior Partial Correlation.** As the subjects switch from the original to the alternative bias distribution, their behavior and attentional modulations change as a function of stimulus position. These changes are correlated. (A) The change in increment sensitivity correlates with the change in attention between the two bias distributions. (B) The change in reaction time shows a trend toward correlation with attentional modulations.

5.3 Discussion

5.3.1 Spatial Attention in Primary Visual Cortex

To date the highest resolution studies of attentional modulations within V1 rely upon electrophysiologic recordings. Even when using small stimuli, much like the single targets used in our study, these typically report modest effects: 0-10% increases in action potential firing rate are accompanied by non-specific changes in current source density or local field potential of the supragranular layers of V1[4, 70, 3]. By contrast, strong modulations (>30% in many neurons) are observed using paradigms that require the animal to make perceptual judgments using information encoded by V1 (e.g. curve tracing[154] or detection of small target changes[153]), but these paradigms do not naturally restrict attention to address the limits of these modulations. In this study, we combine these two concepts, small stimuli and V1-level decision making, to produce a task which evokes strong (±30-40%) attentional modulations within V1 that influence task performance over a measurably limited spatial extent.

Our paradigm was engineered to require the involvement of V1. Even if the stimulus is small and optimal for V1, such as a bar or Gabor, any stimulus presented in isolation can be reliably detected by higher-level visual areas with larger receptive fields by integrating over the task-responsive and unresponsive regions of V1. There is no need to manipulate the visual

representation as the finer V1 scale when modulation of higher areas with better connectivity to putative attention centers within prefrontal cortex[61] (e.g. the frontal eye fields) may be sufficient. As V1 does not receive direct [pre]frontal input[61], any attentional modulation of V1 from these regions must be multi-synaptic and therefore metabolically more expensive than modulation of higher level areas with a shorter network distance. Moreover, as V1 contains the lowest level visual cortical representations it also contains information closer to the ground truth of physical reality. If the attention system can accomplish target selection without perturbing this early map, it will allow one to preserve this representation while also performing the task at hand. This may serve to prevent inattention blindness[17] (which is known to impact early visual area MT[160]) to important low-level stimuli such as brief motion pulses which could signal danger. For these reasons, there is utility in limiting attentional modulations of V1 unless the task is spatially complex[4].

Our task, however, can not be solved simply by increasing the signal gain over the entire array, as might occur if only higher visual areas with larger receptive fields were modulated. Importantly, both subjects found it impossible to reliably detect contrast increments in the singleton stimuli at the same threshold that increments were detected in the array. Our task was only possible if subjects we able to to notice differential contrasts between adjacent stimuli. This forced the monkeys to make perceptual judgments over fine partitions of visual space on the order of V1 neural receptive fields. Note that this task requirement arose naturally from the structure of the stimulus array and was not explicitly instructed- the comparison of neighboring-element contrasts appears to be a natural strategy for both animals.

In contrast it is well-established that imaging studies of attention in V1, particularly fMRI, tend to show large modulations of V1 activity- up to 100% or more, on the order of the underlying visual signal. It has been proposed that this is due to the ability of fMRI to integrate a weak signal over the entire neural population contributing to the voxel's BOLD response (>1 million neurons)[93]. Like BOLD, the AF signal we measured in this study integrates physiologic responses from a population of neural and non-neural cells. While we can not rule out the possibility that AF imaging is similarly sensitive to subthreshold modulations, note that the scale of this averaging operation is much smaller in our imaging than in typical fMRI studies. First, by analyzing early time periods, we may rule out the influence of any hemodynamic signal including the pooling of responses within large venules[93, 161]. Second, the individual pixels in our preparation reflect an area of approximately 4E-4 mm^2, sampling the mitochondrial response from only hundreds of neurons. If the responsivity of imaging signals such as BOLD and AF to attentional modulations in V1 relied on a simple average of the modulations of many neurons, we would expect our modulations measured by AF to be much closer to the responses seen in single-unit studies. Given that we see modulations as strong as 40% at single positions,

this is clearly not the case.

It is also unlikely that the AF signal is representing non-visual and non-attentional information in our task. All modulations reported here are time-locked to the visual stimulation and are base-line subtracted- the signal due to non-neuronal background physiology is removed from our images. Moreover, as action-potential related changes account for the majority of the brain's energy consumption[114], we expect the mitochrondrial AF signal to closely approximate neural processing on short, stimulus-evoked time frames. Our estimates of the attention component of our signal are not corrupted either by visual information or by modulations due to task performance[58], as we only measure attention as a difference between two task conditions with identical task rhythm and visual stimulation.

Rather, we suspect that attentional modulations may readily reach V1, but that this process only exerts a strong effect when required by the task. The addition of this task requirement poses a non-trivial challenge to the simple model of attentional targeting that is proposed in this thesis: regardless of whether the task is easy or difficult, of whether stimuli are presented singly or hidden within an array, the most task-appropriate cell in the brain would remain the same V1 neuron whose receptive field matches the stimulus. Why, then, might attentional targeting be a function of task demands as well as the nature of the attended stimulus?

A substantial clue may arise from the mismatch between the target locations and their attentional modulations: in both animals, several continuous elements showed attentional modulations and a perfect selection of the bias targets appeared impossible, but none-the-less modulations were grossly targetable to at least one half of the array. Assuming the magnification factor of Monkey F and P's underlying V1 retinotopy is similar, this suggests both that attentional modulations may be precise to within 0.5-1 degree of visual space, but no more precise than 0.3-0.4 degrees (the interstimulus spacing of each animal). In cortical space, this represents precision at the scale of 2-3 mm but imprecision under 1mm. In agreement with these values, corticocortical feedback axons from V2 branch along 1-4 mm of the V1 cortical surface.

In postulating that the precision of V2-V1 feedback is a hard limit to the attentional selection of visual space, we imply that these feedback processes carry attentional information. V2 provides equal or greater input to V1 than does the lateral geniculate nucleus[162]- while this feedback has long been known to influence non-attentive processes such as contour end stopping and surround suppression[158], we imply that these same circuits also carry conscious attentional influences which may provide equally strong influences to V1 processing. Moreover, we provide evidence that attentional modulations must reach V1 by traveling through the visual hierarchy and that other feedback projections to V1 do not provide more precise spatial information.

5.3.2 Attentional modulations of V1 variably impact performance

We demonstrate a strong correlation between attentional modulations in V1 and task performance on the scale of fractions of a visual degree, and show that these modulations can support trained(Figure 5.5) and untrained (Figure 5.7) attentional patterns. Moreover, V1 modulations facilitate the change between patterns (Figure 5.1). This suggests that our observed attentional modulations within V1 are not simply the result of longitudinal training but rather do respond flexibly to changing task demands.

However, the nature of the behavioral improvements associated with V1 attentional modulations appear to be a function of other variables in the animal's global state. With the original, highly trained position bias, both subjects were less likely to make a false positive saccade. However, when exposed to an alternative bias distribution, the sudden task uncertainty causes an increase tendency for invalid saccades in both animals. At the same time we observed a strong correlation between positional reaction time and attentional modulation when attending to the alternative but not to the original bias. We interpret this as the animals changing the speed-accuracy trade off of their V1 readout task uncertainty increases and they must learn the new bias distribution. This may occur as a result of coincident modulation of other visual areas, or through changes in how both animals convert continuous visual information into a binary perceptual decision[47]. Thus the effects of V1 attentional modulations on task performance are not constant, but rather change as a function of greater task demand. This provides a novel route for further flexibility within the attention system.

5.4 Methodology

5.4.1 Subjects

Two adult male rhesus macaques (*Macaca mulatta*, 13.5 and 9.8 kg) were enrolled in this study. The two subjects were fluid restricted and trained using positive reinforcement to perform a change detection task in return for a fluid reward (Gatorade). All experimental procedures were approved by the Institutional Animal Care and Use Committee of the University of Minnesota, an Association for Assessment and Accreditation of Laboratory Animal Care International accredited organization. Both subjects were attended daily by professional veterinary staff and had daily access to food, activity, and audiovisual enrichment.

5.4.2 Behavioral Paradigm and Analysis

Two macaques (Monkey F and Monkey P) performed the change-detection task outlined in Figure 5.1. Subjects maintained fixation within 0.5° at a 0.125° white fixation dot for a long

(variably 500-2000 ms, uniform distribution) prestimulus period after which two 3x3 arrays of small (F: 0.3°, P: 0.4° diameter) Gabors appear symmetrically on screen, one each in the left and right visual hemifields. The array elements are positioned such that the middle column is isopolar along the vector from the fixation point to the center of the array- the remaining 6 Gabors are distributed in neighboring columns parallel to the isopolar column. The Gabors are high contrast (F: 35%, P: 20%) and continuously drift (4 Hz) in order to strongly activate V1 neurons. Gabor orientation and drift direction are uniform across each array, but are balanced between stimulus arrays such that net motion along the horizontal axis is zero. The spatial frequency of each element is appropriately scaled such that one full cycle is always present. Visual stimuli were generated using custom software, and presented on a CRT monitor with 85 Hz refresh rate positioned 495 mm from the subject. Subject eye position was continuously monitored with a monocular iViewX infrared camera and analyzed on-line with the same custom software. On-line deviations of 0.9-1.4 degrees from fixation were permitted; this lax window was required for subjects to maintain fixation for 8 seconds per trial. Larger deviations caused trials to immediately abort with no reward; this typically occurred only during saccades or eye blinks. During off-line analysis, only attention data collected from the time period between the onset of the stimulus array and the first fixation deviation greater than 0.5 degrees are analyzed. Typically, this excludes a large microsaccade.

At a random time (400-6150 ms, exponential distribution with uniform hazard function), one of the 18 Gabor elements briefly (94 ms) increased contrast (P: to 32%, F: to 52%). The increments were difficult to detect and the task required the subject's constant vigilance. For both subjects, task performance was well distributed between true positive, false positive, and false negatives. The overall hit rate to detect targets was 62.5% for Monkey F and 81% for Monkey P. The predictive value of a saccade was 52% for F and 70% for P. On 10% of trials, no contrast increment occurred and subjects were rewarded for maintaining fixation. Both subjects performed the task at their maximum tolerated difficulty (the smallest tolerated contrast increment) in order to force the greatest possible amount of attention to the targets- adjustments of 1-2% to the contrast increment caused a precipitous decrease in overall behavioral performance in both animals (observed during on-line analysis but not shown).

If subjects reported detection of the increment via a saccade to the target array, a juice reward was administered along with a positive sound cue. If subjects broke fixation from the central dot for any other reason, the trial was aborted with no reward and a negative sound cue. At this task difficulty, both animals exhibited a strong tendency to make a false positive response early in the trial (consistent with a high-uncertainty, guess-based strategy). To reduce this tendency without sacrificing the visual difficulty (attentional demand) of the task, we made several manipulations to the reward and intertrial schedule. The juice reward administered

on a given trial was non-random and increased exponentially with successive true positive or true negative responses, up to a maximum of one second of continuous fluid administration. This reduced the expected value of continuous guessing, as randomly correct performance would usually administer only the smallest reward. Moreover, when a false positive response was recorded, the next trial was delayed by a period of time equal to the time remaining in the trial. This provided a maximal punishment time-out for early guesses (to discourage the animal from rapidly cycling through trial attempts) but only minimally punished a putatively effortful false positive that occurred later in the trial. While the effect of these performance manipulations was not carefully measured, the end result was that both subjects maintained effort in spite of a very difficult task for which a juice reward was administered infrequently relative to a more typical macaque behavioral paradigm (on some days, including fixation breaks, <30% of trials resulted in a juice reward). Physiologic fluid requirements for each subject were met daily and exceeded weekly via supplementation with unflavored water as necessary.

To manipulate visuospatial attention, the probability that the increment would occur at a given target position was non-uniformly distributed. The subjects were given two different cues to direct attention to a subset of the stimulus elements. First, in each trial block (20-25 trials), the increment would occur in either the left or the right hemifield on 96% of trials. This left/right cue was explicitly given to the subjects by a series of 4-5 instruction trials preceding each block during which only the likely hemifield was stimulated. A second cue was given to the animals in the form of their training history. For months prior to imaging data acquisition, the same two target locations (one on the foveal and one on the peripheral side of the array) were eight times more likely to increment. Prior to imaging, both animals demonstrated a behavioral preference for detecting increments at one or both of these locations. The same locations are biased during training and image acquisition, except that in the final data collection sessions for each subject the intraarray locational bias was abruptly changed. In Monkey F, the bias was remove completely and replaced with a uniform probability distribution. In Monkey P the bias was rotated such that the opposite corners of the array were now eight times more likely to increment. The new bias was then held constant over several imaging sessions.

We estimated the subjects' overall task performance by fitting both increment sensitivity (the percentage of detected contrast increments) and saccade positive predictive value (PPV, the percentage of saccades that correctly identified an increment) over all positions to a binomial distribution. To estimate detection performance at each position, we only considered the sensitivity to each position's increments as we could not reliably determine at which position an increment was falsely perceived during false positive saccades. When plotting these data linearly, we collapsed the two-dimensional array of positions into a one-dimensional representation by averaging all positions that were equidistant from the foveal and peripheral bias location (the

vertical axis in Figure 5.1C).

Each subject also performed a similar task during 'position tuning' sessions in which only a single Gabor was presented, of the same size as and at one position of those in the 3x3 array experiment. The purpose of this was to record the visually evoked activity across V1 attributable to each individual stimulus element. During these position tuning measurement trials, the subjects detected a larger contrast increment which always occurred within the single Gabor; both subjects were unable to detect the original contrast increment within a singleton Gabor and required this easier detection.

In a variant of the position tuning task, subjects detected singleton stimulus contrast increments over a variety of stimulus radii and base contrasts. Imaging data from these trials was used to verify the visual response of the chamber but was not otherwise utilized during subsequent analyses.

Immediately after the chamber implantation and prior to position tuning and task performance, both animals also participated in conventional retinotopic mapping of the chamber. Estimated retinotopy from these methods was used to place the stimulus array in an appropriate location within the visual field, but no analysis of task performance or attentional modulation relies on these traditional retinotopic measurements- all correlation between task signals and individual stimulus positions utilizes the position tuning measurements described above.

5.4.3 Image Acquisition

Utilizing sterile surgical technique while subjects were under general anesthesia, we made a craniotomy and durotomy over V1 of each subject. V1 was identified anatomically by visualization of the operculum of V1 (ensuring that the exposed region of V1 is not near the lunate sulcus and V2/V4) and by cranial landmarks. To maintain patency of the craniotomy and durotomy, a biocompatible polymer (polyethyl ether ketone) imaging chamber and transparent artificial dura were placed over V1. The artificial dura was stabilized between behavioral sessions with a rigid chamber insert. Prior to each imaging session, hygienic cleaning of the skin, exposed implant surface, and the dura margin was performed. To reduce physiologic movement artifacts and glare, the subdural space of each animal was flushed with sterile normal saline via tubing inserted through the artificial dura, and the imaging chamber was filled with sterile normal saline.

After recovery from surgery, both subjects performed the task seated upright and comfortably while V1 was imaged with a Cascade 512b charge-coupled device camera. The camera was suspended over the animal's exposed V1 and held rigidly to the behavioral apparatus. Focus was manually adjusted daily onto a plane 0.5-1.0 mm below the surface of the brain. Differences in the field of view of the camera between different behavioral sessions (due to small changes in

the position of the subjects, their behavior chairs, and the camera) were tolerated and corrected with off-line image registration (see below). The camera acquired a 256x256 pixel image spanning $\approx 8\times8$ mm of the cortical surface five times per second. The implied resolution of these images is thus 23.4×23.4 μm/pixel. The chamber was illuminated with blue light (415-485 nm band-pass Chroma D455/70x filter); with Monkey F we used a DC tungsten light source and with Monkey P we used a light-emitting diode to reduce illumination noise. In a set of control experiments targeting the hemodynamic intrinsic signal instead of the AF signal, the chamber was illuminated with red light. Light entering the camera was again filtered (520 nm long-pass Chroma E515LPv2 filter) before pixel binning, on-chip multiplicative gain (15-20x amplification), and digitization to generate a monochromic, unsigned 16 bit integer image. The same custom software used to present visual stimuli also collected these images, tagged each image with a time stamp relative to behavioral task events, and saved the images to disk for off-line analysis- on-line analysis of images was limited to ensuring appropriate camera positioning and focus.

5.4.4 Off-line Image Processing

Each image was converted from a RAW bytestream to MATLAB 16-bit arrays using custom conversion software. Each image was reoriented to reflect the true left/right and up/down axes, and hardware-level image acquisition errors (e.g. image tears) were detected and eliminated using custom MATLAB code. Within each behavioral trial, motion correction between images was performed by selecting the first image acquired after stimulus onset and then translating all other images from the trial such that the mutual information between all images was maximized. Across behavioral trials, differences in the position and angle of the camera were corrected for by a 6 degree of freedom affine registration between the two images series. Intratrial motion correction was automated using gradient descent methods, but intertrial motion correction required substantial manual intervention. Errors due to manual imprecision were minimized by oversampling the number of registration points between images using 9 instead of the minimum 3 control points.

Because the animals are seated up-right and the chamber protrudes from the parietal bone at an angle, the gravitationally determined water line is not normal to the brain surface and a small hyperintense glare is present from the illuminator in nearly all images from the anterior portion of the chamber. Hyper- and hypointensities are also present near the edges of the artificial dura. Such abnormal regions of each image were liberally masked by thresholding each image and then further removing a 5-pixel edge from the edge of the thresholded image, and the motion-corrected images from each trial were then converted to units of percent-change by dividing each trial's image series by the respective trial's first post-stimulus image. The image series from each trial was aligned to the onset of visual stimulation, and images occurring before

fixation or after either a fixation break/saccade or after a contrast increment were discarded. These aligned image series were averaged for each stimulus condition.

5.4.5 Individual Position Tuning

Once the approximate retinotopic location of V1 within each imaging chamber was found using standard methods[111], we measured the pattern of activity evoked across the chamber when each individual stimulus element of the array was presented in isolation. In Monkey P, the individual stimuli evoked a clear and reliable distribution of V1 activity across adjacent locations that matched the known topology of the retinotopic map. However, the evoked activity from individual stimuli typically demonstrated a negative response that lasted several seconds- this is very typical of the known time course and signal directionality of hemodynamic signals that are known to potentially interfere with AF signals[112]. In relating position tuning from Monkey P to his attentional modulations (which were positively signed), we inverted the sign of his position signals such that estimates of stimulus position were positive for the receptive field centers of each element.

In Monkey F, we mapped position tuning preferences with smaller stimuli, at a higher contrast, at a more foveal location, and through a layer of neomembrane (a thickening of the remaining layers of dura that occurs naturally as the imaging chamber ages). The net result of these differences is that each individual element evoked a wide-spread activation pattern including the entire imaging chamber. None-the-less, this pattern was distinct for each position, with centers-of-mass that crudely aligned with retinotopic topology. Seperable regions of activation for each position emerge in Monkey F's position tuning estimates over the same timecourse as seen in Monkey P. Thus while we could not create a 1-to-1 mapping from V1 pixels to stimulus positions, we could still construct for each pixel a position tuning curve. Using these tuning curves, we can use multi-pixel pattern analyses to decompose primary task activity across the chamber into a discrete prediction of activity within the neural representation of each stimulus position (see below).

Informed by these position tuning estimates, we manually selected a region of interest within each chamber that included responsive pixels for all nine stimulus positions plus surrounding cortex. This ROI included 39,414 pixels (21.6 mm^2) from Monkey F and 16,698 pixels (9.17 mm^2) from Monkey P. The larger ROI of Monkey F includes the larger extent of his position tuning evoked activity. Differences in the images area between animals are controlled by performing pixel-wise analyses separately for each animal before combining data.

5.4.6 Analysis of Attentional Modulations

We observed both a substantial visual-evoked and a non-visual, non-attentive response from V1 under all task conditions. Monkeys performing tasks with a similar structure (cycling between intertrial, stimulus, and response epochs) have shown a large intrinsic signal change in V1 that is correlated with the dynamics of the task independent of visual stimulus[96]. To control for visual and non-visual signals, in our study we exclusively study attentional modulations as defined by the difference between images collected while animals attend the stimulus in the hemifield contralateral to the imaged hemisphere ("attend in") and images collected in the opposite cue condition ("attend out"). We discarded trials which were shorter than 1 second, as they did not contribute sufficiently to our targeted attention period (600-1600 ms post-stimulus).

By averaging hundreds of trials of each type together (Monkey P, 847 Attend In trials, 881 Attend Out trials; Monkey F, 502 Attend In trials, 503 Attend Out trials), we obtained an estimation of the distribution of attentional modulations across the cortical surface. After finding that in both subjects the sign of the attentional modulation is positive from 600-1600 ms after stimulus onset, we averaged data from that time interval to generate a mean attention modulation and mean single position evoked activities. Use of data from the early trial period also avoids conflict between mitochondrial and vascular sources of optical signal[112]. We decomposed this mean attention into an estimate of activity at distinct positions by performing a multiple linear regression of the attention map against the activity patterns evoked by each individual position. That is, we modeled the attentional map as a linear sum of the individual positions' visual activity maps

$$MeanAttentionalModulation = \sum_{pos=1}^{9} \beta_{pos} \times MeanSinglePositionEvokedActivity_{pos} + C \tag{5.1}$$

where the beta values are computed by standard linear regression. We use these beta values as measurements of "Positional Modulation." This regression analysis has one crucial advantage over a region-of-interest based analysis, in that it naturally accommodates pixels that are on the border of the V1 representation of two positions and this respond to both stimulus elements. Due to the point spread function of the AF signal[112], the measured representations may overlap even though the stimuli do not overlap in visual space.

Both attentional and positional activity terms in 5.1 are vectors containing data from all pixels in the visually responsive region of interest within each animal's V1. This regression analysis considers attentional modulations toward a given stimulus as an all-or-nothing linear change including all images pixels in the center and surround fields of each position's visually evoked response. Non-linearities may be implied by the map of residual attentional modulations

which are not accounted for by this model, but such residuals are not further explored in this report due to the inferior retinotopy of Monkey F.

To improve the overlap between position tuning and attentional modulation images, we smoothed all composite images by a 116 μm Gaussian kernel. The activity maps for each position were not normalized- thus each beta may accurately be interpreted as the proportion of that position's activity that is present within the attention map. For example, a beta value of 0.2 would imply an attentional modulation that is 20% of the magnitude of the position's original evoked activity.

To compare V1 physiology with subject behavior, we computed partial correlations between positional attention and sensitivity that remove the influence of the probability distribution of the stimuli from both the positional modulations and the behavioral distributions. This allows us to explore whether variation in attentional modulations correlate with variations in task behavior without confounding this relationship with the increased task performance at high probability locations. The partial correlation is computed as the Pearson's R correlation coefficient between the residuals that remain after the probability distribution is independently regressed out from the positional modulations and behavioral distributions. For this analysis, due to the sparse sampling of behavior at the unbiased locations we used sensitivity computed from all time points. Our major conclusion, that positional attention is correlated with contrast increment sensitivity ($r_{partial}$=0.414,p<0.001, Figure 5.7, still holds when sensitivity is restricted to stimuli presented during the analyzed time period with timing adjusted for the delayed AF impulse response function ($r_{partial} = 0.164, p = 0.014$). The partial correlation for reaction time is reduced to a trend by restricting analysis to early correct trials ($r_{partial} = 0.076, p = 0.108$).

In Monkey F, the same factors that decreased the quality of our position tuning (small, closely packed, high contrast stimuli, larger fixation variance) also may account for increased surround suppression within his stimulus sensitivity measurements. This is readily observable as higher sensitivity to detect increments at the corners of the stimulus array (the least crowded locations) and reaches statistical thresholds for significance in Monkey F but not in Monkey P (Table chapter:imaging::table:betavalues). For Monkey F, we also removed the influence of surround suppression in his partial correlation analyses. This improves the relationship between behavior and positional modulations in Monkey F, but outcome of our correlation analyses over the full data set are robust to the inclusion or exclusion of the surround suppression term in either animal.

	Monkey F				Monkey P			
	Original		Alternate		Original		Alternate	
	Bias	SS	Bias	SS	Bias	SS	Bias	SS
Modulation	0.25	0.01	-	-0.01	-0.22	-0.01	-0.09	-0.04
(p)	0.69	0.97	-	0.44	0.75	0.83	0.82	0.14
Behavior	0.20	*-0.05*	-	*-0.04*	0.28	-0.01	-0.12	*-0.03*
(p)	0.50	*0.04*	-	*0.02*	0.17	0.62	0.35	*0.00*

Table 5.1: Regression beta values for controlled variables in the behavior versus positional modulation partial correlation. Bias term not included in Monkey F's Alternate bias because it was uniform. Suppression term is justified in Monkey F's original bias set, but not Monkey P's. Bias, the probability distribution of increments; SS, surround suppression.

Chapter 6

The biologically plausibility of selective targeting

The data we presented demonstrate that selective targeting of attentional modulations occurs within V1 under two distinct task conditions. Given that V1 is the earliest stage of cortical visual processing and is therefore the furthest (in a hierarchical sense) from the cortical areas thought to mediate attentional selection[61], observing selectivity within V1 is strong evidence that precise selectivity may be a fundamental property of attentional modulations throughout the visual system. From this, we propose that attentional modulations are targeted to the most task-appropriate neurons within the brain, with at least the precision of local horizontal/feedback connections and functional columns. In order to account for the selective modulations we have observed within V1, the neural and cellular mechanics of attentional selection must be inherently flexible and capable of shifting a modulatory signal throughout the visual system in real time to match the current task demands. As discussed in Chapter 2, attention as an "active" selection process requires a greater degree of neural complexity than might an alternative "passive" mechanism.

Our model's relative complexity remains to be addressed: how might the brain implement selective targeting? Is there actually a physical one-to-one map between conscious attentional efforts and functional domains of visual cortex, or do these specific modulations arise as a function of local circuitry? I have not performed rigorous theoretical modeling nor simulated biologically plausible circuitry implementing these selective processes. Moreover, our data only explore the effects of attentional selection upon V1 and provide less evidence for one or another model of attention in higher cortical areas. Thus the optimal neurobiologic explanation of these findings remains to be determined.

In this chapter, I will review the current knowledge about the role of known corticocortical feedback projections in V1, and relate the precision of this feedback to the precision of modulations we have observed. Grossly, our data may be found consistent with two distinct models of attention which postulate distinct origins to the modulations we observe in V1. I will introduce these models, and briefly propose a series of experiments and simulations to disambiguate between these two model families.

6.1 Non-retinal inputs to primary visual cortex

Figure 6.1 schematizes the findings from the two studies presented in this dissertation. In both studies, we find that attention may selectively modulate task-appropriate subpopulations of V1, and that the extent of these modulations may be directly related to overall behavioral performance on sensory tasks. These findings allow us to immediately reject models of attention that postulate an insignificant role of V1 modulations. V1 is not diffusely modulated, but rather appropriate functional domains in V1 are precisely targeted for enhanced processing. These modulations do not merely reflect non-specific feedback from higher areas- we conclude that V1 attentional modulations support improved task performance in a direct manner.

This schematic illustrates significant differences between the two tasks we studied. In attention to orientation, we find a diffuse modulation is (on average) targeted to task-appropriate V1 orientation domains across all of V1. This suggests that attentional modulations within V1 may occur with precision on the scale of orientation tuning columns. However, the spatial attention study demonstrated that attentional modulations had a clearly limited precision- attention may modulate an area of V1 corresponding to a fraction of the 3x3 stimulus array, but we did not measure specificity for the individually trained stimulus elements. This suggests a more limited resolution for attentional modulations, on the order of 2mm of cortical space.

How can attention operate with columnar specificity over a wide swath of V1, but with much poorer specificity when the attentional focus is more narrow? This apparent contradiction suggests that the attentional modulations may not emerge from within V1. As a counterexample, one might postulate that intrinsic microcircuits within V1 may selectively enhance the activity of individual cortical columns to meet task demands, but in such V1-intrinsic models we would expect the emergent attentional modulations to have a similar cortical resolution under all task conditions.

Models overemphasizing V1 are also inconsistent with the general consensus that attentional signals originate outside of early visual cortex[33]. Histologic studies demonstrate that V1 receives feedback and modulatory projections from an enormous range of cortical areas[61, 162, 163], and the neuromodulators acetylcholine[164, 165, 166, 167, 164] and to a lesser degree

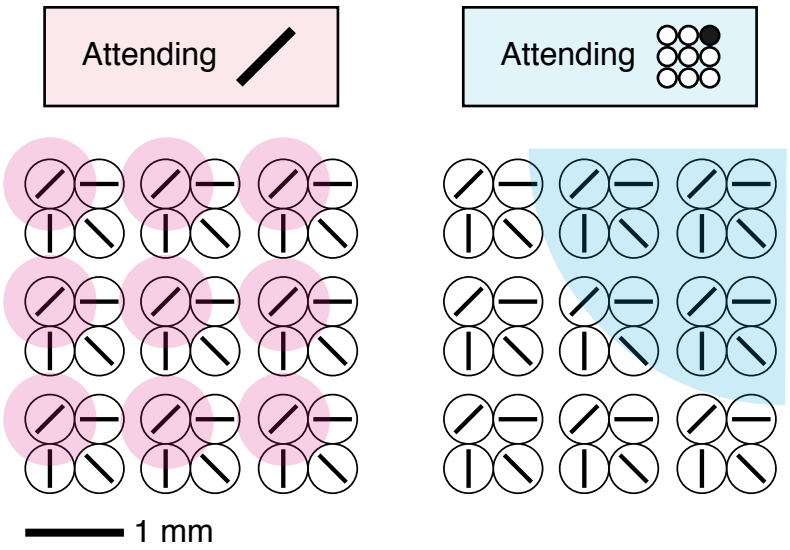

Figure 6.1: **Schematized outcome of presented data.** The inferred distribution of attentional modulation for two orthogonal task conditions is shown on a diagram of V1. Each circle represents a column of neurons with similar orientation tuning, where separation of orientation columns is approximately to scale. In Chapter 4 we demonstrated that attention to one orientation (magenta) caused BOLD signal modulations within voxels whose population-level orientation tuning curve was aligned near the attended orientation. This suggests that attentional modulations must be targetable at or near the scale of cortical columns, with less than 1 mm precision. In Chapter 5 we demonstrated that attention to a small point in visual space (cyan) caused AF signal modulations across a relatively diffuse swath of V1, as though attentional modulations were precise only to a precision of 2 mm or more.

norepinephrine[165] are suspected to play a role on facilitating attentional modulations directly or through subcortical pathways. However, robust feedback connections from dorsal lateral prefrontal cortex, the frontal eye fields, especially of a scale required to facilitate column-specific modulation, have not been discovered in V1[61]. Feedback from posterior parietal cortex (the parietooccipital area[168] and perhaps the posterior[168] or ventral[169] intraparietal area)to V1 has been reported, but these pathways were weakly labeled on only some tracer injections in some animals. We conclude that parietal feedback pathways to V1 are too sparse to represent a high-precision, one-to-one map of the V1 retinotopy as we would expect to see for selectively targeted feedback.

Rather, the primary source of corticocortical feedback projections entering V1 is retinotopically-matched V2, which provides one third of all cortical feedback to V1[162]. The role of V2 feedback in facilitating curve-completion and surround-suppressive responses in V1 has been well-documented[158, 170, 171]. The V2-V1 circuit is a well-studied feedback system, and V2 feedback strongly modulates stimulus representations in V1. V2 has not, to our knowledge, been inactivated or manipulated during measurement of attentional modulations in V1, and so a definitive role of V2 in facilitating attention within V1 is not proven. However, the carefully documented anatomy of the V2 feedback axon is of particular interest in considering possible sources of V1 modulatory signals.

In Figure 6.2, a V2 feedback axon[11, 12] is imposed on our V1 schematic. Three critical properties of the feedback projections are demonstrated. First, the feedback is, to a first approximation, retinotopically matched. Second, the feedback projections are also functionally matched: V2 cells of a given preferred orientation have a tendency to project to similarly oriented functional domains of V1. Finally, many V2 feedback axons are not restricted to a single cortical column in V1. Rather, the axons ascend to Layer 1 and turn, converting into the horizontal projections that are observed in Layer 1 throughout the neocortex. These horizontal projections continue along the cortical surface for 1 to 4 mm, and these feedback axons generate synapses onto V1 pyramidal dendrites along this entire distance. Thus the individual feedback axon is expected to stimulate an approximately elliptical region of V1 with a major axis of 1-4 mm. The direction that V2 feedback horizontal axons travel along the cortical surface is not random- they appears to follow the V2 cell's preferred orientation along the retinotopic map of V1[12]. To simplify this discussion, we will however assume that the precision of the individual V2 feedback axon is a 2 mm circle and not consider the direction of horizontal connections. This simplifying assumption is justified by the fact that our spatial attention data average together modulations to stimuli of different orientations.

These anatomic features of V2 feedback provide an elegant explanation of the differences in precision we observe between our two attention tasks. When attending to one orientation,

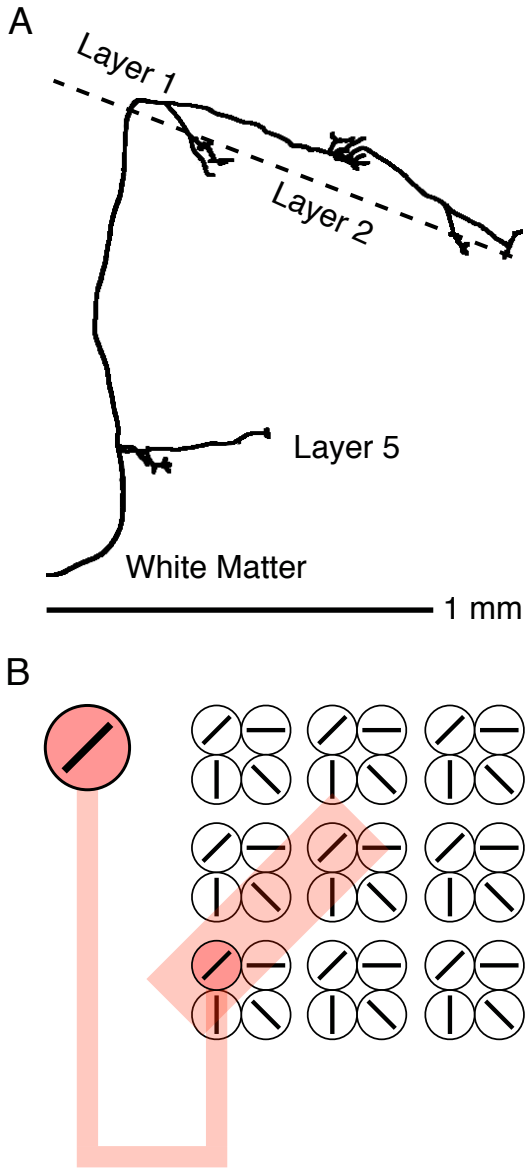

Figure 6.2: **Corticocortical feedback axons in V1.** (A) Reconstruction of a representative feedback axon projecting from V2 into layer 1 of V1, adapted from [11]. The horizontal connection in Layer 1, with multiple synaptic foci made over 1-4mm, is typical of corticocortical feedback in V1[11, 12]. (B) The axon is imposed in our V1 schematic. Above 60% of V2 feedback axons target orientation preference-matched populations in V1[12]. The range of the horizontal connection is similar so the amount of imprecision reported in Chapter 5.

multiple feedback axons from V2 neurons might target different regions of space but always with the center of their modulations appropriately aligned to the attended orientation regions in V1. Modulation of other orientation columns is expected but should be weaker due to the summation of the modulations from multiple feedback axons all converging onto the attended orientations. Meanwhile, when attending to small regions of space, no such averaging is possible- only the retinotopically-matched V2 feedback is useful for the task, and these feedback projections are fundamentally limited to a ≈ 2 mm extent along the cortical surface due to the anatomy of the feedback axon.

For these reasons, I propose that the simplest explanation for the distribution of modulations that we observe within V1 is that the modulations are distributed through and thus limited by V2-V1 cortical feedback. In both cases the modulations we observe are as precise as is permitted by V2 feedback. The attention system does not appear to have direct access to V1, but rather must influence it indirectly through manipulation of V2 or other high-level areas (e.g. the pulvinar[172] or reticular[13] nuclei of the thalamus). This is not to suggest that the modulations we documented in V1 merely represent sub-attentional feedback from V2, but simply that V2 gates and filters attentional modulations before they reach V1. Our model suggests that, for appropriately designed tasks, it is still optimal for attention to modulate V1 neural populations and so it appears to do. It is just that the precision of attentional modulations is limited in this regard.

6.2 A Selective Spotlight Model of Attention

Even given the anatomy of V2-V1 feedback, it is surprising that precision at the level of V2 cells is observed within V1. Consider an ultimate extension of this simple imprecise-feedback model: if feedback is carried through a reverse visual hierarchy, we would expect similar imprecision due to horizontal connections and receptive field divergence between each layer of visual processing. The net result should be that even the most precise modulations are hopelessly blurred by the time they are carried from the forebrain and prefrontal cortex, through temporal and late occipital areas, and finally to V2 and then V1. Given the V2-like precision of modulations that we observe, one must rather conclude that the regions of the brain that originate and target attentional modulations must have direct access to V2 or another very closely located visual area.

Metaphorically, attention has been described as a "spotlight"; attention may be steered, reallocated, and reoriented to improve the processing of different stimuli much in the way a stagehand may steer a spotlight to improve visibility of different areas of a theater. In homage to this description, I describe our postulated direct modulation of the V2 representation as evidence

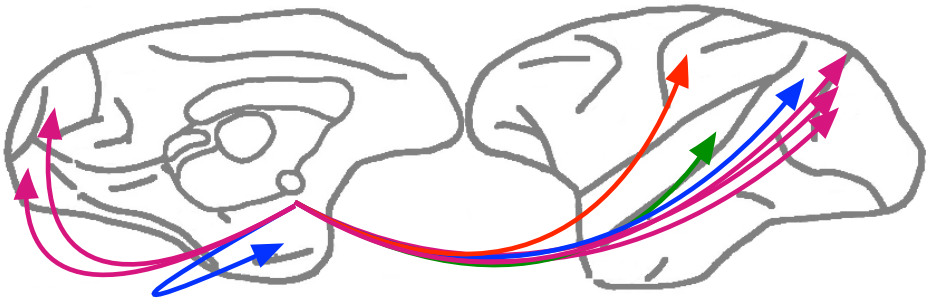

Figure 6.3: **Selective Spotlight Model of Attention** The Selective Spotlight Model assumes that a literal implementation of the metaphorical "attentional spotlight[13]" is the best explanation for our finding that V1 attentional modulations are no more imprecise than V2 feedback axons. A source of attentional modulation (depicted here from the basal forebrain only for the purpose of demonstration) may directly target modulations to V2 (magenta) when attending to small regions of space, but these modulations do not reach V1 with retinotopic precision. Distinct connections to other task-relevant brain regions would underlay attention to higher-order visual stimuli (blue), to sounds (green), to touch (red), et cetera for other forms of attention. However, any region lacking a connection from the spotlight would only receive indirect attentional modulations and so attention to such stimuli would suffer.

toward a Selective Spotlight Model of attention. Here, we describe attentional modulations as a near-literal "spotlight" of enhanced neural activity that may be directed across a wide range of sensory areas. Some representations, such as those in V1, may not be directly modulated but may be influenced by feedback from directly modulated regions. However, in allowing the spotlight to be directed toward as far as V2, we imply that the spotlight has access to an incredible range of sensory areas. This "strong" spotlight might be directed toward V2 for the greatest spatial precision, or it might be directed toward a higher level area with position-invariant orientation tuning for the greatest orientation discrimination (Figure 6.3). Presumably, in order to facilitate other sensory modalities, the spotlight also has direct access to auditory, somatosensory, and other sensory cortices.

6.3 A Selection-Stabilization Model of Attention

Although the Selective Spotlight model provides a parsimonious account for our data, it is weak to several lines of criticism. Foremost, we have only removed one area, V1, from the spotlight's range. We should then still expect to see evidence of direct and retinotopically precise connectivity between V2 and premotor attentional areas sufficient to explain targeted modulations. While V2 does receive more feedback from higher visual areas than V1 (including more of parietal cortex (medial superior temporal area and more from VIP) and conflicting

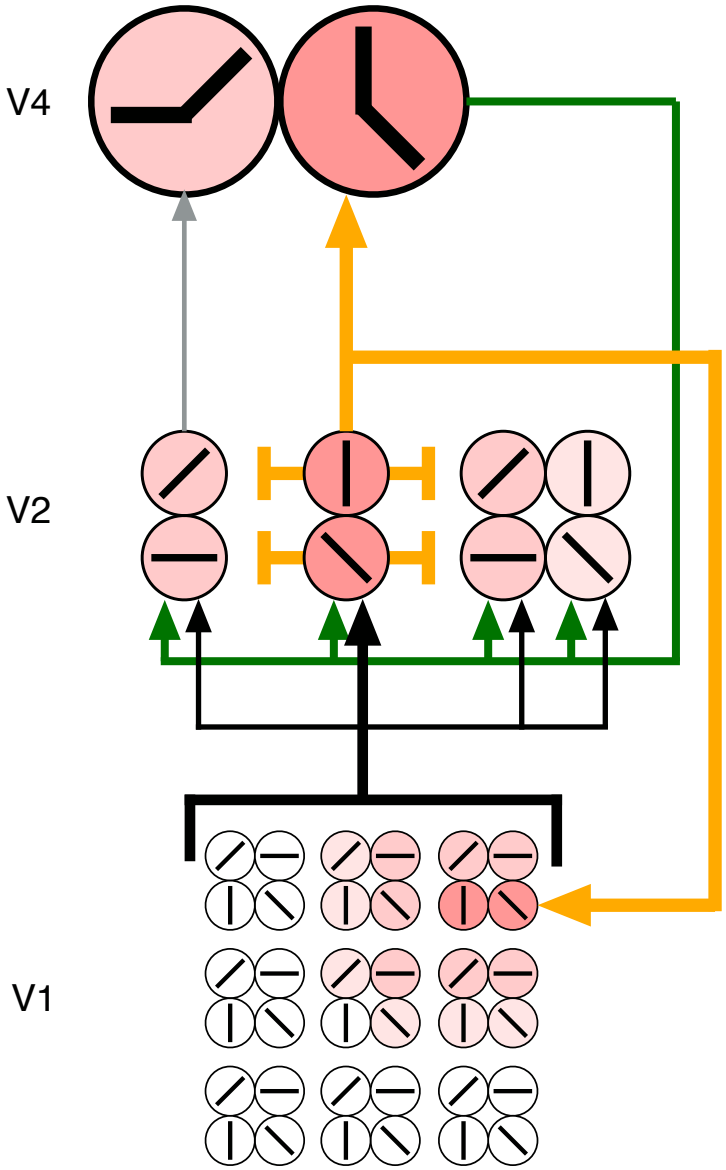

Figure 6.4: **Selection-Stabilization Model of Attention** A hypothetical schematic of attentional modulations propagating from V4 (top) through V2 (middle) and down to V1 orientation columns. A feedback population from V4 diffusely modulates a range of V2 cells with varying tuning properties. However, feedback loops between V2 and V4 along with lateral inhibitory processes within V2 limit the ability to task-inappropriate neurons to provide further feedback to V1. As a result, only task-appropriate modulations are sent from V2 and observed within V1, even though each stage of feedback was initially diffuse- in this manner the selected attentional target is stabilized within each layer of the visual hierarchy.

reports of direct frontal eye field feedback[61]), it is not clear from the available literature that V2 or even area V4 are sufficiently strong recipients of direct, retinotopically matched [pre]frontal feedback. It is possible that attentional modulations reach V4 and V2 with retinotopic precision through the pulvinar or reticular nuclei of the thalamus, which are strongly suspected to play a role in attentional modulations[173, 174, 175]; such cortico-thalamo-cortical modulations are an active topic of research.

A greater philosophical challenge is posed by the Selective Spotlight model. In suggesting that attention is mediated by direct connections to small, task-relevant pools of neurons, one implies that attention is limited by whether such direct connections exist. This is at odds with the ability of human observers to rapidly orient attention to novel or unique visual stimuli[176], or to conjunctions of stimuli that have never been previously encountered[177]. In order to account for the full flexibility of the attention system, one must postulate a nearly infinite number of spotlight-mediating projections even to areas of sensory cortex for which an attentional spotlight has never been required. While attention is known to improve with training, is it conceptually difficult to consider that training might involve the de novo growth of a new white matter tract. One solution to this is that novel attention strategies are generated by combining or sequencing multiple existing strategies[177]- this may account for novel conjunction or multimodal strategies, but still may not explain responses to novel objects, textures, or visual primitives.

In considering this contradiction, one need re-evaluate the central observation that led us to conclude V2 is directly modulated in our task: we expect indirect modulation of V2 to be as diffuse as V2 feedback is onto V1, and thus we would expect that V2 can not transmit indirect modulations with such fidelity as we observe. Suppose, however, that V2 was able to refine its diffuse feedback signal before transmitting it on to V1. As a simple example, a V2 feedback axon might increase its action potential firing rate if it also receives feedforward information from V16.4. In this way, attentional modulations from V2 to V1 would not be a one-directional but rather exhibit positive feedback, actively selecting for and stabilizing only attentional modulations that map onto the observed stimulus while also enhancing visual signals that match the attended stimulus. The combined V2-V1 circuit could thus actively discard task-irrelevant modulations within V2.

Feedback within the visual system is complex[178, 61], and the observed effects of feedback go beyond the simple gain modulations we have proposed to underlay attentive processing. For example, feedback from V2 is thought to be the origin of the surround receptive field of V1 neurons[158]. At a higher level, it has been shown that IT is required for a discrimination task using unexpected stimuli, but is not necessary after the subject has habituated to the stimuli within the experimental day[179], suggesting that feedback interactions may in fact transmit information encoded within a higher visual area into the working memory of a lower visual area.

The impact of intermediate visual regional inactivation on earlier visual attentional modulations has not been directly studied, but the known structure and function of visual feedback provides a rich substrate for attentional modifications of visual processing. Multiplicative gains applied to these feedback pathways could enhance both linear and non-linear computations.

Extending this Selection-Stabilization model through all levels of the visual hierarchy, it is possible that attention need only involve a spotlight-like selection of the highest-level representations of the attended stimulus. This representation diffusely feeds back to lower visual areas, possibly applying a simple-gain like modulation, but at each level the attentional modulations are refined by a feedback/selective enhancement process that stabilizes the attentional "template" against incremental degradation as it travels through the reverse visual hierarchy. Indeed, one might expect the modulation to actually grow in magnitude as the cortical area associated with the attended region of space increases along each level of reverse visual processing. The reason we do not observe a sharpening of modulations in V1 is simply due to the fact that V1 is the earliest visual cortical area and no lower-level representation exists to sharpen V1 modulations. Equally plausibly, our diffuse modulations accurately measures the metabolic extent of modulation but does not reflect a subsequent refinement in the spike response of our V1 units.

The Selection-Stabilization model is anatomically simple and capable of explaining diverse attentional responses across all sensory modalities: there is no requirement that the highest-level attentional template is a visual object, it may just as well be an auditory, tactile, or multimodal sensory percept. Moreover, the requirement of distinct projections to all possible attentional foci is lifted, as the model works entirely within the existing visual hierarchy (although attentional shortcuts through e.g. the pulvinar could be utilized to refine the stabilization process). However, it is also computationally more complex and it is unreasonable to consider our findings as evidence in this model's favor.

6.4 Disambiguation between Attentional Models

Broadly, these two models are representational for two broad classes of general theories of attention. One group postulates direct connections to early visual areas that provide an early and powerful bias in downstream visual processing, while the other postulates that complex modulations are propagated through a reverse visual hierarchy with the ability to gate and be gated by every stage of visual processing. Parameters of both model families may be adjusted to predict our results in V1, primarily due to the fact that V1 is the earliest level of visual hierarchical processing. However, the models make very distinct predictions under several testable conditions.

6.4.1 Criteria for biological plausibility

Neither the Selective Spotlight nor the Selection-Stabilization model meet all criteria for plausibility using the currently existing literature. However, the knowledge gaps facing both models are offer potentially low-hanging fruit.

Spotlight models predict the presence of a single source of richly divergent feedback to a wide swath of sensory cortex (or sensory thalamus). Presumably, a competitive selection process (mediated through divisive normalization, lateral inhibition, higher-level cognitive feedback, or another undiscovered process) occurs within this region in order to drive the spotlight modulations to different white matter tracts projecting to distinct cortical (or thalamic) patches for different attentional states. Some candidate regions of the brain appear to have anatomy consistent with this model. A major candidate region is the nucleus basalis (NB) and related forebrain structures. NB is the primary source of acetylcholine to the cerebral cortex[180], and this neuromodulator evokes gain modulations in monkey[181] and rat[88] V1, and has been shown to be necessary for attentional orienting[167, 164]. NB is divided into several subnuclei, with distinct nuclei projecting to distinct cortical regions[180]. This serves as a crude map of the cerebral cortex within the NB- an ideal substrate for spotlight orientation. However, it is not clear that projections from NB align with local cortical topography with the necessary precision to explain attentional specificity. In addition, it is not known whether the location of activity within NB tracks changes in attentional strategy. As the macaque NB is amenable to electrophysiologic recordings and NB neurons are responsive to visual stimuli[182], this would be a useful target for future research.

NB is not the only potential spotlight origin, and numerous other brain areas may also meet the model's gross criteria. Data from the Human Connectome Project[183] (HCP) may be parsed to identify new candidate spotlight regions whose connectivity patterns match the necessary sensoricorticotopic distribution. One could then measure the connectome of individual subjects (a la the HCP protocols[184]) and obtain differential spotlight "weights" (connectivity strengths) to different sensory areas and determine whether the relative weights predict performance on different attentional tasks. Success in such efforts would demonstrate not only the anatomic plausibility of the spotlight model but also lend direct behavioral evidence across multiple sensory paradigms.

While no new anatomy is necessary to support the Selection-Stabilization model, the computational processes outlined by this or similar models are purely speculative. Thought experimentation alone can not determine whether stable attentional states might emerge purely secondary to innate normalization and surround suppression activity[83], or whether the theory is fundamentally flawed and can not be achieved within the context of known V1/V2 processes.That said, the intrinsic circuitry of V1 and V2, as well as their feedforward and feedback

connections, is extensively studied and has been the subject of numerous computational models ranging from the theoretically abstract[185, 186] to the deeply parameterized[187], from low dimensional simplifications[188] to deep artificial neural networks[189].

Given this rich foundation to draw upon, it is relatively simple to extend such models to test the plausibility of self-stabilizing or positive-reinforcing feedback patterns. I would propose choosing and implementing a working model of hierarchical visual processing, such as the HMAX model[190], and add to the model feedback processes that obey the statistics of V2-V1 cortico-cortial feedback projections as described in Figure 6.2. Presumably, normalization mechanisms speculated to interact with attentional modulations would also be necessary[80, 81]. One may then initiate attention by artificially activating a top-level feedback projection and determine the modulatory effect on lower visual areas. We can test the predictions of this model against our experimental observations. Through a series of simulations implementing alternative feedback pathways, we may address whether and how a top-down hierarchical system might give rise to attentional selectivity in its lowest levels, or alternative whether shortcut pathways (such as a Spotlight-like connection from FEF to V2) are fundamentally required to achieve attentional specificity within low-level vision

6.4.2 Novel forms of Attention

The Selective Spotlight model predicts that attention is limited by the reach of the cortical spotlight- if a direct path from the site of attentional origination to a given cortical location does not exist, then the spotlight can not be cast toward this location and thus that particular attentive state should be impossible (at least, impossible without substantial training efforts).

It is unlikely that the subjects in our tasks ever encountered a need to attend to full-field gratings or to very small perifoveal locations, and thus one may safely assume that these attention conditions were novel. However, there is reason to believe that neither task was of great difficulty for the spotlight model. Attention to regions of space, utilized to plan eye and reach movements, is likely among the most primitive and well-developed forms of attention. We expect a system for presaccadic, covert orientation to be capable of selecting regions of visual space with accuracy on the order of saccade accuracy ($\sigma = \pm 0.26^\circ$ at 5° eccentricity in humans[191]). Similarly, orientation is one of the earliest and most critical visual features. Position invariant, orientation-selective cells exist throughout the visual system: V4[192] and even IT[193, 194] neural tuning functions can be modeled as a function of orientation and curvature, and cortical feedback may modulate orientation processing in V1[12, 195]. One would expect that the spotlight system should have access to the modulation of such an essential, well-represented, and explicitly targetable visual feature.

Modern psychological studies have made careful measurement of the statistical properties of objects[196] and natural scenery[197, 198], as well as observers' ability to utilize such statistics[197, 198]. Given these stimulus models and modern computational power, it is simple enough to develop artificial objects, object-primitives, sounds, or other stimuli which violate these statistics and have never been encountered either by the subject or its evolutionary ancestors. While such objects or patterns would be planely visible, the attentional spotlight's underutilized connections to the relevant cortical areas should be weaker for these synthetic stimuli, and the benefits of attention to unnatural synthetic stimuli should be weaker than those observed while attending to natural stimuli. Moreover, training on attention to unnatural stimuli is expected to be slower and less specific as the spotlight develops or strengthens the required connections.

By contrast, the Selection-Stabilization model predicts that attention to unnatural stimuli should be possible as soon as the brain can generate a template for the attended stimulus, perhaps as soon as a single stimulus is encoded within IT. Moreover, a similar benefit for natural and unnatural stimuli may be expected as they would utilize the same feedback architecture. Any training effects should depend on the individual synapses involved in feed-forward processing of the single unnatural stimulus, and it would be expected that training does not transfer across different unnatural stimuli.

In summary, by carefully controlling the subjects' exposure to unnatural stimulation, one might observe subtle differences in attentional performance that implicate one or the other model of attention. One might consider that our measurements of spatially precise attention also utilized an unnatural form of attention to two nearby locations. However, the subjects in our experiment were extensively trained on one novel attention condition, with months of successful performance at criterion before data were collected. While we did abruptly switch the probability distribution, forcing the subjects to adopt an altered attentional allocation, the animals had to learn this new cue probabilistically and it is not clear when and how completely they switched their attentional efforts. For these reasons it is not possible to conclude from our study how a naive observer would allocate attention to our or another novel stimulus.

6.4.3 Off-target modulation of intermediate visual areas

Few investigations of single-unit responses have dared to intentionally miss their recording site. Outside of careful studies of surround interaction, the stimuli used to stimulate a neuron under investigation are typically matched to the receptive field structure of that one neuron. However, for such a stimulus the Spotlight and Stabilization models make similar predictions- attention to the stimulus should modulate the stimulus-matched neuron as needed for the task[2]. The theories differ as to what modulation is expected outside the field of attentional focus. A precise

Spotlight should exclude the recorded neuron, or a less precise modulation would act a function of its retinotopic distance from the focus of attention. If the specificity emerges through an internal state stabilization process, then we may expect the recorded neuron to be modulated early in the trial but to have this modulation suppressed during the later response phase.

A major confound for this analysis, present in most single-unit studies of attention (and against my own imaging studies) is that the position of the attended stimulus is kept constant across many trials such that it always falls within the receptive field of the units under investigation. A consequence of this design is that the animal may "preload" its attentional state[179], potentially allocating attentional resources to this position with greater precision than it may do so if the actual position of the attended stimulus were more uncertain. These anticipatory signals, along with synaptic potentiation along the repeatedly invoked attentional path to the studied neuron, may obscure efforts to determine whether attentional modulations appear suddenly due to a single spotlight of modulation or evolve over time as a function of both feedforward and feedback interactions.

An alternative is available through the use of a 2-dimensional electrode array. By covering a range of cortical space, attentional modulations might be simultaneously recorded inside and outside of a range of different V4 neurons' receptive fields. In this hypothetical study, V4 is preferred over V1 as we infer that a Spotlight does not reach V1. Based off the known scale of the retinotopic map in V4[199] and the expected placement of a recording array on the exposed surface of V4[108], we expect a 4×4 mm array to cover ≈4×4° of visual space. This is a sufficient area to place a large array of stimuli[108], much the same as we presented in V1.

This provides a rich substrate to study the initiation and evolution of an attentional state. One may present an array of symbolic stimuli of different orientation/curvature, and cue the subject to attend to one stimulus element for e.g. a change detection task[2]. However, the use of symbols allows for a novel manipulation- the animal will have to use endogenous attention to select one stimulus element, but within each trial he must determine which element by parsing the symbols and applying a simple rule (e.g. "one position clockwise from the square"). We could then measure, on a trial-to-trial basis, the activity of task-involved and task-uninvolved neurons over the time of attentional orientation. We may then determine whether these modulations involve the entire array and evolve as a function of sensory input within both task-involved and task-neutral V4 neurons, as expected if attentional specificity emerges within V4, or whether the modulations appear instantaneously in task-involved neurons once the spotlight is appropriately allocated.

References

[1] Michael I. Posner, Charles R. R. Snyder, and Brian J. Davidson. Attention and the detection of signals. *Journal of experimental psychology*, 109(2):160–74, jun 1980.

[2] Geoffrey M. Ghose and John H. R. Maunsell. Spatial summation can explain the attentional modulation of neuronal responses to multiple stimuli in area V4. *The Journal of Neuroscience*, 28(19):5115–26, may 2008.

[3] Jeffrey Moran and Robert Desimone. Selective attention gates visual processing in the extrastriate cortex. *Science (New York, N.Y.)*, 229(4715):782–4, aug 1985.

[4] Brad C. Motter. Focal attention produces spatially selective processing in visual cortical areas V1, V2, and V4 in the presence of competing stimuli. *Journal of Neurophysiology*, 70(3):909–19, sep 1993.

[5] R B Tootell, N Hadjikhani, E K Hall, S Marrett, W Vanduffel, J T Vaughan, and a M Dale. The retinotopy of visual spatial attention. *Neuron*, 21(6):1409–22, dec 1998.

[6] Daniel Baldauf and Robert Desimone. Neural mechanisms of object-based attention. *Science (New York, N.Y.)*, 344(6182):424–7, apr 2014.

[7] Maria G. Veldhuizen, Genevieve Bender, R. Todd Constable, and Dana M. Small. Trying to detect taste in a tasteless solution: Modulation of early gustatory cortex by attention to taste. *Chemical Senses*, 32:569–581, 2007.

[8] Christina Zelano, Moustafa Bensafi, Jess Porter, Joel Mainland, Brad Johnson, Elizabeth Bremner, Christina Telles, Rehan Khan, and Noam Sobel. Attentional modulation in human primary olfactory cortex. *Nature Neuroscience*, 8(1):114–120, 2005.

[9] Annette Sterr, Shan Shen, Arshad Zaman, Neil Roberts, and Andre Szameitat. Activation of SI is modulated by attention: a random effects fMRI study using mechanical stimuli. *Neuroreport*, 18(6):607–611, 2007.

[10] Aspasia E. Paltoglou, Christian J. Sumner, and Deborah a. Hall. Mapping feature-sensitivity and attentional modulation in human auditory cortex with functional magnetic resonance imaging. *European Journal of Neuroscience*, 33(November 2010):1733–1741, 2011.

[11] Kathleen S. Rockland and Agnes Virga. Terminal arbors of individual "feedback" axons projecting from area V2 to V1 in the macaque monkey: a study using immunohistochemistry of anterogradely transported Phaseolus vulgaris-leucoagglutinin. *The Journal of Comparative Neurology*, 285(1):54–72, 1989.

[12] Amir Shmuel, Maria Korman, Anna Sterkin, Michal Harel, Shimon Ullman, Rafael Malach, and Amiram Grinvald. Retinotopic axis specificity and selective clustering of feedback projections from V2 to V1 in the owl monkey. *The Journal of neuroscience : the official journal of the Society for Neuroscience*, 25(8):2117–31, feb 2005.

[13] Francis Crick. Function of the thalamic reticular complex: the searchlight hypothesis. *Proceedings of the National Academy of Sciences of the United States of America*, 81(14):4586–90, jul 1984.

[14] Alex C. Huk and David J. Heeger. Task-related modulation of visual cortex. *Journal of Neurophysiology*, 83(6):3525–3536, jun 2000.

[15] Elias H Cohen and Frank Tong. Neural Mechanisms of Object-Based Attention. *Cerebral Cortex*, Online, nov 2013.

[16] William Prinzmetal, Christin McCool, and Samuel Park. Attention: reaction time and accuracy reveal different mechanisms. *Journal of Experimental Psychology: General*, 134(1):73–92, 2005.

[17] Daniel J Simons and Christopher F Chabris. Gorillas in our midst: sustained inattentional blindness for dynamic events. *Perception*, 28(9):1059–74, 1999.

[18] Adam Gazzaley and Anna C. Nobre. Top-down modulation: Bridging selective attention and working memory. *Trends in Cognitive Sciences*, 16(2):129–135, 2012, NIHMS150003.

[19] Hagit Magen. The role of central attention in retrieval from visual short-term memory. *Psychonomic Bulletin & Review*, 2016.

[20] K J Hawley and W a Johnston. Long-term perceptual memory for briefly exposed words as a function of awareness and attention. *Journal of experimental psychology. Human perception and performance*, 17(3):807–815, 1991.

[21] M J Morgan, R M Ward, and E Castet. Visual search for a tilted target : Tests of spatial uncertainty models. *The Quarterly journal of experimental psychology. A, Human experimental psychology*, 51A(2):347–370, 1998.

[22] Barbara Anne Dosher and Zhong-Lin Lu. Noise exclusion in spatial attention. *Psychological science*, 11(2):139–46, mar 2000.

[23] Louise Whiteley and Maneesh Sahani. Attention in a bayesian framework. *Frontiers in human neuroscience*, 6(June):100, 2012.

[24] Ryan T. Maloney, Jaikishan Jayakumar, Ekaterina V. Levichkina, Ivan N. Pigarev, and Trichur R. Vidyasagar. Information processing bottlenecks in macaque posterior parietal cortex: An attentional blink? *Experimental Brain Research*, 228(3):365–376, 2013.

[25] Jesse Prinz. A Neurofunctional Theory of Visual Consciousness. *Consciousness and Cognition*, 9(2):243–259, 2000.

[26] John R Searle. Consciousness. *Annual review of neuroscience*, 23:557–78, 2000.

[27] Yuhong V Jiang, Bo-Yeong Won, and Khena M Swallow. First saccadic eye movement reveals persistent attentional guidance by implicit learning. *Journal of experimental psychology. Human perception and performance*, 40(3):1161–73, 2014.

[28] Geoffrey M. Ghose and John H. R. Maunsell. Attentional modulation in visual cortex depends on task timing. *Nature*, 419(6907):616–20, oct 2002.

[29] Scott G. Warren, Essa Yacoub, and Geoffrey M. Ghose. Featural and temporal attention selectively enhance task-appropriate representations in human primary visual cortex. *Nature communications*, 5:5643, 2014.

[30] Yao Chen, Susana Martinez-Conde, Stephen L Macknik, Yulia Bereshpolova, Harvey A Swadlow, and Jose-Manuel Alonso. Task difficulty modulates the activity of specific neuronal populations in primary visual cortex. *Nature neuroscience*, 11(8):974–982, 2008.

[31] Steven J. Luck, Leonardo Chelazzi, Steven A. Hillyard, and Robert Desimone. Neural mechanisms of spatial selective attention in areas V1, V2, and V4 of macaque visual cortex. *Journal of neurophysiology*, 77(1):24–42, 1997.

[32] Leonardo Chelazzi, E K Miller, J Duncan, and R Desimone. Responses of neurons in macaque area V4 during memory-guided visual search. *Cerebral cortex (New York, N.Y. : 1991)*, 11:761–72, 2001.

[33] Fumi Katsuki and Christos Constantinidis. Bottom-Up and Top-Down Attention: Different Processes and Overlapping Neural Systems. *The Neuroscientist*, 20(5):509–521, 2014.

[34] Kareem M Ahmad, Karl Klug, Steve Herr, Peter Sterling, and Stan Schein. Cell density ratios in a foveal patch in macaque retina. *Visual neuroscience*, 20(2003):189–209, 2003.

[35] David C. Van Essen, William T. Newsome, and John H. R. Maunsell. The visual field representation in striate cortex of the macaque monkey: asymmetries, anisotropies, and individual variability. *Vision research*, 24(5):429–48, jan 1984.

[36] Dennis M. Levi, Stanley A. Klein, and A. P. Aitsebaomo. Vernier acuity, crowding and cortical magnification. *Vision Research*, 25(7):963–977, 1985.

[37] H Bouma. Interaction Effects in Parafoveal Letter Recognition. *Nature*, 226(5241):177–178, 1970.

[38] Amelia R. Hunt and Alan Kingstone. Covert and overt voluntary attention: Linked or independent? *Cognitive Brain Research*, 18(1):102–105, 2003.

[39] Bianca de Haan, Paul S. Morgan, and Chris Rorden. Covert orienting of attention and overt eye movements activate identical brain regions. *Brain Research*, 1204:102–111, 2008, NIHMS150003.

[40] Caroline E Robertson, Dwight J Kravitz, Jan Freyberg, Simon Baron-Cohen, and Chris I Baker. Tunnel vision: sharper gradient of spatial attention in autism. *The Journal of neuroscience : the official journal of the Society for Neuroscience*, 33(16):6776–81, apr 2013.

[41] Milind Gadgil, Eric Peterson, Jason Tregellas, Susan Hepburn, and Donald C Rojas. Differences in global and local level information processing in autism: An fMRI investigation. *Psychiatry research*, 213(2):115–21, aug 2013.

[42] P M Greenwood, R Parasuraman, and G E Alexander. Controlling the focus of spatial attention during visual search: effects of advanced aging and Alzheimer disease. *Neuropsychology*, 11(1):3–12, jan 1997.

[43] J N Epstein, C K Conners, D Erhardt, J S March, and J M Swanson. Asymmetrical hemispheric control of visual-spatial attention in adults with attention deficit hyperactivity disorder. *Neuropsychology*, 11(4):467–73, 1997.

[44] J M Swanson, M Posner, S Potkin, S Bonforte, D Youpa, C Fiore, D Cantwell, and F Crinella. Activating tasks for the study of visual-spatial attention in ADHD children: a cognitive anatomic approach. *Journal of child neurology*, 6 Suppl:S119–S127, 1991.

[45] G. P. Novak, M. Solanto, and H. Abikoff. Spatial orienting and focused attention in attention deficit hyperactivity disorder, 1995.

[46] Marisa Carrasco. Visual attention: the past 25 years. *Vision Research*, 51(13):1484–525, jul 2011.

[47] Rafal Bogacz, Eric Brown, Jeff Moehlis, Philip Holmes, and Jonathan D Cohen. The physics of optimal decision making: A formal analysis of models of performance in two-alternative forced-choice tasks. *Psychological Review*, 113(4):700–765, 2006, arXiv:1011.1669v3.

[48] S. Saberi-Moghadam, S. Ferrari-Toniolo, S. Ferraina, R. Caminiti, and A. Battaglia-Mayer. Modulation of Neural Variability in Premotor, Motor, and Posterior Parietal Cortex during Change of Motor Intention. *Journal of Neuroscience*, 36(16):4614–4623, 2016.

[49] I Toni, D Thoenissen, and K Zilles. Movement preparation and motor intention. *NeuroImage*, 14(1 Pt 2):S110–S117, 2001.

[50] Nelly Amador and Itzhak Fried. Single-neuron activity in the human supplementary motor area underlying preparation for action. *Journal of neurosurgery*, 100(2):250–259, 2004.

[51] D Boussaoud. Attention versus intention in the primate premotor cortex. *NeuroImage*, 14(1 Pt 2):S40–5, 2001.

[52] Oren Cohen, Efrat Sherman, Nofya Zinger, Steve Perlmutter, and Yifat Prut. Getting ready to move: Transmitted information in the corticospinal pathway during preparation for movement. *Current Opinion in Neurobiology*, 20(6):696–703, 2010, NIHMS150003.

[53] B. M. Sheliga, L. Riggio, and G. Rizzolatti. Orienting of attention and eye movements. *Experimental Brain Research*, 98(3):507–522, 1994.

[54] Giacomo Rizzolatti, Lucia Riggio, Isabella Dascola, and Carlo Umiltá. Reorienting attention across the horizontal and vertical meridians: Evidence in favor of a premotor theory of attention. *Neuropsychologia*, 25(1 PART 1):31–40, 1987.

[55] Daniel T. Smith and Thomas Schenk. The Premotor theory of attention: Time to move on? *Neuropsychologia*, 50(6):1104–1114, 2012, arXiv:0811.2183v2.

[56] Valérie Hospod, Jean-Marc Aimonetti, Jean-Pierre Roll, and Edith Ribot-Ciscar. Changes in human muscle spindle sensitivity during a proprioceptive attention task. *The Journal of neuroscience : the official journal of the Society for Neuroscience*, 27(19):5172–8, 2007.

[57] Todd a. Kelley and Steven Yantis. Neural Correlates of Learning to Attend. *Frontiers in Human Neuroscience*, 4(November):1–11, 2010.

[58] Mariana M B Cardoso, Yevgeniy B Sirotin, Bruss Lima, Elena Glushenkova, and Aniruddha Das. The neuroimaging signal is a linear sum of neurally distinct stimulus- and task-related components. *Nature Neuroscience*, 15(9):1298–1306, 2012.

[59] Amir Shmuel, Essa Yacoub, Denis Chaimow, Nikos K Logothetis, and Kamil Ugurbil. Spatio-temporal point-spread function of fMRI signal in human gray matter at 7 Tesla. *NeuroImage*, 35(2):539–52, apr 2007.

[60] Eric M. Bowman, Verity J. Brown, Caroline Kertzman, Urs Schwarz, and David Lee Robinson. Covert orienting of attention in macaques. I. Effects of behavioral context. *Journal of Neurophysiology*, 70(1):431–443, 1993.

[61] Daniel J Felleman and David C Van Essen. Distributed hierarchical processing in the primate cerebral cortex. *Cerebral cortex (New York, N.Y. : 1991)*, 1(1):1–47, 1991.

[62] David H. Hubel and T N Wiesel. Receptive fields of single neurones in the cat's striate cortex. *Journal of Physiology*, 148:574–591, 1959.

[63] David H. Hubel and Torsten N. Wiesel. Sequence regularity and geometry of orientation columns in the monkey striate cortex. *The Journal of Comparative Neurology*, 158(3):267–93, dec 1974.

[64] James J. DiCarlo, Davide Zoccolan, and Nicole C. Rust. How Does the Brain Solve Visual Object Recognition? *Neuron Perspective*, 73(3):415–434, 2012.

[65] Marino Pagan and Nicole C Rust. Dynamic target match signals in perirhinal cortex can be explained by instantaneous computations that act on dynamic input from inferotemporal cortex. *The Journal of neuroscience : the official journal of the Society for Neuroscience*, 34(33):11067–84, 2014.

[66] J Bachevalier, M Meunier, M X Lu, and L G Ungerleider. Thalamic and temporal cortex input to medial prefrontal cortex in rhesus monkeys. *Experimental brain research*, 115(3):430–44, 1997.

[67] Jena B Hales, Nicola J Broadbent, Priya D Velu, Larry R Squire, and Robert E Clark. Hippocampus, perirhinal cortex, and complex visual discriminations in rats and humans. *Learning & Memory*, 22(2):83–91, 2015.

[68] Corbin A Cunningham, Michael A Yassa, and Howard E Egeth. Massive memory revisited: Limitations on storage capacity for object details in visual long-term memory. *Learning & memory (Cold Spring Harbor, N.Y.)*, 22(11):563–6, 2015.

[69] Ying Zhang, Ethan M Meyers, Narcisse P Bichot, Thomas Serre, Tomaso A Poggio, and Robert Desimone. Object decoding with attention in inferior temporal cortex. *Proceedings of the National Academy of Sciences*, 108(21):8850–8855, 2011.

[70] Ashesh D. Mehta, I Ulbert, and Charles E. Schroeder. Intermodal selective attention in monkeys. I: distribution and timing of effects across visual areas. *Cerebral Cortex*, 10(4):343–58, apr 2000.

[71] David H. Hubel and Torsten N. Wiesel. Receptive fields and functional architecture of monkey striate cortex. *The Journal of physiology*, 195(1):215–43, mar 1968.

[72] D G Albrecht and D B Hamilton. Striate cortex of monkey and cat: contrast response function. *Journal of neurophysiology*, 48(1):217–37, jul 1982.

[73] K H Foster, J P Gaska, M Nagler, and Daniel a Pollen. Spatial and temporal frequency selectivity of neurones in visual cortical areas V1 and V2 of the macaque monkey. *The Journal of physiology*, 365:331–63, aug 1985.

[74] J C Gardner and E J Raiten. Ocular dominance and disparity-sensitivity: why there are cells in the visual cortex driven unequally by the two eyes. *Experimental brain research. Experimentelle Hirnforschung. Experimentation cerebrale*, 64:505–514, 1986.

[75] S. Marčelja. Mathematical description of the responses of simple cortical cells*. *Journal of the Optical Society of America*, 70:1297, 1980.

[76] John H Reynolds, Leonardo Chelazzi, and Robert Desimone. Competitive mechanisms subserve attention in macaque areas V2 and V4. *The Journal of neuroscience : the official journal of the Society for Neuroscience*, 19(5):1736–1753, 1999.

[77] John H. Reynolds and Robert Desimone. Interacting roles of attention and visual salience in V4. *Neuron*, 37(5):853–863, 2003.

[78] Carrie J. McAdams and John H. R. Maunsell. Effects of attention on orientation-tuning functions of single neurons in macaque cortical area V4. *The Journal of Neuroscience*, 19(1):431–41, jan 1999.

[79] Stefan Treue and Julio C. Martínez Trujillo. Feature-based attention influences motion processing gain in macaque visual cortex. *Nature*, 399(6736):575–9, jun 1999.

[80] Geoffrey M. Ghose. Attentional modulation of visual responses by flexible input gain. *Journal of Neurophysiology*, 101(4):2089–106, apr 2009.

[81] Marlene R Cohen and John H. R. Maunsell. Attention improves performance primarily by reducing interneuronal correlations. *Nature neuroscience*, 12(12):1594–600, dec 2009.

[82] Matteo Carandini and David J. Heeger. Normalization as a canonical neural computation. *Nature reviews. Neuroscience*, 13(1):51–62, jan 2012.

[83] John H Reynolds and David J. Heeger. The normalization model of attention. *Neuron*, 61(2):168–85, jan 2009.

[84] Anita A Disney, Kunal V Domakonda, and Chiye Aoki. Differential expression of muscarinic acetylcholine receptors across excitatory and inhibitory cells in visual cortical areas V1 and V2 of the macaque monkey. *J Comp Neurol*, 499(1):49–63, nov 2006.

[85] Emilio Salinas and P Thier. Gain modulation: a major computational principle of the central nervous system. *Neuron*, 27(1):15–21, 2000.

[86] Frances S. Chance, Larry F. Abbott, and Alex D. Reyes. Gain modulation from background synaptic input. *Neuron*, 35(4):773–782, aug 2002.

[87] Asli Ayaz and Frances S. Chance. Gain modulation of neuronal responses by subtractive and divisive mechanisms of inhibition. *Journal of Neurophysiology*, 101(2):958–968, feb 2009.

[88] Shogo Soma, Satoshi Shimegi, Naofumi Suematsu, and Hiromichi Sato. Cholinergic modulation of response gain in the rat primary visual cortex. *Scientific reports*, 3:1138, 2013.

[89] Timothy J. Ebner and Gang Chen. Use of voltage-sensitive dyes and optical recordings in the central nervous system. *Progress in Neurobiology*, 46(5):463–506, 1995.

[90] T. Robert Husson and Naoum P. Issa. *Functional Imaging with Mitochondrial Flavoprotein Autofluorescence: Theory, Practice, and Applications.* 2009.

[91] Anna W Roe. Long-term optical imaging of intrinsic signals in anesthetized and awake monkeys. *Applied optics*, 46(10):1872–1880, 2007.

[92] Elizabeth M.C. C Hillman. Coupling Mechanism and Significance of the BOLD Signal: A Status Report. *Annual review of neuroscience*, 37(1):161–181, 2014.

[93] Geoffrey M. Boynton. Spikes, BOLD, attention, and awareness: a comparison of electrophysiological and fMRI signals in V1. *Journal of Vision*, 11(5):12, jan 2011, NIHMS150003.

[94] Sunil P. Gandhi, David J. Heeger, and Geoffrey M. Boynton. Spatial attention affects brain activity in human primary visual cortex. *Proceedings of the National Academy of Sciences of the United States of America*, 96(6):3314–3319, mar 1999.

[95] Nikos K Logothetis, J Pauls, M Augath, T Trinath, and a Oeltermann. Neurophysiological investigation of the basis of the fMRI signal. *Nature*, 412(6843):150–7, jul 2001.

[96] B. Lima, M. M. B. Cardoso, Y. B. Sirotin, and Aniruddha Das. Stimulus-Related Neuroimaging in Task-Engaged Subjects Is Best Predicted by Concurrent Spiking. *Journal of Neuroscience*, 34(42):13878–13891, oct 2014.

[97] O J Arthurs, H Johansen-Berg, P M Matthews, and S J Boniface. Attention differentially modulates the coupling of fMRI BOLD and evoked potential signal amplitudes in the human somatosensory cortex. *Exp Brain Res*, 157(3):269–274, 2004.

[98] Arthur R Houweling, Guy Doron, Birgit C Voigt, Lucas J Herfst, and Michael Brecht. Nanostimulation: manipulation of single neuron activity by juxtacellular current injection. *Journal of neurophysiology*, 103(3):1696–704, mar 2010.

[99] David H. Hubel and T N Wiesel. SHAPE AND ARRANGEMENT OF COLUMNS IN CAT'S STRIATE CORTEX. *Journal of Physiology*, 165:559–568, 1963.

[100] Ichiro Fujita, K Tanaka, M Ito, and K Cheng. Columns for visual features of objects in monkey inferotemporal cortex. *Nature*, 360(6402):343–6, nov 1992.

[101] Valery A Kalatsky and Michael P Stryker. New paradigm for optical imaging: temporally encoded maps of intrinsic signal. *Neuron*, 38(4):529–45, may 2003.

[102] Pavlos Gourtzelidis, Charidimos Tzagarakis, Scott M Lewis, David a Crowe, Edward Auerbach, Trenton a Jerde, Kamil Ugurbil, and Apostolos P Georgopoulos. Mental maze solving: directional fMRI tuning and population coding in the superior parietal lobule. *Experimental brain research. Experimentelle Hirnforschung. Expérimentation cérébrale*, 165(3):273–82, sep 2005.

[103] Essa Yacoub, Noam Harel, and Kamil Ugurbil. High-field fMRI unveils orientation columns in humans. *Proceedings of the National Academy of Sciences of the United States of America*, 105(30):10607–12, jul 2008.

[104] Yukiyasu Kamitani and Frank Tong. Decoding the visual and subjective contents of the human brain. *Nature Neuroscience*, 8(5):679–85, may 2005.

[105] Jeremy Freeman, Gijs Joost Brouwer, David J. Heeger, and Elisha P. Merriam. Orientation decoding depends on maps, not columns. *The Journal of Neuroscience*, 31(13):4792–804, mar 2011.

[106] Janneke F M Jehee, Devin K Brady, and Frank Tong. Attention improves encoding of task-relevant features in the human visual cortex. *The Journal of Neuroscience*, 31(22):8210–8219, jun 2011.

[107] Katherine F Weiner and Geoffrey M. Ghose. Population coding in area V4 during rapid shape detections. *Journal of neurophysiology*, 113(7):3021–34, 2015.

[108] Katherine F. Weiner and Geoffrey M. Ghose. Rapid shape detection signals in area V4. *Frontiers in Neuroscience*, 8(SEP):1–15, 2014.

[109] Takayuki Sato, Go Uchida, and Manabu Tanifuji. Cortical columnar organization is reconsidered in inferior temporal cortex. *Cerebral cortex (New York, N.Y. : 1991)*, 19(8):1870–88, aug 2009.

[110] Barbara Heider, Jason L. Nathanson, Ehud Y. Isacoff, Edward M. Callaway, and Ralph M. Siegel. Two-photon imaging of calcium in virally transfected striate cortical neurons of behaving monkey. *PLoS ONE*, 5(11):1–13, 2010.

[111] Stephen A. Engel, Gary H. Glover, and Brian A. Wandell. Retinotopic organization in human visual cortex and the spatial precision of functional MRI. *Cerebral Cortex*, 7(2):181–92, mar 1997.

[112] Yevgeniy B. Sirotin and Aniruddha Das. Spatial relationship between flavoprotein fluorescence and the hemodynamic response in the primary visual cortex of alert macaque monkeys. *Frontiers in Neuroenergetics*, 2(June):6, 2010.

[113] T Robert Husson, Atul K Mallik, Jing X Zhang, and Naoum P Issa. Functional imaging of primary visual cortex using flavoprotein autofluorescence. *The Journal of neuroscience : the official journal of the Society for Neuroscience*, 27(32):8665–75, aug 2007.

[114] David Attwell and Simon B. Laughlin. An energy budget for signaling in the grey matter of the brain. *Journal of cerebral blood flow and metabolism : official journal of the International Society of Cerebral Blood Flow and Metabolism*, 21:1133–45, 2001.

[115] Melissa Vos, Elsa Lauwers, and Patrik Verstreken. Synaptic mitochondria in synaptic transmission and organization of vesicle pools in health and disease. *Frontiers in Synaptic Neuroscience*, 2(SEP):1–10, 2010.

[116] Christopher M. Anderson and Raymond A. Swanson. Astrocyte glutamate transport: Review of properties, regulation, and physiological functions. *Glia*, 32(1):1–14, 2000.

[117] Kamil Ugurbil, Wei Chen, Xiaoping Hu, Seong-Gi Kim, Xiao-Hung Zhu, and Seiji Ogawa. Functional MRI at high fields: Practice and utility. *eMagRes*, pages 1–20, 2007.

[118] David A. Feinberg and Essa Yacoub. The rapid development of high speed, resolution and precision in fMRI. *NeuroImage*, 62(2):720–725, 2012, NIHMS150003.

[119] Jeff H. Duyn. The future of ultra-high field MRI and fMRI for study of the human brain. *NeuroImage*, 62(2):1241–1248, 2012, NIHMS150003.

[120] Charles W. Eriksen and J. D. St James. Visual attention within and around the field of focal attention: a zoom lens model. *Perception & Psychophysics*, 40(4):225–40, oct 1986.

[121] Anna C. Nobre. Orienting attention to instants in time. *Neuropsychologia*, 39(12):1317–28, jan 2001.

[122] Taosheng Liu and Youyang Hou. Global feature-based attention to orientation. *Journal of Vision*, 11(10):1–8, jan 2011.

[123] Taosheng Liu, Franco Pestilli, and Marisa Carrasco. Transient attention enhances perceptual performance and FMRI response in human visual cortex. *Neuron*, 45(3):469–77, feb 2005.

[124] Marlene R Cohen and John H. R. Maunsell. Using neuronal populations to study the mechanisms underlying spatial and feature attention. *Neuron*, 70(6):1192–1204, jun 2011.

[125] Geoffrey M. Boynton. A framework for describing the effects of attention on visual responses. *Vision Research*, 49(10):1129–1143, jun 2009.

[126] Mark Roberts, Louise S Delicato, Jose Herrero, Mark A Gieselmann, and Alexander Thiele. Attention alters spatial integration in macaque V1 in an eccentricity-dependent manner. *Nature neuroscience*, 10(11):1483–91, nov 2007.

[127] Julio C Martinez-Trujillo and Stefan Treue. Feature-based attention increases the selectivity of population responses in primate visual cortex. *Current Biology*, 14(9):744–751, 2004.

[128] Pei Sun, Justin L Gardner, Mauro Costagli, Kenichi Ueno, R Allen Waggoner, Keiji Tanaka, and Kang Cheng. Demonstration of tuning to stimulus orientation in the human visual cortex: a high-resolution fMRI study with a novel continuous and periodic stimulation paradigm. *Cerebral Cortex*, 23(7):1618–29, jun 2012.

[129] Joanna R Doherty, Anling Rao, M Marsel Mesulam, and Anna C. Nobre. Synergistic effect of combined temporal and spatial expectations on visual attention. *The Journal of Neuroscience*, 25(36):8259–8266, 2005.

[130] Peter Lakatos, Gabriella Musacchia, Monica N O'Connel, Arnaud Y Falchier, Daniel C Javitt, and Charles E Schroeder. The spectrotemporal filter mechanism of auditory selective attention. *Neuron*, 77(4):750–61, feb 2013.

[131] Christoph Braun, Monika Haug, Katja Wiech, Niels Birbaumer, Thomas Elbert, and Larry E. Roberts. Functional Organization of Primary Somatosensory Cortex Depends on the Focus of Attention. *NeuroImage*, 17(3):1451–1458, nov 2002.

[132] Taosheng Liu, Jonas Larsson, and Marisa Carrasco. Feature-Based Attention Modulates Orientation-Selective Responses in Human Visual Cortex. *Neuron*, 55(2):313–323, jul 2007.

[133] Daniel Yoshor, Geoffrey M. Ghose, William H Bosking, Ping Sun, and John H. R. Maunsell. Spatial attention does not strongly modulate neuronal responses in early human visual cortex. *The Journal of Neuroscience*, 27(48):13205–9, nov 2007.

[134] Tolga Çukur, Shinji Nishimoto, Alexander G Huth, and Jack L. Gallant. Attention during natural vision warps semantic representation across the human brain. *Nature neuroscience*, 16(6):763–70, jun 2013.

[135] Essa Yacoub, Amir Shmuel, Josef Pfeuffer, Pierre-François Van de Moortele, Gregor Adriany, P Andersen, J T Vaughan, H Merkle, Kamil Ugurbil, and X Hu. Imaging brain function in humans at 7 Tesla. *Magnetic Resonance in Medicine*, 45(4):588–94, apr 2001.

[136] Michael S. Beauchamp, Robert W. Cox, and Edgar A. DeYoe. Graded effects of spatial and featural attention on human area MT and associated motion processing areas. *Journal of neurophysiology*, 78(1):516–20, jul 1997.

[137] Benjamin Y. Hayden and Jack L. Gallant. Combined effects of spatial and feature-based attention on responses of V4 neurons. *Vision Research*, 49(10), 2009.

[138] Jasper Poort, Florian Raudies, Aurel Wannig, Victor a F Lamme, Heiko Neumann, and Pieter R. Roelfsema. The role of attention in figure-ground segregation in areas V1 and V4 of the visual cortex. *Neuron*, 75(1):143–56, jul 2012.

[139] David H. Hubel and Torsten N. Wiesel. Receptive fields, binocular interaction and functional architecture in the cat's visual cortex. *The Journal of Physiology*, 160:106–54, jan 1962.

[140] George Azzopardi and Nicolai Petkov. A CORF computational model of a simple cell that relies on LGN input outperforms the Gabor function model. *Biological Cybernetics*, 106(3):177–89, mar 2012.

[141] Takayuki Sato, Go Uchida, Mark D Lescroart, Jun Kitazono, Masato Okada, and Manabu Tanifuji. Object representation in inferior temporal cortex is organized hierarchically in a mosaic-like structure. *The Journal of neuroscience : the official journal of the Society for Neuroscience*, 33(42):16642–56, oct 2013.

[142] Jerrold H. Zar. *Biostatistical Analysis*. Prentice Hall, Upper Saddle River, NJ, fourth edition, 1999.

[143] Pierre-François Van de Moortele, Edwards J Auerbach, Cheryl Olman, Essa Yacoub, Kamil Ugurbil, and Steen Moeller. T1 weighted brain images at 7 Tesla unbiased for Proton Density, T2* contrast and RF coil receive B1 sensitivity with simultaneous vessel visualization. *NeuroImage*, 46(2):432–46, jun 2009.

[144] Mark Jenkinson, Christian F. Beckmann, Timothy E. J. Behrens, Mark W. Woolrich, and Stephen M. Smith. Fsl. *NeuroImage*, 62(2):782–790, aug 2012.

[145] Bruce Fischl. FreeSurfer. *NeuroImage*, 62(2):774–781, aug 2012.

[146] Yoav Benjamini and Yosef Hochberg. Controlling the False Discovery Rate: a Practical and Powerful Approach to Multiple Testing. *Journal of the Royal Statistical Society*, 57(1):289–300, 1995.

[147] Ludwig Fahrmeir and Heinz Kaufmann. Consistency and Asymptotic Normality of the Maximum Likelihood Estimator in Generalized Linear Models. *The Annals of Statistics*, 13(1):342–368, 1985.

[148] Andrea Benucci, Aman B Saleem, and Matteo Carandini. Adaptation maintains population homeostasis in primary visual cortex. *Nature Neuroscience*, 16(6):724–729, jun 2013.

[149] Notger G Müller, Oliver a Bartelt, Tobias H Donner, Arno Villringer, and Stephan a Brandt. A physiological correlate of the "Zoom Lens" of visual attention. *The Journal of neuroscience : the official journal of the Society for Neuroscience*, 23(9):3561–5, may 2003.

[150] Julie A. Brefczynski and Edgar A. DeYoe. A physiological correlate of the 'spotlight' of visual attention. *Nature Neuroscience*, 2(4):370–4, apr 1999.

[151] Sirawaj Itthipuripat, Javier O Garcia, Nuttida Rungratsameetaweemana, Thomas C Sprague, and John T Serences. Changing the spatial scope of attention alters patterns of neural gain in human cortex. *The Journal of neuroscience : the official journal of the Society for Neuroscience*, 34(1):112–23, jan 2014.

[152] Manfred Fahle. Perception of Oppositely Moving Verniers and Spatio-temporal Interpolation. 35(7):925–937, 1995.

[153] Carrie J McAdams and R Clay Reid. Attention modulates the responses of simple cells in monkey primary visual cortex. *The Journal of neuroscience : the official journal of the Society for Neuroscience*, 25(47):11023–33, nov 2005.

[154] Pieter R. Roelfsema, V A Lamme, and H Spekreijse. Object-based attention in the primary visual cortex of the macaque monkey. *Nature*, 395(6700):376–81, 1998.

[155] D.C. Somers, A.M. Dale, A.E. Seiffert, and R.B.H. Tootell. Functional MRI reveals spatially specific attentional modulation in human primary visual cortex. *Proceedings of the National Academy of Sciences, USA*, 96(4):1663–1668, 1999.

[156] Jens-Max Hopf, Steven J. Luck, Kai Boelmans, Mircea a Schoenfeld, Carsten N Boehler, Jochem Rieger, and Hans-Jochen Heinze. The neural site of attention matches the spatial scale of perception. *The Journal of neuroscience : the official journal of the Society for Neuroscience*, 26(13):3532–40, mar 2006.

[157] Eero P Simoncelli and Odelia Schwartz. Modeling Surround Suppression in V1 Neurons with a Statistically-Derived Normalization Model. *Advances in Neural Information Processing Systems*, 11:153–159, 1998.

[158] J. J. Nassi, S. G. Lomber, and Richard T Born. Corticocortical feedback contributes to surround suppression in V1 of the alert primate. *The Journal of neuroscience : the official journal of the Society for Neuroscience*, 33(19):8504–17, 2013.

[159] Vitaly Chicherov, Gijs Plomp, and Michael H Herzog. Neural correlates of visual crowding. *NeuroImage*, feb 2014.

[160] Ian T Harrison, Katherine F Weiner, and Geoffrey M. Ghose. Inattention blindness to motion in middle temporal area. *The Journal of neuroscience : the official journal of the Society for Neuroscience*, 33(19):8396–410, may 2013.

[161] Robert Turner. How much cortex can a vein drain? Downstream dilution of activation-related cerebral blood oxygenation changes. *NeuroImage*, 16:1062–1067, 2002.

[162] Lars Muckli and Lucy S. Petro. Network interactions: non-geniculate input to V1. *Current Opinion in Neurobiology*, 23(2):195–201, 2013.

[163] Kathleen S. Rockland and G W Van Hoesen. Direct temporal-occipital feedback connections to striate cortex (V1) in the macaque monkey. *Cerebral cortex (New York, N.Y. : 1991)*, 4(3):300–13, 1991.

[164] Inge Klinkenberg, Anke Sambeth, and Arjan Blokland. Acetylcholine and attention. *Behav Brain Res*, 221(2):430–442, aug 2011.

[165] Angela J Yu and Peter Dayan. Uncertainty, neuromodulation, and attention. *Neuron*, 46(4):681–92, may 2005.

[166] Martin Sarter, Cindy Lustig, William M Howe, Howard Gritton, and Anne S Berry. Deterministic functions of cortical acetylcholine. *Eur J Neurosci*, mar 2014.

[167] J L Herrero, M J Roberts, L S Delicato, Mark A Gieselmann, P Dayan, and Alexander Thiele. Acetylcholine contributes through muscarinic receptors to attentional modulation in V1. *Nature*, 454(7208):1110–4, aug 2008.

[168] D C Van Essen, W T Newsome, J H Maunsell, and J L Bixby. The projections from striate cortex (V1) to areas V2 and V3 in the macaque monkey: asymmetries, areal boundaries, and patchy connections. *The Journal of comparative neurology*, 244(4):451–480, 1986.

[169] D J Perkel, J. Bullier, and H Kennedy. Topography of the afferent connectivity of area 17 in the macaque monkey: a double-labelling study. *The Journal of comparative neurology*, 253(3):374–402, nov 1986.

[170] Jonathan J Nassi, Camille Gómez-Laberge, Gabriel Kreiman, and Richard T Born. Corticocortical feedback increases the spatial extent of normalization. *Frontiers in Systems Neuroscience*, 8(May):105, 2014.

[171] J. Bullier, J. M. Hupé, A. James, and P. Girard. Functional interactions between areas V1 and V2 in the monkey. *Journal of Physiology Paris*, 90(3-4):217–220, 1996.

[172] Leslie G Ungerleider, Thelma W Galkin, Robert Desimone, and Ricardo Gattass. Subcortical projections of area V2 in the macaque. *Journal of cognitive neuroscience*, 26(6):1220–33, jun 2014, 1511.04103.

[173] Yuri B. Saalmann, Mark a. Pinsk, Liang Wang, Xin Li, and Sabine Kastner. The pulvinar regulates information transmission between cortical areas based on attention demands. *Science (New York, N.Y.)*, 337(6095):753–6, aug 2012, NIHMS150003.

[174] Huihui Zhou, Robert John Schafer, and Robert Desimone. Pulvinar-Cortex Interactions in Vision and Attention. *Neuron*, 89(1):209–220, 2016.

[175] Didier Pinault. *The thalamic reticular nucleus: Structure, function and concept*, volume 46. 2004.

[176] Alexandra Woolgar, Mark A. Williams, and Anina N. Rich. Attention enhances multi-voxel representation of novel objects in frontal, parietal and visual cortices. *NeuroImage*, 109:429–437, 2015.

[177] Giles M. Anderson, Dietmar Heinke, and Glyn W. Humphreys. Top-down guidance of eye movements in conjunction search. *Vision Research*, 79:36–46, 2013.

[178] J M Budd. Extrastriate feedback to primary visual cortex in primates: a quantitative analysis of connectivity. *Proceedings. Biological sciences / The Royal Society*, 265(1400):1037–1044, 1998.

[179] James A. Horel. Retrieval of active and inactive visual discriminations while temporal cortex is suppressed with cold. *Behavioural Brain Research*, 51(2):193–201, 1992.

[180] James Gratwicke, Joshua Kahan, Ludvic Zrinzo, Marwan Hariz, Patricia Limousin, Thomas Foltynie, and Marjan Jahanshahi. The nucleus basalis of Meynert: A new target for deep brain stimulation in dementia? *Neuroscience and Biobehavioral Reviews*, 37(10):2676–2688, 2013.

[181] Anita a. Disney and Chiye Aoki. Muscarinic acetylcholine receptors in macaque V1 are most frequently expressed by parvalbumin-immunoreactive neurons. *Journal of Comparative Neurology*, 507(December 2007):1748–1762, apr 2008, NIHMS150003.

[182] H. Santos-Benitez, C. M. Magariños-Ascone, and E. Garcia-Austt. Nucleus basalis of Meynert cell responses in awake monkeys. *Brain Research Bulletin*, 37(5):507–511, 1995.

[183] David C. Van Essen, Stephen M. Smith, Deanna M. Barch, Timothy E. J. Behrens, Essa Yacoub, and Kamil Ugurbil. The WU-Minn Human Connectome Project: An overview. *NeuroImage*, 80:62–79, 2013, NIHMS150003.

[184] Stephen M. Smith, Christian F. Beckmann, Jesper Andersson, Edward J. Auerbach, Janine Bijsterbosch, Gwenaëlle Douaud, Eugene Duff, David A. Feinberg, Ludovica Griffanti,

Michael P. Harms, Michael Kelly, Timothy Laumann, Karla L. Miller, Steen Moeller, Steve Petersen, Jonathan Power, Gholamreza Salimi-Khorshidi, Abraham Z. Snyder, An T. Vu, Mark W. Woolrich, Junqian Xu, Essa Yacoub, Kamil Uurbil, David C. Van Essen, and Matthew F. Glasser. Resting-state fMRI in the Human Connectome Project. *NeuroImage*, 80:144–168, 2013, NIHMS150003.

[185] Elena Y. Smirnova, Ekaterina A. Chizhkova, and Anton V. Chizhov. A mathematical model of color and orientation processing in V1. *Biological Cybernetics*, 109(4-5):537–547, 2015.

[186] Alexandre Afgoustidis. Orientation Maps in V1 and Non-Euclidean Geometry. *Journal of mathematical neuroscience*, 5(1):24, 2015.

[187] Y Banitt, K A C Martin, and I Segev. A biologically realistic model of contrast-invariant orientation tuning by thalamocortical synaptic depression. 27(38):10230–10239, 2007.

[188] Cong Wang and Louis Tao. Dimensional reduction of a V1 ring model with simple and complex cells. *Journal of Computational Neuroscience*, 37(3):481–492, 2014.

[189] Yinlin Li, Wei Wu, Bo Zhang, and Fengfu Li. Enhanced HMAX model with feedforward feature learning for multiclass categorization. *Frontiers in Computational Neuroscience*, 9(October):1–14, 2015.

[190] Maximilian Riesenhuber and Tomaso Poggio. Hierarchical models of object recognition in cortex. *Nature neuroscience*, 2(11):1019–25, 1999.

[191] Z Kapoula and D A Robinson. Saccadic undershoot is not inevitable: saccades can be accurate. *Vision research*, 26(5):735–43, 1986.

[192] a Pasupathy and C E Connor. Shape representation in area V4: position-specific tuning for boundary conformation. *Journal of neurophysiology*, 86(5):2505–2519, 2001.

[193] Greet Kayaert, Irving Biederman, Hans P. Op De Beeck, and Rufin Vogels. Tuning for shape dimensions in macaque inferior temporal cortex. *European Journal of Neuroscience*, 22(1):212–224, 2005.

[194] Scott L Brincat and Charles E Connor. Underlying principles of visual shape selectivity in posterior inferotemporal cortex. *Nature neuroscience*, 7(8):880–6, 2004.

[195] D. L. Ringach, M. J. Hawken, and R. Shapley. The dynamics of orientation tuning in macaque primary visual cortex. *Investigative Ophthalmology and Visual Science*, 38, 1997, 9810036.

[196] Antonio Torralba and Aude Oliva. Statistics of natural image categories. *Network (Bristol, England)*, 14(3):391–412, 2003.

[197] Anthony D. D'Antona, Jeffrey S. Perry, and Wilson S. Geisler. Humans make efficient use of natural image statistics when performing spatial interpolation. *Journal of Vision*, 13:1–13, 2013.

[198] DustinE Stansbury, Thomas Naselaris, and Jack L. Gallant. Natural Scene Statistics Account for the Representation of Scene Categories in Human Visual Cortex. *Neuron*, 79(5):1025–1034, 2013.

[199] Ricardo Gattass, a P Sousa, and Charles G. Gross. Visuotopic organization and extent of V3 and V4 of the macaque. *The Journal of neuroscience*, 8(6):1831–1845, 1988.